Doctoral Dissertations   Dissertations and Theses

November 2018

IDENTIFYING FUNCTIONAL COMPONENTS OF THE ENDOPLASMIC RETICULUM QUALITY CONTROL AND DEGRADATION FACTOR EDEM1

Lydia Lamriben

Recommended Citation

IDENTIFYING FUNCTIONAL COMPONENTS OF THE ENDOPLASMIC RETICULUM QUALITY CONTROL AND DEGRADATION FACTOR EDEM1

A Dissertation Presented

By

LYDIA LAMRIBEN

Submitted to the Graduate School of the

University of Massachusetts Amherst in partial fulfillment

of the requirements for the degree of

DOCTOR OF PHILOSOPHY

September 2018

Molecular and Cellular Biology

IDENTIFYING FUNCTIONAL COMPONENTS OF THE ENDOPLASMIC RETICULUM QUALITY CONTROL AND DEGRADATION FACTOR EDEM1

A Dissertation Presented

by

LYDIA LAMRIBEN

Approved as to style and content by:

_____

Daniel N. Hebert, Chair

_____

Scott C. Garman, Member

_____

Danny J. Schnell, Member

_____

Igor A. Kaltashov, Member

_____

Scott C. Garman, Director

Molecular and Cellular Biology

DEDICATION

To my loving parents Malek and Nassima, my siblings Nabil and Danil, and my wonderful partner Kevin.

ACKNOWLEDGMENTS

I owe a great deal of thanks to my mentor, Dr. Daniel Hebert, for all of his support, advice and patience during my training in his lab. Dan was pivotal to my success as a graduate student; he provided a stimulating research environment that allowed me to develop my critical thinking skills and provided me with the necessary tools to become an independent researcher. I am grateful to Dan for giving me the opportunity to contribute to a book chapter and a number of review articles as well as to present my research in numerous forums. I would also like to thank my committee members, Dr. Garman, Dr. Kaltashov and Dr. Schnell, for their support and helpful feedback.

I would like to acknowledge previous and current members of the Hebert lab, specifically Abla Tannous, Johan Sunryd and Kristina Giorda, for teaching me the ropes, training me and for being such wonderful role models, Jill Graham for her friendship and resourcefulness in lab and Michela Oster, Yekaterina Kori and Haiping Ke who have helped me carry this project through and assisted me on numerous other projects. I would also like to thank the CBI and MCB programs for providing a collaborative and fun learning environment through which I have met and made a number of friends.

Lastly, I would like to thank my parents for their unconditional love and support and my partner for his patience, kindness and for agreeing to spend almost all of his weekends in lab with me.

ABSTRACT

IDENTIFYING FUNCTIONAL COMPONENTS OF THE ENDOPLASMIC RETICULUM QUALITY CONTROL AND DEGRADATION FACTOR EDEM1

SEPTEMBER 2018

LYDIA LAMRIBEN, B.S., NORTHEASTERN UNIVERSITY

Ph.D., UNIVERSITY OF MASSACHUSETTS AMHERST

Directed by: Professor Daniel N. Hebert

The ER Degradation-Enhancing Mannosidase-Like protein 1 (EDEM1) is a critical endoplasmic reticulum (ER) quality control factor involved in identifying and directing non-native proteins to the ER-associated protein degradation (ERAD) pathway. However, its recognition and binding properties have remained enigmatic since its discovery. Here we provide evidence for an additional redox-sensitive interaction between EDEM1 and Z/NHK that requires the presence of the single Cys on the α-1 antitrypsin ERAD clients. Moreover, this Cys-dependent interaction is necessary when the proteins are isolated under stringent detergent conditions, ones in which only strong covalent interactions can be sustained. This interaction is inherent to the mannosidase-like domain (MLD) of EDEM1, for which we demonstrate substrate-binding and glycan-trimming properties. EDEM1 appears to possess bipartite binding properties as it also binds these ERAD variants in a Cys-independent manner under milder detergent conditions. In addition, a second intrinsically disordered region (IDR) was identified and both are required for machinery interaction, but they are not necessary for Z/NHK binding. Interestingly, although the N-terminal IDR is required for binding to another ERAD substrate, in this case, neither IDR is required for Z/NHK binding, as the MLD, which lacks both IDRs, exhibits glycan-independent and redox-sensitive binding to

Z/NHK. Not only is the MLD sufficient to preferentially interact with the α-1 antitrypsin ERAD clients, it also possesses, as demonstrated for the first time, catalytic properties as observed through glycan-trimming. Although the IDRs do not contribute to Z/NHK binding, they are required for binding to the oxidoreductase, ERdj5. These results expand our understanding of the range of binding interactions implemented by EDEM1 and help elucidate its role as an active mannosidase involved in the quality control machinery of the Endoplasmic Reticulum (ERQC).

TABLE OF CONTENTS

LIST OF FIGURES

CHAPTER 1

INTRODUCTION

(Sections from this chapter are adapted from (Lamriben et al. 2016)

Protein folding in the endoplasmic reticulum

Approximately one third of the mammalian proteome is composed of proteins that traverse the secretory pathway (Stolz and Wolf, 2010). These membrane and soluble proteins are co-translationally translocated into the endoplasmic reticulum (ER). The majority of these proteins undergoes processing as well as acquires covalent modification in order to reach their native states. The oxidizing nature of the ER lumen provides a suitable environment for proper disulfide bond formation. Additional modifications that occur in the ER include signal sequence cleavage, glycosylation, and glycan modification. The goal of the quality control (ERQC) machinery in the ER is to differentiate between proteins that have reached their native state from those that are terminally misfolded.

Proteins that have successfully folded are released from the folding machinery of the ERQC and sorted depending on their target destinations (Dancourt and Barlowe, 2010; Barlowe and Helenius, 2016). Protein cargo that is destined to reside in other organelles or in the extracellular space is packaged into specialized COPII-coated vesicles, which exit the ER and transport it to the Golgi as the first step in protein trafficking (Barlowe et al., 1994; Belden and Barlowe, 1996; Bi et al., 2007). Once in the Golgi, some proteins are further modified and properly folded and assembled cargo is

transported out and continues trafficking. Proteins that are improperly folded or misassembled are retrieved from the Golgi compartment and returned to the ER. COPI-coated vesicles carry out this retrograde transport (Hara-Kuge et al., 1994). Proteins that are identified as terminally misfolded are extracted from folding attempts and targeted for proteasome-dependent degradation through ER-Associated Degradation (ERAD) or through autophagy (Figure 1.1). Here, we will focus solely on the events that precede and lead to ERAD. For a detailed review on mammalian autophagy please consult the article by Bento and colleagues (Bento et al., 2016).

Secretory protein trafficking begins as nascent secretory polypeptides are targeted to the ER through N-terminal signal peptides that are comprised of a large hydrophobic domain flanked by an N-terminal basic domain and C-terminal acidic domain (Hegde and Bernstein, 2006). Once synthesized and exposed, the signal peptide engages the translocation machinery by docking onto the signal peptide recognition particle (SRP), which allows it to engage the Sec61 translocation channel (Hegde and Kang, 2008). Inside the ER lumen, the nascent polypeptide is modified depending on its ultimate topology. For instance, soluble proteins possess cleavable signal peptides, while the signal peptide of Type II membrane proteins remains uncleaved and inserts into the ER membrane through the hydrophobic domain of the signal peptide.

The modified luminal polypeptide engages the ERQC machinery once inside the lumen. The ERQC is comprised of a network of maturation and quality control factors that can be organized into three categories: classical molecular chaperones, redox enzymes, and carbohydrate-binding chaperones (Figure 1.1).

Classical molecular chaperones

Classical chaperones recognize exposed hydrophobic surfaces on folding or misfolded proteins. The immunoglobulin heavy chain binding protein (BiP) is a member of the heat shock protein (Hsp)70 chaperone family and is one of the most abundant chaperones in the ER. BiP is comprised of three domains: an N-terminal nucleotide-binding domain (NBD); a central substrate-binding domain (SBD); and a C-terminal lid domain. The NBD and SBD are connected by a linker (Bukau and Horwich, 1998). The chaperone activity of the SBD is regulated by the adenosine diphosphate (ADP) and adenosine triphosphate (ATP) bound states of the NBD; wherein an ATP-bound NBD yields an open SBD conformation, and an ADP-bound NBD yields a closed SBD with a high binding affinity for substrates. BiP associates with a number of cofactors in the J-domain containing protein family, which when bound to BiP result in ATP hydrolysis.

In addition to functioning as a classical chaperone in protein folding, BiP also facilitates protein translocation into the lumen through its channel-gating properties on the Sec61 complex, and contributes to the activation of the unfolded protein response (UPR) in its direct association with the ER stress sensor IRE1α (Haßdenteufel et al., 2018; Bertolotti et al., 2000). Additionally, BiP plays a role in ERAD as indicated by binding to and promoting the degradation of misfolded ER-retained immunoglobulin light chains as well as associating with the J-domain containing cofactors ERdj4 and ERdj5, which have both been linked to ERAD (Knittler et al., 1995; Lai et al., 2012; Ushioda et al., 2008).

Oxidative folding and thiol oxidoreductases

The oxidative nature of the ER lumen provides an ideal environment for the folding of secretory proteins, which unlike other proteins; tend to be richer in cysteine (Cys) residues. These Cys are able to undergo oxidation events and form disulfide bonds in the ER that they otherwise would not form in the reducing cytoplasm. These disulfide bonds are crucial for the structural integrity and function of many secretory proteins. A large portion of secretory proteins possesses intra- or inter-molecular disulfide bonds, which facilitate the assembly of multimeric proteins in the ER. To accommodate these requirements, the ER has evolved into a specialized organelle for oxidative folding, in which pairing of disulfide bonds and correcting improperly paired disulfides, although a rate-limiting step, drives protein folding (van den Berg et al., 1999; Matagne and Dobson, 1998).

To promote oxidative folding, the ER lumen is equipped with redox components such as oxidized glutathione (GSSG) and glutathione (GSH) and approximately 20 disulfide exchange proteins that belong to the protein disulfide isomerase (PDI) family of dithiol-disulfide oxidoreductases (Ellgaard and Ruddock, 2005). The common characteristic shared among this protein family is the presence of the conserved thioredoxin domain(s), with an active Cys-Xxx-Xxx-Cys (CXXC) site (Ellgaard and Ruddock, 2005). These oxidoreductases perform dual functions, as they can either accept or donate electrons depending on whether they are forming (oxidation) or breaking (reduction) disulfide bonds, respectively. In addition to oxidation and reduction, PDI

proteins are also able to shuffle non-native disulfides to obtain native disulfides, in a process termed isomerization.

PDI possesses four thioredoxin-like domains termed a, b, b' and a' where only the a and a' domain possess active CXXC motif (Hatahet and Ruddock, 2009). The reduced and oxidized structure of human PDI has been solved and revealed that the protein adopts a twisted "U" conformation with the active domains a and a' located at the two ends of the structure (Wang et al., 2013; Tian et al., 2006). The catalytically inactive b and b' domains are situated at the center of the structure, or the bottom of the "U", in a region that is highly hydrophobic and proposed to serve as a binding site for misfolded proteins and give the protein chaperone-like properties (Tian et al., 2006; Denisov et al., 2009; Cai et al., 1994).

Likewise, the putative substrate-binding cleft that is generated from the twisted "U" structures of PDI changes in dimension depending on whether the protein is oxidized or reduced, as demonstrated from their respective solved crystal structures (Wang et al., 2013; Tian et al., 2006). It has been proposed that the size of the cleft created by the open (oxidized) versus the closed (reduced) conformation serves to bind substrates that have achieved different folding stages, the former being larger, folded polypeptides whose disulfides will be formed through an exchange reaction with the active PDI thioredoxin site (Oka and Bulleid, 2013). In order to remain catalytically active, PDI undergoes constant re-oxidizing events by members of the ER oxidoreductin 1 (Ero1) protein family (Frand and Kaiser, 1999; Tu et al., 2000).

In addition to PDI, the mammalian ER is equipped with other PDI family oxidoreductases that function in protein folding or protein degradation. Like PDI, ERp57 consists of four thioredoxin domains of which the two positioned at each termini, possess the active CXXC motifs, while the central thioredoxin folds lack enzymatic activity (Ellgaard and Ruddock, 2005). ERp57 associates with the carbohydrate-binding chaperones, calnexin and calreticulin in the ER and promotes oxidative folding.

Another oxidoreductase involved in ERQC is ERp72, which possesses three catalytically active domains and two inactive domains (Mazzarella et al., 1990). Although the sequence similarity between ERp72 and ERp57 is high, ERp72 does not interact with either calnexin or calreticulin, which is likely due to lacking a similar P-domain binding patch (Kozlov et al., 2009; Rutkevich et al., 2010). Likewise, mixed disulfides were observed between ERp72 and the glycoprotein thyroglobulin, it is unclear how ERp72 binds these substrates as it lacks any obvious hydrophobic cleft and does not interact with lectin chaperones (Menon et al., 2007; Rutkevich et al., 2010).

The other well-characterized oxidoreductase that contributes to ERQC belongs to the HSP40 J-domain containing BiP cofactor family and has been implicated in the degradation of misfolded proteins. Of the six J-domain containing proteins identified in the ER ERdj5 is the only one to possess a BiP-binding J-domain and thioredoxin domains. Structural analyses of ERdj5 revealed an N-terminal J-domain followed by six thioredoxin and thioredoxin-like domains labeled in sequential order as Trx1, Trxb1, Trxb2, Trx2, Trx3, and Trx4. All of the domains except for Trxb1/ b2 possess reactive Cys-Xxx-Xxx-Cys domains (Hagiwara et al., 2011).

ERdj5 has been implicated in ERAD as it is able to interact with misfolded proteins through BiP, on which it is hypothesized to functions as a reductase to unfold the polypeptides and facilitate their extraction from the ER and ultimate destruction (Ushioda et al., 2008; Hagiwara et al., 2011). Upon completing its function, ERdj5 was proposed to be reduced and returned to its active state by the flavoprotein-associated with degradation (ERFAD) (Riemer et al., 2009).

N-linked glycosylation and the protein folding lectin chaperone network

The vast majority of mammalian secretory proteins are modified with N-linked glycans, which are sugar appendages that are composed of 3 glucoses, 9 mannoses and 2 N-acteylglucosamines ($Glc_3Man_9GlcNAc_2$) (Figure 1.2) (Hebert and Molinari, 2007; Helenius, 1994). Glycans are covalently attached to the amide side chain of Asn located within the N-glycosylation sequence Asn-Xxx-Ser/Thr, where Xxx is any amino acid except Pro (Apweiler et al., 1999; Freeze et al., 2014). These glycans are synthesized in the ER membrane by a number of cytoplasmic and ER dolichol pyrophosphate lipid carrier proteins (Burda and Aebi, 1999). Once synthesized, $Glc_3Man_9GlcNAc_2$ glycans are transferred by the oligosaccharyltransferase (OST) complex *en bloc* co- and/or post-translationally to folding glycoproteins. Glycans are bulky amphipathic sugar structures, which possess intrinsic properties that promote the solubility of glycoproteins, disfavor aggregation, and promote native folding (O'Connor and Imperiali, 1998; Hoffmann and Flörke, 1998; Shental-Bechor and Levy, 2008; Jitsuhara et al., 2002).

N-linked glycans also possess extrinsic properties that allow glycoproteins to engage the calnexin/calreticulin folding cycle that constitutes the lectin chaperone

machinery of the ER, through a series of glycan-trimming events. The first glycan-trimming step to occur is deglucosylation. The deglucosylation events in the ER occur in a controlled sequential manner which is initiated by α-glucosidase I that cleaves the outer most α-1,2-linked glucose (Kornfeld and Kornfeld, 1985) (Figure 1.3). α-glucosidase I is a Type-II single pass transmembrane protein with a large globular luminal portion that contains the catalytic domain and a short N-terminal cytoplasmic tail (Shailubhai et al., 1991). α-glucosidase I isolated from mouse fibroblasts was found in a complex with Sec61 as observed in proteomics studies of translocon-associated factors, which supports early intervention by the enzyme in the protein folding pathway (Dejgaard et al., 2010).

Once the terminal glucose has been trimmed, the di-glucosylated glycan becomes a substrate for α-glucosidase II, a soluble ER resident enzyme that specifically cleaves the two α-1,3-linked glucose moieties to generate deglucosylated glycans (Kornfeld and Kornfeld, 1985). Human α-glucosidase II is comprised of a large α-subunit (∼100 kDa) and a smaller β-subunit (∼50 kDa) that associate non-covalently (Trombetta et al., 1996; Stigliano et al., 2011). The α-subunit possesses catalytic activity and is retained in the ER by its association with the β-subunit, which possesses an ER retention (KDEL) sequence (Pelletier et al., 2000). The β-subunit is not required for the catalytic activity of the enzyme; however, it appears necessary for its maturation, solubility and stability. The β-subunit contains a mannose 6-phosphate receptor homology (MRH) domain, which has been proposed to bind the terminal mannose on the trimmed C-branch of glycans, as well as the B-branch in order for the enzyme to efficiently act on the A-branch glucoses (Munro, 2001; Stigliano et al., 2011).

The glycan processing achieved by α-glucosidase I/II results in the transient formation of mono-glucosylated glycan, which serves as a substrate for calnexin and calreticulin. The type I membrane protein calnexin and its soluble paralog calreticulin share a similar general organization. Each is comprised of an N-terminal globular domain, a central proline-rich domain and a C-terminal domain. The N-termini of the two proteins fold into globular domains consisting of a single carbohydrate-binding site, which supports binding specifically to monoglucosylated glycans (Schrag et al., 2001; Helenius, 1994). Calcium is important for stabilizing the lectin chaperones and regulating their binding to substrates (Li et al., 2001; Brockmeier and Williams, 2006). ATP also appears to modulate the conformation of the lectin chaperones, as they become more resistant to proteases in its presence, suggestive of their adoption of a more compact conformations (Ou et al., 1995; Wijeyesakere et al., 2015).

Calnexin and calreticulin possess proline-rich domains called P-domains, which are the site of interaction with two folding factors: ERp57, a protein disulfide isomerase; and cyclophilin B (CyB), a peptidyl prolyl isomerase (Ellgaard and Ruddock, 2005). ERp57 contains a P-domain-binding region that localizes it to the vicinity of lectin chaperone substrates so it can assist with disulfide bond formation and rearrangement on lectin chaperone associated substrates. The interaction between the lectin chaperones and ERp57 is transient and occurs in the absence of a client substrate (Frickel et al., 2004; Kozlov et al., 2006). The direct association of ERp57 with calnexin and calreticulin has been suggested to be important for bringing ERp57 and its substrates together, thereby enhancing the local concentration of the isomerase for the catalysis of disulfide bonds.

ERp57 knockdown   specifically delays the secretion of glycosylated substrates (Rutkevich et al., 2010).

Calnexin and calreticulin also appear to bind client proteins in a glycan-independent manner (Danilczyk and Williams, 2001). *In vitro* studies show that they can inhibit the aggregation of non-glycosylated substrates (Saito et al., 1999). The peptide-binding site is likely located in the vicinity of the glycan binding site within the globular domain (Wijeyesakere et al., 2013). While the affinity of calreticulin for glycosylated and non-glycosylated substrates appear to be similar, their kinetics is distinct, binding to glycosylated clients is more rapid. Glycosylated and non-glycosylated clients support the formation of open and closed conformations, respectively, where the closed conformation involves the clamping down of the P-domain on the substrate stabilizing substrate interactions. The co-factor ERp57 also induces the closed conformation of calreticulin as probed using FRET measurements with purified components (Wijeyesakere et al., 2013).

If a glycoprotein has not reached its native state in a timely manner, it is able to re-engage the calnexin/calreticulin folding cycle through a concerted effort by UDP-glucose glycoprotein glucosyltransferase 1 (UGGT1), which keeps the glycan in a mono-glucosylated state (Helenius, 1994; Sousa and Parodi, 1995). Once the glycoprotein is in a mono-glucosylated state, it also becomes a substrate for α-glucosidase II, which competes with UGGT1 with opposing effects (Caramelo and Parodi, 2008). This positions UGGT1 as a central gatekeeper in the ER that decides whether glycoproteins traffic onto the Golgi and beyond, or are retained in the ER for further assistance.

Human UGGT1 is a soluble resident ER enzyme. It possesses a catalytic glucosyltransferase domain at its C-terminus. This domain contains a DxD motif that is required for its catalytic activity (Tessier et al., 2000; Breton et al., 2006). In an *in vitro* study, purified rat UGGT1 required calcium to transfer glucose onto deglucosylated glycoprotein acceptors, suggesting calcium dependence for the catalytic activity of UGGT1 (Trombetta and Parodi, 1992). Similar to α-glucosidase II, the catalytic activity of UGGT1 is more effective on glycans with high mannose content (Sousa et al., 1992). UGGT1 also has a homologue UGGT2 that shares 55% sequence identity with UGGT1 (Arnold et al., 2000). The C-terminal glucosyltransferase domain appears to be active when swapped with the catalytic domain of UGGT1 or when tested *in vitro* against synthetic substrates (Arnold and Kaufman, 2003; Takeda et al., 2014). Currently, no biological role has been assigned nor natural substrates of UGGT2 have been identified.

Mannose trimming direct glycoprotein degradation through ERAD

Terminally misfolded or irreparably folded glycoproteins are efficiently reglucosylated by UGGT1 supporting persistent binding to the lectin chaperones (Tannous et al., 2015b). If upon additional rounds of calnexin/calreticulin folding cycles the glycoproteins remain misfolded, they are then targeted for destruction (Figure 1.3). One way the ERQC machinery is able to distinguish between properly folded proteins from aberrantly folded glycoproteins is through the glycan composition they exhibit, or glycoform. Specifically, proteins that exhibit extensive demannosylation become poorer substrates for calnexin/calreticulin. This is especially true when the A-branch mannoses

have been removed resulting in a glycan that can no longer be reglucosylated (Figure 1.4).

The process of mannose trimming is suggested to function as a timer mechanism in which mannoses are removed slowly and sequentially from the glycans on misfolded proteins, reducing the amount of time remaining for the protein to fold with each mannose trimming event (Hebert and Molinari, 2012). However, the duration for which any given protein is allowed to fold is not a set timeframe and varies for each protein. Exactly what causes a protein to be deemed terminally misfolded remains undetermined but likely involves bearing a combination of hallmarks of misfolded proteins, such as exposing hydrophobic patches, unpaired Cys or mispaired disulfides, and extensive de-mannosylation.

Evidence linking de-mannosylation to protein destruction stems from a number of early studies into ER degradation. Glycan profiling of terminally misfolded proteins revealed extensively trimmed glycoforms ($Man_{7-5}GlcNAc_2$) (Ermonval et al., 2001; Frenkel et al., 2003). Experiments in which mannosidase inhibitors such as kifunensine (KIF) or 1-deoxymannojirimycin (DMJ) delayed the degradation of terminally misfolded substrates (Su et al., 1993). Likewise, exposure of the α1,6-linked mannoses (Figure 1.2), which occurs as a result of demannosylation of α1,2-linked mannoses on the B- and C-branch, may also serve as an protein destruction signal (Clerc et al., 2009; Hosokawa et al., 2001; Jakob et al., 2001; Nakatsukasa et al., 2001). Together, these results support the presence and function of a single or multiple α1,2 mannosidases in ERQC and ERAD.

12

In mammalian cells, the mannose-trimmed glycans on ERAD targeted polypeptides are recognized by the two mannose-6-phosphate receptor homology domain (MRH)-containing lectins, Os-9 and XTP3-B (Hosokawa et al., 2009; Cruciat et al., 2006; Groisman et al., 2011). Yos9p is the yeast OS-9 ortholog (Cormier et al., 2005). Thus, Os-9/Yos9p and XTP3-B are proposed to function as ERAD receptors that prepare and present the misfolded substrate to the retrotranslocation machinery. Os-9 and Yos9p possess a single MRH domain, and Yos9p also possesses a C-terminal ER retrieval and retention sequence that is absence in OS-9. Unlike Os-9, XTP3-B possesses two MRH domains, although only one is thought to actively bind mannose-trimmed glycans (Yamaguchi et al., 2010; Fujimori et al., 2013).

The role of Os-9/Yos9p in glycoprotein degradation through ERAD has been demonstrated through gene deletion studies that resulted in the stability of the misfolded mutant variants of carboxypeptidase yscY (CPY*) and α1-antitrypsin *Null* Hong Kong (NHK) (Jaenicke et al., 2011; Christianson et al., 2008; Bernasconi et al., 2008). However, no effects were observed for Os-9 on non-glycosylated substrates, although Yos9p appears to bind both glycosylated and non-glycosylated substrates (Jaenicke et al., 2011; Benitez et al., 2011). The carbohydrate binding affinity of Os-9/Yos9p for ERAD glycoforms is stronger than that of XTP3-B (Yamaguchi et al., 2010; Fujimori et al., 2013).

Unlike Os-9/Yos9p, the role of XTP3-B in ERAD is less obvious. Some studies propose that XTP3-B serves an opposing role to Os-9 and may function as a recognition unit for proteins that were accidentally targeted to ERAD, as it appeared to delay the

degradation of NHK bearing high mannose glycoforms (Fujimori et al., 2013). XTP3-B also interacted with and prevented the degradation of the non-glycosylated ERAD substrates transthyretin and NHK (Hosokawa et al., 2008; Christianson et al., 2008). It is postulated that XTP3-B prevents the degradation of non-glycosylated substrates by interacting with the translocation machinery component Sel1L, thereby delaying their degradation and allowing more time for the polypeptides to fold (van der Goot et al., 2018).

Os-9/Yos9p and XTP3-B deliver misfolded substrates to the ERAD translocation machinery through the mammalian membrane-bound adaptor protein Sel1L or yeast adaptor protein Hrd3p (Hampton et al., 1996; Mueller et al., 2006). Sel1L and Hrd3p possess multiple glycans and tetricopeptide repeats (TPRs), both of which mediate protein-protein interactions, specifically the C-terminal TPR clusters appear necessary for Os9/Yos9p and XTP3-B binding and the glycans are also involved in XTP3-B (Denic et al., 2006; Carvalho et al., 2006).

Once the misfolded substrates are localized to the ERAD retrotranslocation machinery they interact with ERAD E3 ligases such as the mammalian Hrd1 and yeast Hrd1p, and E2 ligases which tag them for degradation through ubiquitination (Carvalho et al., 2006; Christianson et al., 2008; Claessen et al., 2012; Denic et al., 2006; Neutzner et al., 2011). The ubiquitin-tagged substrates are dislocated from the ER with the help of an AAA-ATPase and once in the cytoplasm the substrates are de-glycosylated and sent to the cytoplasmic 26S proteasome (Wolf and Stolz, 2012; Saeki et al., 2009). ER-localized

mannosidases are proposed to play a critical role in creating the carbohydrate degradation signal that supports recognition by these ERAD receptors.

Mannosidases and Mannosidase-like proteins of the secretory pathway

ER resident mannosidases were first discovered from *Saccharomyces cerevisiae* genetic studies and were determined to trim N-linked glycans from $Man_9GlcNAc_2$ structures to $Man_8GlcNAc_2$ (Burke et al., 1996). The yeast Mns1p is a Type II ER membrane localized alpha1,2-mannosidase involved in glycan trimming and belongs to the Class I mannosidase CAZy glycosyl hydrolase (GH family 47 (Henrissat and Bairoch, 1996). Proteins belonging to the GH47 family share a conserved $(\alpha\alpha)_7$-barrel structure and catalytic residues (Karaveg et al., 2005; Mast and Moremen, 2006) (Figure 1.5). Mns1p was first implicated in ERAD as its overexpression accelerated the degradation of ERAD glycoproteins and its deletion had the opposite effect (Knop et al., 1996; Jakob et al., 1998, 2001) (Figure 1.5). Mns1p removes the terminal mannose of the B-branch, which is believed to be the first step required for generating the glycoforms exposing $\alpha1,6$-linked mannoses that are recognized by Yos9p and targeted for ERAD (Figure 1.2) (Jakob et al., 1998). Removing the terminal B-branch mannose also occurs on properly folded glycoproteins; however, the mannoses on ERAD bound glycoproteins are extensively trimmed in comparison. It is likely that the terminal mannose on the A-branch of the glycan is removed to prevent re-glucosylation of mature glycoproteins; however, the identity of mannosidase responsible for this trimming event is not known.

A mammalian ortholog of Mns1p was identified and named ER $\alpha1,2$-mannosidase 1 or ERman1 (Man1B1) (Figure 1.5). Searches into $Man_8ClcNAc_2$ glycan binding lectins

in mammalian cells revealed ERman1 as an ideal candidate as it was upregulated upon ER stress (Gonzalez et al., 1999). Like Mns1p, overexpression of ERman1 accelerated the degradation of the ERAD substrate NHK and glycan analysis of NHK isolated from these cells revealed an accumulation of $Man_8GlcNAc_2$ (Hosokawa et al., 2001). The mannosidase domain of ERman1 was expressed as a soluble recombinant protein and exhibited mannosidase activity toward the B-branch of $Man_9GlcNAc_2$ glycans. The catalytic activity of ERman1 was abolished upon treatment with the mannosidase inhibitors kifunensine and 1-deoxymannojirimycin (Tremblay and Herscovics, 1999).

ERman1 like its yeast ortholog is a type II membrane protein; however, its cellular localization is under debate. Golgi co-localization indicate that it may reside in the Golgi as an O-glycosylated protein, and its amino acid sequence, although similar to the ER localized Mns1p, is homologous to the Golgi α1,2-mannosidases (Tremblay and Herscovics, 1999; Pan et al., 2011; Iannotti et al., 2014). Golgi localization of ERman1 is further supported from data indicating that it interacts with the protein γ-COPI, a member of the Golgi-ER retrograde transport complex, to enhance the degradation of NHK (Pan et al., 2013). ERman1 is proposed to interact with γ-COPI to retrieve ERAD substrates that evaded the ERQC machinery.

The mammalian Golgi is equipped with multiple α1,2-mannosidases belonging to the Class I GH47 family as well as Class II mannosidases belonging to the GH38 family mannosidases; which possesses different catalytic properties (Henrissat, 1991; Moremen et al., 1994; Daniel et al., 1994). The GH47 family Golgi mannosidases is comprised of α mannosidase class IA (Man1a1 and Man1a2), class IB (Man1b1 or ERman1) and class

16

IC (Man1c1) (Herscovics, 2001).Man1a1/a2/b1/c1 are type II transmembrane proteins that expose a short cytoplasmic facing tail and a conserved Golgi localized mannosidase domain, which requires a calcium ion for catalytic activity (Herscovics et al., 1994; Lal et al., 1994). Like other members of the GH47 family, the Golgi class 1 α mannosidases are inhibited by the inhibitors kifunensine and deoxymannojirimycin (Lal et al., 1994).

The catalytic activity of mouse Golgi mannosidases was determined using purified recombinant proteins and glycan components. These studies revealed that the mannosidases exhibit similarities and redundancies in their trimmed glycan products although the glycoforms generated and their substrate specificities are not identical (Tulsiani and Touster, 1988; Bause et al., 1992; Lal et al., 1998).

A homolog of Mns1p was also identified in yeast and termed Htm1p (also known as Mnl1p) (Jakob et al., 2001) (Figure 1.5). Although Htm1p was originally thought to lack mannosidase activity and thus believed to function as a lectin, it was later determined to possess hydrolytic activity (Jakob et al., 2001; Quan et al., 2008; Clerc et al., 2009; Liu et al., 2016). Specifically, $Man_8ClcNAc_2$ glycans are further demannosylated by Htm1p on the C-branch, which exposes the ERAD signal α1,6-linked mannoses (Quan et al, 2008; Clerc et al., 2009).

Htm1p mannosidase activity is coupled to its association with the oxidoreductase Pdi1p as a mutation on Pdi1p that abolished complex formation between the two proteins resulted in less $Man_7GlcNAc_2$ glycoforms and delayed the degradation of CPY[*] (Gauss et al., 2011). Furthermore, Htm1p in complex with Pdi1p is able to distinguish between proteins that are misfolded from those that have reached their native folds (Liu et al.,

17

2016). This substrate selectivity and mannosidase activity is attributed to a disulfide on Htm1p that is introduced by Pdi1p (Sakoh-Nakatogawa et al., 2009).

The proposed function of EDEM1 and EDEMs in ERAD

The search and discovery of ERman1 revealed an Htm1p mammalian ortholog, the stress-induced mammalian putative mannosidase, ER degradation-enhancing mannosidase-like protein 1, or EDEM1 (Hosokawa et al., 2001) (Figure 1.5). Two additional ER mannosidase-like proteins are present in the mammalian ER, but are absent in the yeast ER, EDEM2 and EDEM3, which share a conserved mannosidase-like domain with EDEM1 and are both ER-stress induced and proposed to function in ERAD (Olivari et al., 2005; Hirao et al., 2006) (Figure 1.5).

Although EDEM1 accelerates the degradation of the ERAD substrates and misfolded variants of α1-antitrypsin, β-secretase, cystic fibrosis transmembrane conductance regulator, rhodopsin and the asialoglycoprotein receptor when overexpressed and delay their degradation upon knockdown or knockout, the role of EDEM1 in ERAD is not completely understood (Gnann et al., 2004; Hosokawa et al., 2001; Kosmaoglou et al., 2009; Molinari et al., 2003; Ninagawa et al., 2015; Shenkman et al., 2013). For instance, early studies suggested EDEM1 was a catalytically inactive mannosidase with lectin-like functions as evidenced by a lack of demannosylation of [^{3}H]-Man$_9$GlcNAc substrate by EDEM1-IgG immobilized beads (Hosokawa et al., 2001).

As a lectin, EDEM1 was proposed to recognize misfolded substrates through the composition of their glycans, specifically the Man$_8$GlcNAc$_2$ glycoform, and subsequently

18

deliver them to the retrotranslocon (Hosokawa et al., 2010). However, later studies showed that EDEM1 promoted glycan trimming on misfolded glycoproteins. Overexpression of EDEM1 increased the SDS-PAGE mobility of the ERAD substrates NHK and BACE457 compared to when the proposed catalytically inactive EDEM1 mutant E220Q is overexpressed or in non-transfected cells (Olivari et al., 2006). Similarly, Hosokawa and colleagues showed an accumulation of $[^3\text{H}]$-Man$_{8\text{-}6}$GlcNAc$_2$ in cell lysates in which EDEM1 was overexpressed, providing further evidence of mannosidase activity (Hosokawa et al., 2010). However, direct evidence that EDEM1 itself contributes to glycan trimming using purified components is lacking.

Like EDEM1, EDEM2 was originally thought to lack mannosidase activity as EDEM2 isolated from mammalian cell lysates appeared to be inactive (Mast et al., 2005). Later it was determined that RNAi silencing of EDEM2 resulted in the accumulation of untrimmed glycoforms on ERAD substrates, which implicated a role for EDEM2 in the early stages of mannose trimming and labelling terminally misfolded proteins for ERAD (Ninagawa et al., 2014).

Although EDEM2 contributed to glycan demannosylation and generated the Man-$_8$GlcNAc$_2$ glycoform, which likely results from trimming of the terminal mannose of the B-branch *in vivo*, an *in vitro* mannosidase assay showed that purified EDEM2 did not possess mannosidase activity (Ninagawa et al., 2014; Olivari et al., 2005). This disparity could be attributed to the absence of EDEM2 binding partners in the *in vitro* study. It is likely that EDEM2, like Htm1p, requires a binding partner in order to function. Furthermore, EDEM2 lacks an ER retention sequence but appears to reside in the ER. It

is possible that EDEM2 interacts with ER-resident binding partners in order to remain and function in the ER.

EDEM3 is the largest member of the EDEM protein family, as it possesses an uncharacterized region C-terminal of the mannosidase-like domain, which is approximately equal in length to the mannosidase-like domain. Structural homology analysis predicts a protease-associated (PA) domain of unknown function, which is located within this region. The PA domain is predicted to be similar in structure to the PA domain of the E3 ubiquitin-protein ligase RNF128 (Anandasabapathy et al., 2003). The role of the PA domain in ERAD or other functions has yet to be assessed.

The KDEL sequence located at the C-terminus of EDEM3 allows its ER retrieval and retention. Glycans released from EDEM3 knockout cell lysates were subjected to HPLC analysis and were identified as Man_8-B glycoforms, indicating that in this experiment EDEM3, like EDEM1, acts after the Man_8-B glycoform is generated on the ERAD substrate (Ninagawa et al., 2014). Thus, EDEM3 is postulated to generate the Man_8-C glycoform which results in the exposure of α1,6-linked mannose that is required for ERAD lectin binding (Ninagawa et al., 2014).

The substrate binding properties of EDEM1

The mannosidase-like domain of EDEM1 makes up nearly 70% of the protein; however, there is still uncertainty as to whether this domain is required for ERAD of misfolded secretory proteins. It is required for interacting with SEL1L, a member of the ERAD machinery, as this interaction was abolished upon treatment with the mannosidase

inhibitor kifunensine (KIF) and mutation of the putative catalytic residues (Cormier et al., 2009; Saeed et al., 2011). However, the same study showed that abolishing the putative mannosidase activity of EDEM1 or its potential carbohydrate-binding properties did not affect the interaction between EDEM1 and the substrate NHK as this association was shown to be glycan-independent, indicating that EDEM1 substrate binding and machinery binding involves different components (Cormier et al., 2009).

Similarly, exogenously expressed EDEM1 was shown to associate with and accelerate the degradation of other non-glycosylated substrates; a non-glycosylated version of H2a, the precursor of asialoglycoprotein receptor, and the non-glycosylated protein non-secreted-1 (NS-1) kappa light chain, all of which undergo EDEM1-dependent degradation (Shenkman et al., 2013). Although these results suggest that the substrate-binding properties of EDEM1 reside outside the mannosidase-like domain, other data indicate contrary results. For instance, EDEM1 no longer interacted with the ERAD substrate BACE457 upon removing its glycans (Molinari et al., 2003).

EDEM1 was determined to possess an intrinsically disordered region (IDR) located at the N-terminus (Marin et al., 2012). EDEM1 lacking its IDR no longer associated with a soluble truncation of tyrosinase and surprisingly binding of this N-terminal truncation to Sel1L was observed; however, its function is unknown (Marin et al., 2012). Similarly, an EDEM1 N-terminal truncation that occluded the majority of the mannosidase-like domain was sufficient to bind H2a, although at the time this was not attributed to the IDR (Shenkman et al., 2013). In addition to the mannosidase-like domain and the IDR, it appears that hydrophobic interactions are likely involved in mediating

EDEM1-BACE457 binding (Sokołowska et al., 2015). Taken together, these results illustrate that the modes of interaction involved between EDEM1 and either ERAD substrates or ERQC machinery is specific to each protein's requirements.

Conclusions

Although much is known about the key players and major events involved in ERAD and ERQC many details remain elusive to this day. The connection between ERAD and glycan-trimming is clear, however the role of each mannosidase, which in many cases appears overlapping is less so. EDEM1 is an enigmatic protein and efforts to determine whether EDEM1 truly possesses catalytic activity have been hindered by the presence of numerous ER and Golgi α1,2-mannosidases and by the inability to isolate and purify EDEM1 for downstream *in vitro* biochemical analyses. Likewise, difficulties in determining the binding properties of EDEM1 is compounded by the fact that multiple modes of interactions are employed and each appear binding partner- and ERAD substrate-specific. EDEM1 has to be fully characterized before we can address its true role in ERAD and ERQC.

The present work examines novel EDEM1 substrate-binding requirements that were identified in cells using lysis detergents of varying strengths. EDEM1 exhibited bipartite binding properties toward the same substrate, NHK, depending on the detergent strength. A redox-sensitive binding interaction was identified from this study and required the presence of a Cys residue on NHK. Additionally, the EDEM1 mannosidase-like domain was successfully expressed in cells and its *in vivo* properties were characterized and it was determined to promote glycan trimming and the redox sensitivity

binding property was maintained. Since the mannosidase like domain is functional, purifying it alone will be a powerful tool to properly study the *in vitro* enzymatic properties of EDEM1. Lastly, a second IDR was identified on EDEM1 and contributed to its rapid turnover. Both IDRs are involved in mediating the EDEM1-ERdj5 interaction.
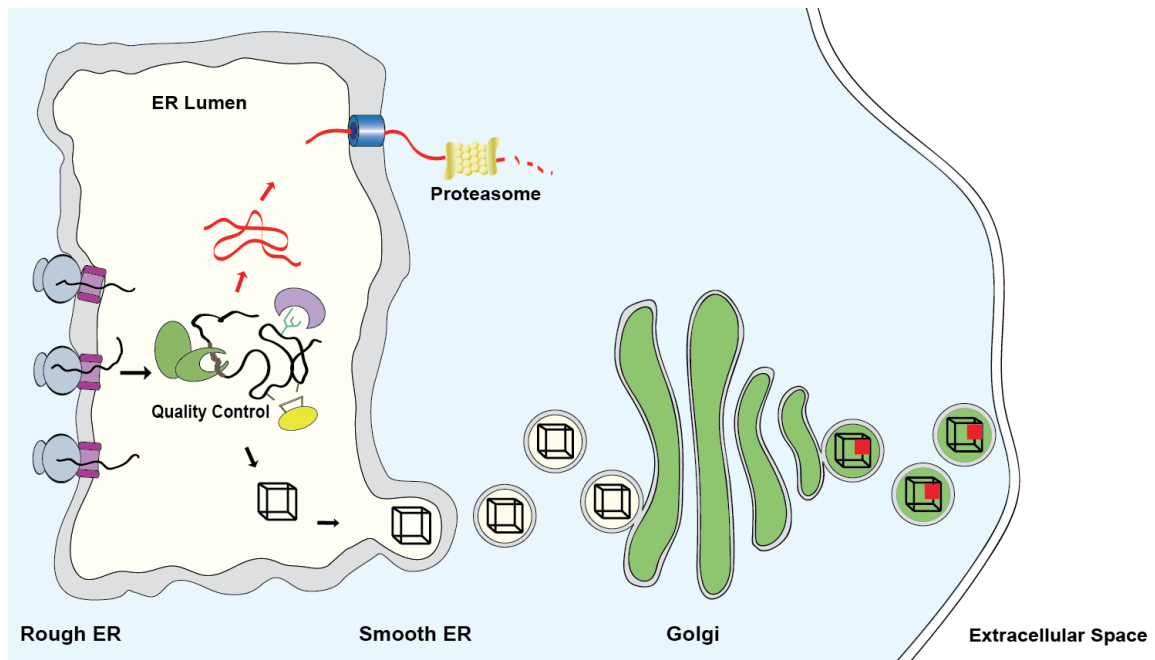
Figure 1.1 Secretory protein trafficking

Secretory polypeptides are co-translationally translocated into the ribosome-studded endoplasmic reticulum (Rough ER). Once inside the ER lumen, the polypeptides engage the ER quality control (ERQC) machinery, which is composed of molecular chaperones (green), redox enzymes (yellow), and glycan modifying enzymes (purple). The ERQC assists in protein folding and possess the ability to differentiate between mature, properly folded proteins (black cube) from terminally misfolded proteins (red). The mature proteins are allowed to exit the ER through vesicles of the smooth ER and are transported to the Golgi where they acquire further modifications that include additional assembly processes, and glycan modification. The mature proteins are then sorted to their final destination. Proteins that are terminally misfolded (red) are extracted from futile folding cycles and targeted for degradation by the proteasome.

Figure 1.2   Structure
of N-linked glycan

N-linked glycans are transferred *en bloc* to asparagine residues in the sequon Asn-X-Ser/Thr, where X denotes any amino acid except for Pro. The precursor structure is composed of three glucoses (blue circles), nine mannoses (green circles) and two N-acetylglucosamines (blue squares). Glycosidic bonds are noted. (Lamriben et al., 2016)
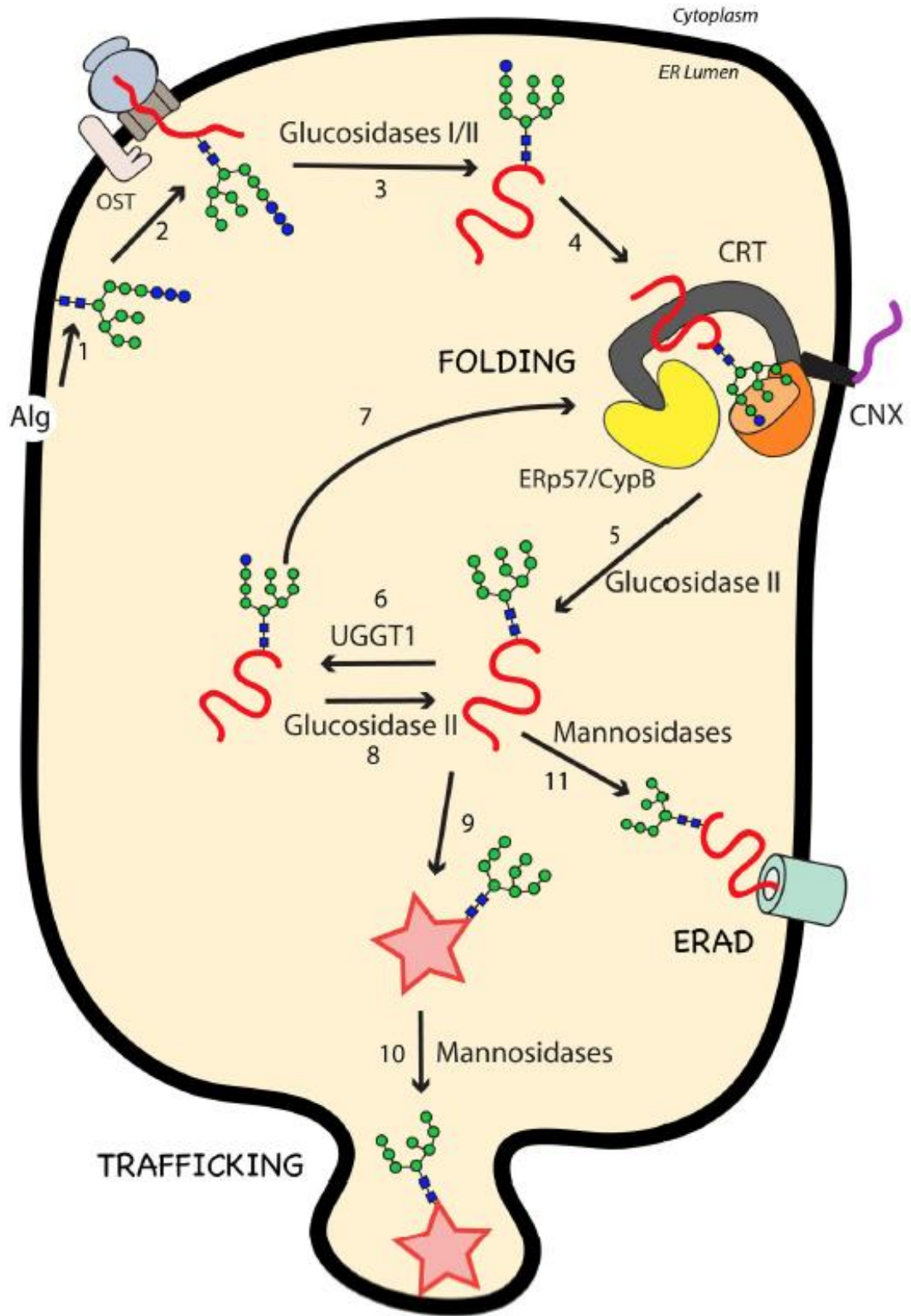
Figure 1.3 Processing of N-linked glycans and folding pathway of secretory glycoproteins in the Endoplasmic Reticulum

N-linked glycans, assembled by *Alg* gene protein products (1), are transferred via the OST complex to proteins translocated into the ER lumen (2). Glucosidases I and II trim the first two glucoses (blue circles) from the glycan (3), generating a monoglucosylated glycoform, which is a substrate for calnexin (CNX) and calreticulin (CRT) (4). Trimming of the remaining glucose by glucosidase II releases the substrate from CNX/CRT (5). Glycoproteins that do not reach their native folded state can be reglucosylated by UGGT1 (6), redirecting them to CNX/CRT binding (7) or trimming by glucosidase II (8). Glycoproteins that have reached their native state (star) (9) are trimmed by mannosidases and directed for trafficking out of the ER (10). Proteins that are terminally misfolded are trimmed by mannosidases and directed for ERAD (11). (Lamriben et al., 2016)
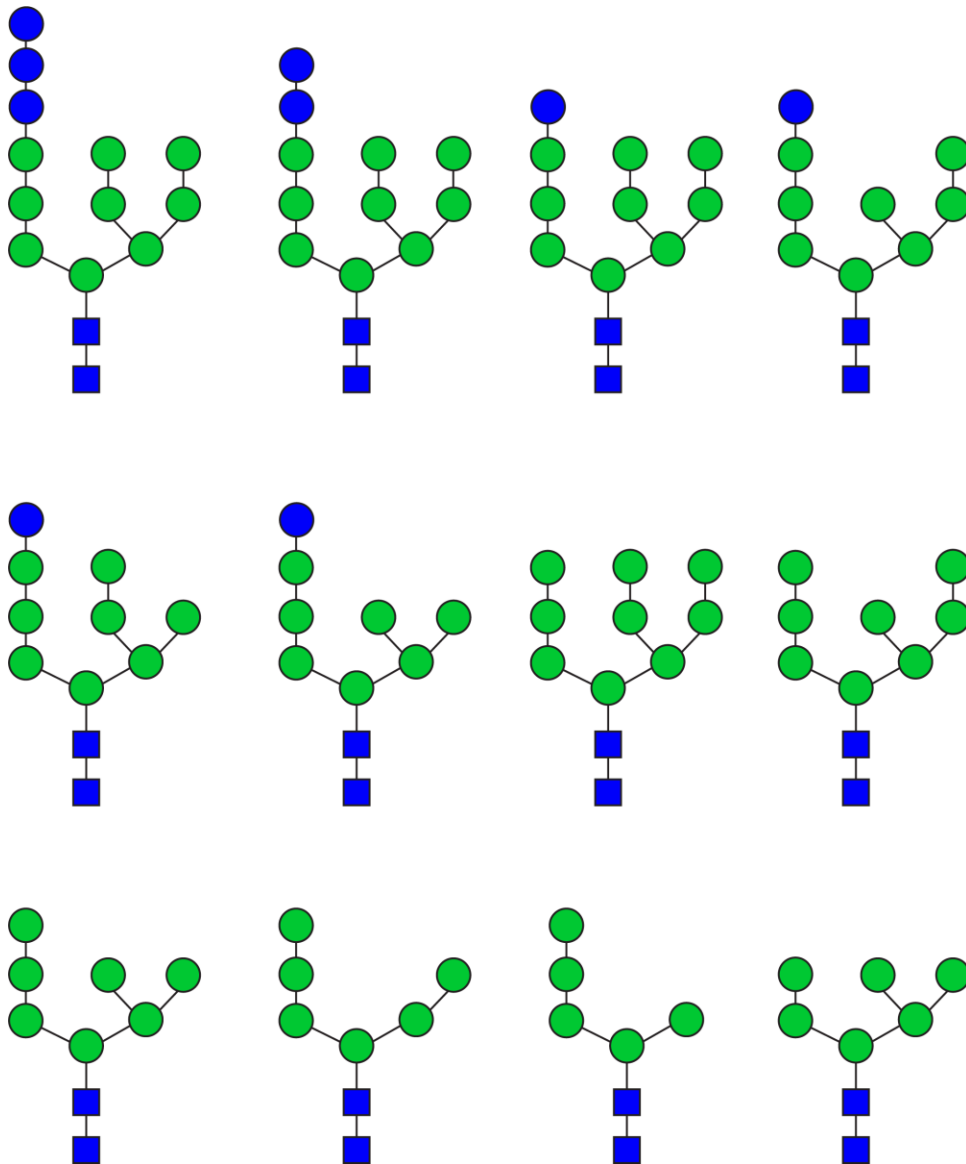
Figure 1.4 Glycoforms of the endoplasmic reticulum

N-linked glycans are processed in the ER through many trimming events that remove glucoses or mannoses depending on the processing enzyme. N-linked glycans exhibiting glucoses (blue circles) are found on newly synthesized polypeptides or on proteins that are undergoing folding. High mannose (green circles) content glycans consisting of 9-7 mannoses are present on mature proteins. Glycans possessing fewer mannoses (7 or less) are typically found on misfolded, ERAD targeted substrates.

Glycosylhydrolase 47 Family Protein Domain
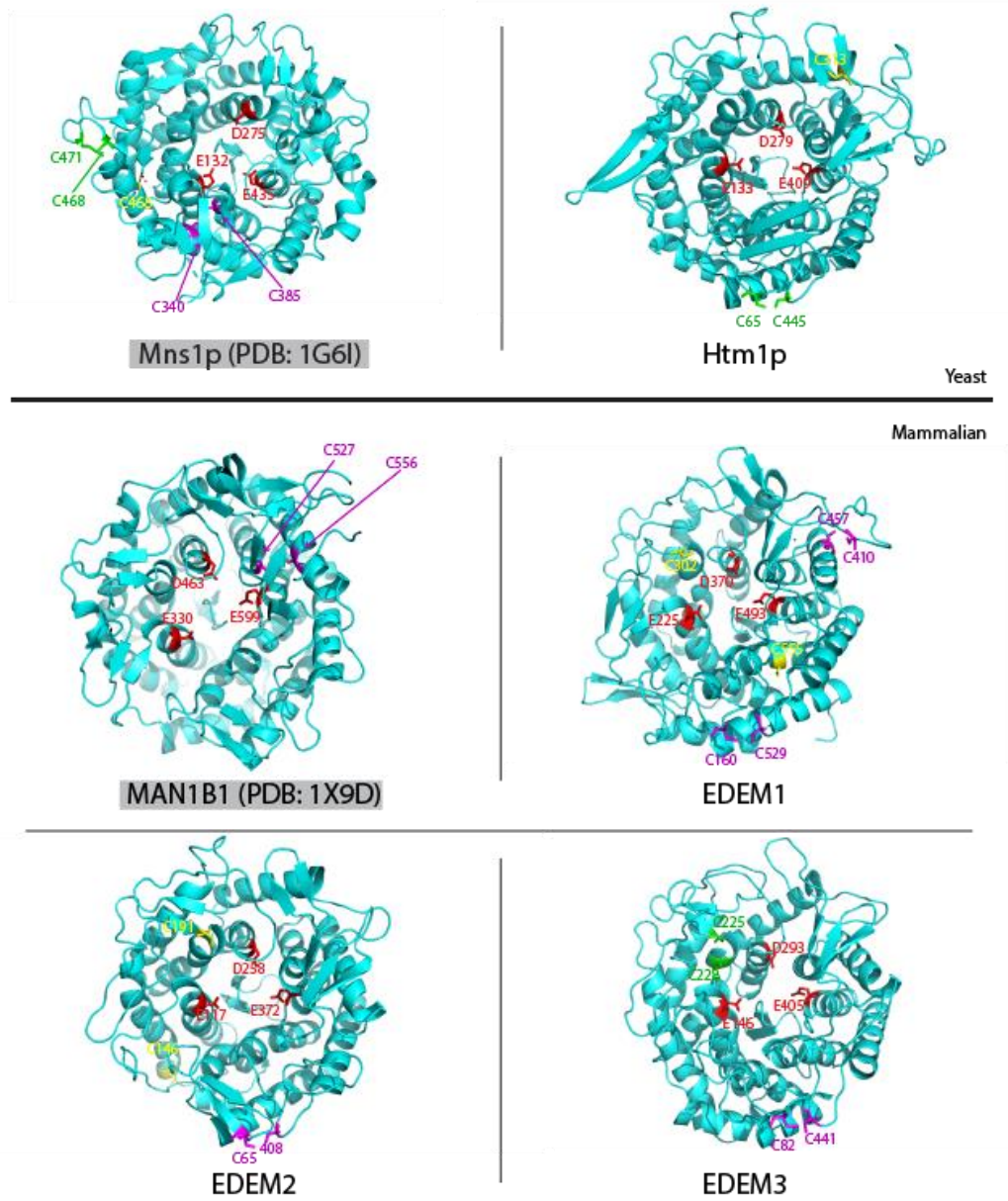
Figure 1.5 GH47 family proteins members of the yeast and mammalian ER

The solved and predicted structures of selected Glycosylhydrolase 47 Family Protein domains. Structural predictions of the Htm1p and EDEM1-3 mannosidase-like domains were generated through the PHYRE2 Protein Fold Recognition Server. The conserved putative mannosidase acidic residues located at the core of the $(\alpha\alpha)_7$-barrel structure are labeled in red. Cysteines that are in close proximity and may form disulfide linkages are labeled in magenta. Cysteines that appear free are labeled in yellow and those that exist as a Cys-X-X-Cys motif are labeled in green.

CHAPTER 2

METHODS AND EXPERIMENTAL PROCEDURES

Reagents

Dulbecco's modified Eagle's medium (DMEM) minimum essential media alpha (αMEM), fetal bovine serum (FBS), penicillin and streptomycin (P/S) were purchased from Invitrogen. Endo H, PNGase F, and all cloning reagents were acquired from New England Biolabs. Human embryonic kidney (HEK) 293 cells were purchased from ATCC (Lot#: 6322631) and HEK293A from Invitrogen (Lot#1806222). Cells were authenticated by universal mycoplasma detection kit (Cat. No. 30-1012K, ATCC). $[^{35}S]$-Met/Cys was acquired from PerkinElmer. Protein A Sepharose 4B was from GE Healthcare. Methoxypolyethelene glycol maleimide was purchased from Sigma-Aldrich (Cat. No. 63187). The following antibodies were used: αFLAG (Cat. No. F3165, Sigma), αA1AT (Cat. No. A0012, Dako), αMYC (Cat. No. 9B11, Cell Signaling), and αGlucosidase II (Cat. No. PA5-21431, Thermo Fisher). The following C-terminally tagged EDEM1 truncations were generated by PCR amplification and subcloned into p3XFLAG-CMV-14 (Addgene): EDEM1 IDR-ΔN (Δ48-119), EDEM1 IDR-ΔC (Δ 583-652), and EDEM1 MLD (Δ48-119 and Δ 583-652). EDEM3-MYCFLAG was purchased from Origene Technologies (Cat. No. RC222885). Transfections were carried out with polyethyleneimine "MAX" (PEI) (Cat. No. 24765, Polysciences, Inc.).

Cell culture and Transfections

HEK293T, HEK293A and CHO (KO man1a1/1a2/1b1/1c1) cell were cultured in DMEM (for HEK) and αMEM supplemented with 10% (FBS) and 100 U/ml penicillin and 100 mg/ml streptomycin at 37°C in 5% CO_2. Transfections were carried out using PEI at a ratio of 1:3 (PEI (ug): DNA (ug)) for all transient transfections except in the immunofluorescent microscopy assay for which Lipofectamin 2000 was used at a 1:2 ratio (Lipofectamine (ug): DNA (ug)).

Protein Radiolabeling and pulse chase analysis

HEK293 or CHO (KO man1a1/1a2/1b1/1c1) cells were grown in 35 or 60 mm dishes where indicated and all transfections were carried out for 18 h in DMEM (or MEM for CHO cells) supplemented with 10% FBS and 1% P/S and incubated at 37°C in 5% CO_2. Cells were lysed on ice with either CHAPS buffer (2% 3-[(3-cholamidopropyl) dimethylammonio]-1-propanesulfonate in 50 mM 4-(2-hydroxyethyl)-1-piperazineethanesulfonic acid and 200 mM NaCl, pH 7.5 (HBS)), or with MNT buffer (0.5% Triton X-100, 20mM MES, 100 mM NaCl, 20 mM Tris-HCl (pH 7.5)). The post-nuclear supernatant was isolated by centrifugation followed by pre-clearing with unbound protein-A Sepharose beads, and subsequent incubation with the corresponding antibody and Sepharose beads overnight. Immunopellets were isolated and washed with 0.5% CHAPS in HBS or Connie's wash buffer (100 mM Tris-HCl, 300 mM NaCl, 0.1% SDS, 0.05% Triton X-100 (pH 8.6)) where indicated. Proteins were eluted from beads with reducing sample buffer, followed by SDS-PAGE. Radiolabled samples were visualized

using phosphorimaging (FLA-500; Fujifilm) and quantified using ImageQuant TL 1D gel analysis software (GE Healthcare Life Science).

Sequential immunoprecipitation

Immunopellets were washed with 0.5% CHAPS in HBS or Connie's wash buffer (100 mM Tris-HCl, 300 mM NaCl, 0.1% SDS, 0.05% Triton X-100 (pH 8.6)) and eluted from beads with reducing sample buffer. When followed by a second immunoprecipitation, samples were eluted with 1% SDS in 10 mM Tris, pH 7.5, and 150 mM NaCl at 100°C and quenched with excess 2% CHAPS in HBS, followed by incubation with the corresponding antibody and Sepharose beads overnight and washing with 0.5% CHAPS in HBS or Connie's wash buffer where indicated.

In vivo reactive thiol analysis

HEK293T cells were transfected with EDEM1 constructs and incubated overnight. The next day (~20 h later), a subset of the samples were pretreated with 5 mM DTT for 1 hr. Cells were lysed with sample buffer (30 mM Tris pH 6.8, 9% SDS, 15% glycerol) containing 5 mM Peg maleimide or 20 mM NEM. Lysates were incubated for 1 hr. Step-by-step protocol is published in Current Protocols Protein Science (Braakman et al., 2017).

Immunoblotting and imaging

HEK293T cells were grown in 35 or 60 mm dishes and all transfections were carried out for 18 h in DMEM supplemented with 10% FBS and 1% P/S and incubated at 37°C in 5% CO_2. Cells were lysed on ice with either CHAPS buffer (2% 3-[(3-

cholamidopropyl) dimethylammonio]-1-propanesulfonate in 50 mM 4-(2-hydroxyethyl)-1-piperazineethanesulfonic acid and 200 mM NaCl, pH 7.5 (HBS)), or with MNT buffer (0.5% Triton X-100, 20mM MES, 100 mM NaCl, 20 mM Tris-HCl (pH 7.5)). The post-nuclear supernatant (PNS) was isolated by centrifugation followed by pre-clearing with unbound protein-A Sepharose beads, and subsequent incubation with the corresponding antibody and Sepharose beads overnight. A fraction of the PNS (10%) was treated with 10% trichloroacetic acid to collect the whole cell lysate, where indicated. Immunopellets were isolated and washed with 0.5% CHAPS in HBS or Connie's wash buffer (100 mM Tris-HCl, 300 mM NaCl, 0.1% SDS, 0.05% Triton X-100 (pH 8.6)), where indicated. Proteins were either subjected to glycosidase digestion (following New England Biolabs protocol) (where indicated) or eluted from beads with reducing sample buffer, followed by SDS-PAGE. Proteins were transferred onto nitrocellulose membrane (LI-COR, Inc.) and blocked in 1X PBS containing 5% Milk and 2% bovine serum albumin. Membranes were blocked overnight at 4°C, followed by an over night incubation with primary antibody at 4°C. LI-COR IRDye fluorescent secondary antibodies were used for detection at 1:10,000 dilution. Blots were imaged and analyzed using the Odyssey Sa imaging system (LI-COR, Inc).

CRISPR/Cas9 targeted KO man1a1/1a2/1b1/1c1 in CHO cells.

Clustered Regularly Interspaced Short Palindromic Repeats/CRISPR-associated protein 9 (CRISPR/Cas9) system was used for gene knockout (KO) in CHO cells as described preciously (Schulz et al., 2018). CHOZN GS$^{-/-}$ cells with stable expression of human alpha-galactosidase A were used as parental clone for KO *man1a1/1a2/1b1/1c1*.

Cells were maintained as suspension cultures in EX-CELL CHO CD Fusion serum-free media (Cat. No. 14365C, Sigma) in 50 mL TPP TubeSpin® and incubated at 37°C and 5% CO_2. Cells were seeded at 0.5×10^6 cells/mL in T25 flask (NUNC, Denmark) one day prior to transfection. Electroporation was conducted with $2x10^6$ cells with a DNA mixture of 1 µg of Cas9-GFP plasmid and 1µg of gRNA plasmid (U6GRNA, Addgene Plasmid #68370) using Amaxa kit V and program U24 with Amaxa Nucleofector 2B (Lonza, Switzerland). 48 hrs after nucleofection the 10-15% highest GFP expression pool of cells were enriched by FACS, and after 1 week cultured cells were single cell sorted by FACS into 96-wells. Gene disruption was identified by Indel Detection by Amplicon Analysis (IDAA) as described (Yang et al., 2015) and was further verified by Sanger sequencing

Immunofluorescent microscopy

HEK293A cells were transfected with indicated EDEM1 constructs and incubated for 24 hr at 37°C and 5% CO_2. Transfected cells were fixed with 3.7% paraformaldehyde in 1X phosphate-buffered saline (PBS) for 15 min at room temperature followed by permeabilization with 0.1% Triton X-100 in 1X PBS for 30 min at room temperature. Slides were rinsed in 1X PBS followed by blocking with 10% fetal bovine serum in 1X PBS for 30 min at room temperature. Cells were rinsed and stained with the indicated primary antibody solution at a 1:200 dilution factor followed by staining with the respective Alexa Fluor 488 or 594 secondary antibodies at a 1:400 dilution factor in blocking buffer. Cells were rinsed and mounted onto coverslips pretreated with VectaShield (Vector Laboratories). Images were acquired using $A1^+/A1R^+$ confocal

microscope (Nikon). The microscopy data was gathered in the Light Microscopy Facility and Nikon Center of Excellence at the Institute for Applied Life Sciences, UMass Amherst with support from the Massachusetts Life Science Center.

Sucrose gradient centrifugation

HEK293T cells were transfected with EDEM1 MLD and incubated for 48 hr. DTT was added to appropriate samples at (5 mM) for 1 hr prior to lysis in MNT buffer. The post-nuclear supernatant was layered atop a continuous 10-40% sucrose gradient in MNT buffer. The gradients were centrifuged for 18 hr at 4 °C with a Beckman SW41 at 38,000 rpm. After centrifugation, 8.5% of total gradient volume was collected per fraction, and proteins were isolated by trichloroacetic acid precipitation. Samples were resuspended in reducing sample buffer and analyzed by immunoblotting with the anti-FLAG antisera. The pellet was processed by adding sample buffer directly to the ultracentrifugation tube, after the last fraction was collected.

Alkaline extraction

Alkaline extraction was performed as previously described (Tamura et al., 2011). HEK293T cells expressing EDEM1 and IDR constructs were resuspended in homogenization buffer (20 mM HEPES, pH 7.5, 5 mM KCl, 120 mM NaCl, 1 mM EDTA, and 0.3 M sucrose) on ice and passed through a 22-gauge needle 20 times. All subsequent steps were conducted at 4 0C. The homogenate was centrifuged at 1,000 g for 10 min to pellet the nuclear fraction. The post nuclear fraction was centrifuged for 10 min at 45,000 rpm in a Beckman rotor (TLA 120.2) to separate the cytosol (supernatant) from

35

the cellular membranes (pellet). The cellular membrane fraction was resuspended in homogenization buffer, and a portion of the resuspended membranes was incubated with 0.1M Na2CO3 (pH 11.5) for 30 min on ice. The alkaline extracted portion was centrifuged at 65,000 rpm for 20 min through a sucrose cushion (50 mM triethanolamine, 0.3 M sucrose, pH 7.5) to separate soluble proteins from membrane proteins in the supernatant and pellet, respectively. The pH was adjusted in the alkaline extracted sample with 1M Tris-HCl (pH 7.5). Proteins were isolated by trichloroacetic acid precipitation. Samples were resuspended in reducing sample buffer and analyzed by immunoblotting with the anti-FLAG antisera

CHAPTER 3

EDEM1 MANNOSIDASE-LIKE DOMAIN BINDS ERAD CLIENTS IN A REDOX-SENSITIVE MANNER AND POSSESSES CATALYTIC ACTIVITY

Abstract

The endoplasmic reticulum (ER) degradation-enhancing α-mannosidase-like 1 protein (EDEM1) is a quality control factor that was initially proposed to recognize N-linked glycans on misfolded proteins through its mannosidase-like domain (MLD). However, recent studies have demonstrated that EDEM1 binds to some misfolded proteins in a glycan-independent manner. In this study, we have identified a thiol-dependent substrate interaction between EDEM1 and the α-1 Antitrypsin ERAD clients, Z and NHK, specifically though the single Cys residue on Z/NHK (Cys256), under stringent detergent conditions. In addition to the thiol-dependent interaction, the presence of weaker protein-protein interactions was confirmed, suggestive of bipartite client binding properties. Reactive thiols on EDEM1 (~4) were identified and are not directly responsible for the observed EDEM1 redox-sensitive binding. Moreover, a construct comprised of the EDEM1 MLD was expressed and its thiol-dependent binding properties were observed along with its active glycan-trimming properties. Lastly, an additional intrinsically disordered region (IDR) located at the C-terminus of EDEM1 was identified in addition to the previously identified N-terminal IDR and it was determined that either IDR is required for binding to ERdj5 as an interaction with ERdj5 was not recovered with the MLD alone. Together, our findings indicate that EDEM1 employs different binding modalities to interact with ERAD clients and ER quality control (ERQC) machinery

machinery partners and some of these properties are shared with its homologues EDEM2 and EDEM3.

Introduction

In the ER lumen, nascent polypeptides gain access to an array of molecular chaperones and foldases such as BiP, lectin molecular chaperones such as calnexin (CNX) and calreticulin (CRT), and oxidoreductases like PDI and ERp57, all of which comprise part of the ERQC machinery (Appenzeller-Herzog and Ellgaard, 2008; Lamriben et al., 2016; Parodi et al., 2015; Tannous et al., 2015b). The ERQC attempts to fold and rescue aberrantly folded proteins by protecting exposed hydrophobic regions (BiP), binding to N-linked glycans (CNX and CRT), and catalyzing the formation of the correct disulfide bonds (PDI, ERp57 etc.).

Terminally misfolded proteins are extracted from futile folding cycles, prevented from re-engaging the ERQC machinery and ultimately targeted for degradation via the ER-Associated Degradation (ERAD) pathway (Nakatsukasa and Brodsky, 2008; Hebert and Molinari, 2007). Numerous ERAD components have previously been characterized that recognize exposed hydrophobic regions, mispaired disulfide bonds, or specific N-linked glycan structures. For instance, mannosidases contribute to the extensive glycan trimming that occurs on ERAD-bound clients, and oxidoreductases are proposed to facilitate retrotranslocation by unfolding and reducing ERAD clients to make them translocation competent (Ermonval et al., 2001; Frenkel et al., 2003; Ushioda et al., 2008).

The ER Degradation Enhancing Mannosidase-Like protein-1 (EDEM1) has been proposed to select and sequester terminally misfolded proteins away from productive folding cycles and target them for degradation as evidenced by its preferential interaction with misfolded ERAD clients, direct interaction with ERAD machinery components such as Sel1L and ERdj5, and acceleration of the degradation of misfolded clients when overexpressed (Cormier et al., 2009; Hosokawa et al., 2001; Molinari et al., 2003; Oda et al., 2003; Kosmaoglou et al., 2009).

Although EDEM1 and its role in ERAD has been extensively studied and characterized since its discovery in 2001 (Hosokawa et al., 2001; Oda et al., 2003), much of the protein's properties remain enigmatic. For instance, early EDEM1 studies suggested that EDEM1 lacked mannosidase activity although it shares a mannosidase-like domain similar to that of the active ER mannosidase, Man1b1 (ER ManI) (Hosokawa et al., 2001). However, several groups have demonstrated contradictory cellular findings showing EDEM1 has weak mannosidase activity (Hosokawa et al., 2010; Ninagawa et al., 2014; Olivari et al., 2006). Additionally, attempts to ascertain on which glycan branch EDEM1 acts have been conducted by determining the glycan profile of cells in which EDEM1 was overexpressed or knocked out, but *in vitro* analyses using recombinant EDEM1 or its MLD are lacking, likely due to difficulty in expressing recombinant EDEM1 and its MLD (Ninagawa et al., 2015, 2014).

EDEM1 has been implicated to play a role in ERAD and function in the ER lumen; however, how the protein is retained in the ER lumen remains undetermined. EDEM1 exhibits dual topology as a result of inefficient cleavage of its signal peptide,

39

which yields a membrane-bound protein that is able to act on membrane-associated ERAD clients (Tamura et al., 2011). However, EDEM1 also exists as a soluble luminal protein that remains in the ER while lacking a known ER retention/retrieval sequence. EDEM1 interacts with numerous ER-localized binding partners and is proposed to exist in a multiprotein complex; which may mediate its ER retention, although this has yet to be shown.

The client- or machinery-binding properties of EDEM1 appear multifaceted and specific to each binding-partner. For instance, the Lederkremer group showed that N-terminal truncation of EDEM1 possessing a portion of the MLD is sufficient for binding to H2a (Shenkman et al., 2013). Petrescu and colleagues identified an N-terminal IDR that is required for interaction with a unnatural soluble form of tyrosinase, further supporting the nonessential role of the MLD in the interaction between EDEM1 and H2a or soluble tyrosinase (Marin et al., 2012). Likewise, the role of glycans in EDEM1 client binding is perplexing and appears substrate-specific, as in some cases (NHK, H2a, and SHH) interactions with EDEM1 were independent of substrate glycosylation; however, in other cases glycans appeared required (BACE457) (Cormier et al., 2009; Molinari et al., 2003; Shenkman et al., 2013; Tang et al., 2014). Interactions between EDEM1 and ER machinery binding partners have been reported and characterized, most notably being that the EDEM1 MLD was involved in the interaction with Sel1L, as mutating the putative catalytic triad or using mannosidase inhibitors abolished this interaction (Cormier et al., 2009; Saeed et al., 2011).

Combined, these results illustrate a much more complex binding landscape of EDEM1 that involves distinct protein-dependent modes of interactions. In this study, we have identified bimodal interactions between EDEM1 and the α1-antitrypsin (A1AT) disease-associated and ERAD variants Z and NHK. The interactions between EDEM1 and Z/NHK involve covalent and weaker protein-protein interactions that were identified under different detergent conditions. We also provided evidence that the MLD of EDEM1 possesses glycosidase activity. Altogether, these findings broaden the scope of the EDEM substrate-binding properties and provide further evidence supporting cellular mannosidase activity of the EDEM1 MLD.

Results

The binding of EDEM1 to misfolded A1AT is bipartite and involves oxidation-dependent and weak protein-protein interactions

EDEM1 preferentially interacts with misfolded A1AT variants NHK and Z in a glycan-independent manner (Cormier et al., 2009). Given the oxidative nature of the ER lumen, we determined whether this preferential interaction is oxidation-dependent. A pulse-chase experiment was performed to compare the protein interactions in the absence or presence of the reducing agent dithiothreitol (DTT) (Figure 3.1). EDEM1-FLAG was co-expressed in HEK293T cells with wild type (WT) A1AT, Z or NHK. The proteins were radiolabeled for 30 min, followed by a 15-min chase, to allow EDEM1 to reach its mature folded state. A 30-min chase with or without 5 mM DTT was performed (+/- lanes) following the initial 15 min chase (Figure 3.1). Cells were lysed with 0.5% Triton X-100 in MNT buffer (TX) or with 2% 3-[(3-cholamidopropyl)dimethylammonio]-1-

41

propanesulfonate (CHAPS or CH) in HBS. Cell lysates were divided into equal fractions and subjected to anti-A1AT (Figure 3.1, lanes 1-12) and anti-FLAG (Figure 3.1, lanes 13-24) immunoprecipitations. Immunoprecipitations obtained from "TX" lysates were washed under stringent buffer conditions containing 0.1% SDS while those obtained from "CH" lysates were washed under milder conditions using 0.5% CHAPS.

The DTT treatment did not affect the maturation or secretion of WT A1AT as the protein appears to have reached its mature state as indicated by the presence of complex sugars acquired in the Golgi as demonstrated by the higher molecular weight species (Figure 3.1, lanes 1-4). Additionally, the DTT treatment did not appear to affect the inherent binding properties of EDEM1 as it did not bind to WT A1AT regardless of the of the addition of DTT using either TX/SDS or CHAPS washes (Figure 3.Figure 3.1, lanes 1-4 and 13-16).

Under mild detergent conditions (CHAPS), the interaction between EDEM1 and NHK (Figure 3.Figure 3.1, lanes 5, 6, 17, and 18) or Z (Figure 3.Figure 3.1, lanes 9, 10, 21, and 22) was maintained regardless of the whether DTT was added. However, under stringent detergent conditions (TX/SDS), the interaction between EDEM1 and NHK (Figure 3.Figure 3.1, lanes 7, 8, 19, and 20) or Z (Figure 3.Figure 3.1, lanes 11, 12, 23, and 24) was disrupted upon addition of DTT indicating the presence of an oxidation requirement, as well as the involvement of weaker protein-protein interactions.

WT A1AT and the misfolded variants NHK and Z possess a single cysteine (Cys or C) residue at position 256 and three N-linked glycosylation sites (Figure 3.Figure 3.2A). We have previously determined that the interaction between EDEM1 and NHK is

42

glycan-independent under stringent detergent conditions (Cormier et al., 2009). Next, A1AT Cys256 was determined as a possible mediator of the interaction between A1AT and EDEM1.

Cys256Ser mutants of Z and NHK were generated and tested for their binding to EDEM1 (Figure 3.Figure 3.2B). EDEM1-FLAG was co-expressed in HEK293T cells with WT A1AT, Z, Z C256S, NHK, or NHK C256S. The proteins were radiolabeled for 30 min, followed by 1 hr chase. Cells were lysed in MNT buffer and washed in buffer containing 0.1% SDS. EDEM1 no longer interacted with Z or NHK when the Cys was mutated to a Ser (Figure 3.Figure 3.2B, lanes 21-24), suggesting that the previously observed covalent-like interaction between the misfolded A1AT ERAD variants and EDEM1, involved the single Cys256 from A1AT.

EDEM1-FLAG possesses multiple reactive maleimide-modifiable Cys

To determine whether the interaction between EDEM1 and NHK or Z involves reactive thiols or unpaired Cys on EDEM1, we conducted an in cell maleimide modification assay using mehtoxypolyethelene glycol maleimide (PEG-Maleimide) (Figure 3.Figure 3.3A). HEK293T cells were transfected with EDEM1-FLAG and a 1 hr DTT pre-treatment was added to designated dishes. Cells were lysed in sample buffer containing 5 mM PEG-Maleimide (+ PEG-Maleimide) or 20 mM NEM (- PEG-Maleimide) to modify reactive thiols (Figure 3.Figure 3.3B).

Human EDEM1 possesses eight Cys residues that are well conserved across metazoan species (Figure 3.Figure 3.3C). All eight Cys were modified upon treatment

43

with PEG-maleimide following DTT-pretreatment (Figure 3.Figure 3.3B, compare mobility shift between lanes 3 and 4). However, under oxidizing conditions (- DTT pretreatment), approximately half of the Cys were accessible to maleimide modification (Figure 3.Figure 3.3B, compare lane 2 to lane 1, 3 and 4) as the modified protein migrates slower than the unmodified but faster than the fully modified sample, indicating that a subset of the Cys on EDEM1 was accessible and reactive at steady state.

The oxidized and maleimide-modified sample (Figure 3.Figure 3.3B, lane 2) was compared to series of EDEM1 constructs on which a single Cys to Ser mutation was generated in order to obtain EDEM1 comprised of 7, 6, 5, and 4 total Cys residues (Figure 3.Figure 3.3D). The number of accessible and reactive Cys on EDEM1 under oxidizing conditions can be estimated as four, as the protein migrates at approximately the same level as EDEM1 4Cys on SDS-PAGE (Figure 3.Figure 3.3D, compare lane 2 to lane 3).

Furthermore, modeling of the conserved EDEM1 MLD predicts that four of the Cys are in sufficient proximity to form two disulfide bonds (Cys160-Cys529 and Cys410-Cys457) (Figure 3.Figure 3.3E, left panel). The two remaining Cys in the MLD (Cys302 and Cys555) might act as free thiols. There are two additional Cys found outside the predicted mannosidase domain, one N-terminal and the other C-terminal, which could pair up with each other, or with Cys302 or Cys555, or remain free thiols. This information was used to derive a predicted disulfide map of EDEM1 (Figure 3.Figure 3.3E, right panel).

We next sought to identify the reactive thiols at steady state, using the maleimide modification assay and monitoring the mobility shifts of each sample under oxidizing conditions compared to that of WT EDEM1 (Figure 3.4A). Combinational Cys to Ser mutants of the predicted reactive Cys (C95/302S, C555/629S, C95/302/629S, and C95/302/555/629S) were generated and transfected in HEK293T cells. Proteins were subjected to PEG-maleimide modification under reducing (+ DTT pretreatment) and non-reducing (- DTT pretreatment) conditions. Proteins were resolved on SDS-PAGE and subjected to immunoblotting.

The resulting blots were positioned such that the reduced protein samples in each condition were aligned (Figure 3.4A, lanes 1, 2, 5, 7, 9, 10, 13, 15, 17, and 19). The mobility shifts of the oxidized and maleimide-labeled combinational mutants C95/302S and C95/302/629S were compared to WT EDEM1 (Figure 3.4A, compare lanes 6 and 14 to lane 3) and in both instances the proteins migrated faster through the gel, with the triple mutant migrating the fastest, indicating that these constructs possess fewer accessible thiols than the WT protein, likely two and one, respectively.

The same analysis was performed with constructs in which C555 was mutated to Ser (C555/629S and C95/302/555/629S); however, both mutations resulted in a smear when labeled with PEG-maleimide under oxidizing conditions (Figure 3.4A, lanes 11 and 18). The same result was obtained with the single C555S point mutant (data not shown), which may implicate Cys555 in forming transient intermediate disulfides, perhaps as the resolving Cys residue, which when mutated to a Ser results in mixed disulfide species.

The interaction between EDEM1 comprising single Cys to Ser mutations and NHK was maintained under stringent detergent conditions (Figure 3.4B), indicating that a single EDEM1 Cys residue was not solely responsible for maintaining the interaction. We then determined whether the reactive thiols contributed to the thiol-dependent interaction that was observed under stringent detergent conditions. To this end, WT EDEM1-FLAG, C95/302/629S, and C95/302/555/629S were co-expressed with A1AT WT, Z and NHK (Figure 3.4C).

The EDEM1-FLAG C95/302/629S, and C95/302/555/629S construct both co-immunoprecipitated with Z and NHK as observed by the presence of EDEM1-FLAG protein (Figure 3.4A, lanes 5, 6, 8 and 9, compared to WT in lanes 1, 4 and 7) with the anti-A1AT immunoprecipitation. These interactions were verified using anti-FLAG immunoprecipitations where the presence of Z and NHK was observed with the EDEM1 pull-downs (Figure 3.4A, lanes 11, 12, 14, 15, 17 and 18, compared to WT in lanes 10, 13 and 16).

Similar to the WT EDEM1, EDEM1-FLAG C95/302/629S, and C95/302/555/629S exhibit preferential interaction with ERAD clients, as neither protein interact with ATAT WT (Figure 3.4A, lanes 10, 13, and 16). Taken together, EDEM1-FLAG possesses multiple reactive thiols, as Cys at positions 95, 302, 555, and 629 appear unpaired and accessible to maleimide modification at steady state; however, these residues do not appear to mediate the thiol-dependent interaction that was observed between EDEM1 and NHK/Z.

Identification of EDEM1 IDRs

Previous studies by Petrescu and colleagues have identified an IDR at the N-terminus of EDEM1 that was required for soluble tyrosinase binding (Marin et al., 2012). To address whether other IDRs are present on EDEM1, the full-length protein sequence was queried using PONDR-FIT, DISOPRED, DisProt, FoldIndex (Prilusky et al., 2005; Sickmeier et al., 2007; Ward et al., 2004; Xue et al., 2010). Each algorithm, with the exception of one, identified two regions that are predicted as IDRs, located at the N- and C-termini of the protein (Figure 3.5A, left panel). These IDRs constitute the bulk of the sequence flanking the MLD, making them potential modes of interaction between EDEM1 and ER quality control machinery or other possible ERAD clients.

ER Localization of the EDEM1 constructs

To investigate the role of the EDEM1 IDRs in localization and to determine if a construct comprised solely of the MLD lacking both IDRs remains ER localized, we generated constructs lacking either IDRs (ΔIDR (N), and ΔIDR (C)) or both (MLD), which comprises the mannosidase-like domain alone (Figure 3.5A, right panel). Each construct contains the putative WT EDEM1 signal sequence, as well as the same FLAG epitope at the C-terminus. In order to address whether the truncated constructs are targeted to the ER, their subcellular localization was monitored by confocal immunofluorescence microscopy (Figure 3.5B) and by endoglycosidase sensitivity (Fig. 3A).

Single transfections of FLAG-tagged EDEM1 FL, ΔIDR(N), ΔIDR(C), and MLD were performed in HEK293A cells and staining was compared against ER (CRT) or Golgi (Giantin) markers (Figure 3.5B). Signals from each EDEM1 construct colocalized with CRT; however, no colocalization was observed with the Golgi marker, suggesting that all constructs were ER resident proteins.

EDEM1 and the IDR constructs are predicted to possess multiple N-linked glycosylation consensus sites. EDEM1 FL was previously shown to be N-glycosylated, thus an N-glycosylation assay would reveal if the EDEM1 constructs lacking the IDRs were targeted to and reside in the ER (Tamura et al., 2011). The proteins were isolated by immunoprecipitation from cells expressing EDEM1 FL, ΔIDR(N), ΔIDR(C), and MLD, and were de-glycosylated using PNGase F (F), Endo H (E), or untreated (U) (Figure 3.6A) and visualized by immunoblotting. PNGase F removes mannose-rich N-glycans found in the ER, as well as complex N-glycans that are acquired in the Golgi, while Endo H only trims high mannose N-glycans encountered in the ER. Since the molecular mass of an N-linked glycan is approximately 2.5 kDa, glycosylated proteins should migrate slower on an SDS-PAGE gel compared to de-glycosylated proteins.

Mobility shifts upon PNGase F and Endo H treatment were observed for all EDEM1 IDR constructs (Figure 3.6A, compare "U" lanes to "P" and "E" lanes), indicating that ΔIDR(N), ΔIDR(C), and MLD were all targeted to the ER and glycosylated with high mannose carbohydrates and did not receive complex N-glycans in the Golgi. Together, these observations are consistent with ΔIDR(N), ΔIDR(C), and MLD being targeted to and residing in the ER.

EDEM1 MLD preferentially interacts with ERAD substrates

To attempt to reduce EDEM1 down to a smaller functional unit and to determine if the conserved N- and C-terminal MLD flanking regions are required for ERAD client binding, the binding of the EDEM1 constructs to A1AT WT and its mutant variants was characterized using a radiolabel pulse-chase approach (Figure 3.6B). The IDRs were not required for the interaction with Z and NHK as binding to Z and NHK but not WT occurred for both EDEM1 □IDR(N) and (C) (Figure 3.6B, lanes 8, 9 14 and 15, compared to lanes 7 and 13). The MLD construct, which is missing both the N- and C-terminal IDRs, also preferentially binds to misfolded variants Z and NHK over WT (Figure 3.6B, lanes 16-18).

Moreover, the three-acidic putative active site residues were replaced with positively charged Lys residues (MLD (3K)) to abolish any potential carbohydrate binding (Figure 3.6C, lanes 7-9). Interestingly, the interaction between MLD (3K) and both NHK and Z was maintained while no interaction was observed with WT A1AT; which further validates the ERAD-client specific glycan-independent binding property of the MLD. The MLD also bound to a non-glycosylated NHK indicating that binding was glycan-independent (Figure 3.6D). Taken together, these results demonstrate that the EDEM1 MLD possesses the ability to preferentially interact with the non-native ERAD clients NHK and Z, in a glycan-independent manner.

MLD substrate binding is redox sensitive

Since the EDEM1 MLD exhibits preferential interaction with ERAD clients, we next determined if this interaction involves thiols by monitoring binding upon the addition of DTT (Figure 3.7A). A pulse chase analysis was performed (as described in Fig. 1*A*) using a sequential immunoprecipitation of the protein with anti-FLAG followed by anti-A1AT (Figure 3.7A, lanes 7-12). As expected, the MLD did not interact with WT A1AT (Figure 3.7A, lanes 7 and 8). However, like full length EDEM1, the interaction between Z and NHK was oxidation dependent under stringent detergent conditions (Figure 3.7A, compare lanes 10 to 9, and 12 to 11).

We next determined if the thiol-dependent interaction involves Cys256 for Z/NHK (Figure 3.7B). The MLD was co-expressed in HEK293T cells with A1AT WT, Z, Z Cys256Ser, NHK, NHK Cys256Ser, NHK NOG, and NHK NOG Cys256Ser. The proteins were radiolabeled for 30 min, and chased for 1 hr. The cells were lysed under stringent detergent conditions (TX/SDS) and protein complexes were isolated by single anti-A1AT and anti-FLAG immunoprecipitation, as well as sequential immunoprecipitation. The Cys256 residue on NHK/Z also plays a role in the interaction with the MLD, as the Cys to Ser mutations abolished the interaction (Figure 3.7B, compare lanes 6 to 5, 15 to 14, and 17 to 16).

The EDEM1 Cys at position 160, 410, 457, and 529 are predicted to be involved in disulfides (Figure 3.3E) and are all found in the MLD. Additionally, our PEG-maleimide analysis revealed that these Cys do not appear modified under oxidizing

conditions, suggesting that they are either involved in disulfide interactions or not accessible to maleimide modification.

The modeled structure of the MLD predicts two potential disulfides and two unpaired Cys (Figure 3.3E). Our PEG-maleimide analysis on full-length EDEM1 identified approximately four reactive thiols and approximately four thiols that are inaccessible to maleimide modification (Figure 3.3B and Figure 3.4A). Based on these results, we expect that a subset (~2) of the Cys on the MLD will be accessible to maleimide modification, while the remaining four would not be. Like the full-length EDEM1, a subset of the Cys residues on MLD is reactive at steady state (Figure 3.7C, compare lane 3 to lanes 1, 2 and 4).

Next, we determined whether the Cys that are predicted to be paired and experimentally inaccessible to PEG-maleimide (Cys160, 529, 410, and 457) are involved in the thiol-dependent interaction between MLD and Z/NHK (Figure 3.8). Each of the Cys/Ser combinational mutants were co-expressed in HEK293T cells with WT A1AT, Z and NHK. Radiolabeled proteins were isolated using single immunoprecipitation with anti-A1AT antibody (Figure 3.8, lanes 1-3, 10-12, 19-21, 28-30, and 37-39), anti-FLAG (Figure 3.8, lanes 7-9, 16-18, 25-27, 34-36, and 43-45), and by sequential immunoprecipitation (Figure 3.8, lanes 4-6, 13-15, 22-24, 31-33, and 40-42).

Binding to WT A1AT was not observed, regardless of the mutation (Figure 3.8, compare lanes 13, 22, 31 and 40 to lane 4). Binding to Z and NHK persisted when either predicted disulfide pairs, or free thiols were mutated (Figure 3.8, compare lanes 14, 15, 23, 24, 32, 33, to lanes 5 and 6). However, the Cys-less construct did not exhibit any

51

binding to Z or NHK (Figure 3.8, compare lanes 41 and 42 to lanes 5 and 6), which is likely due to which is likely due to the resulting compromised structural integrity of the Cys-less MLD.

Altogether, the MLD possesses the ability to bind NHK and Z in a thiol-dependent manner, involving Cys256 on Z/NHK. However, the MLD Cys that are predicted to be involved in disulfides, like the predicted unpaired Cys, are not directly involved in this interaction. Cys residues appear to function as structural components of the MLD, and at least one of these disulfides pairs is required for ERAD client binding.

EDEM1 MLD promotes glycan trimming

To further characterize the MLD and elucidate whether it possesses mannose-trimming properties, the mobility of NHK on SDS-PAGE was monitored (Figure 3.9). A quadruple knockout CRISPR/Cas9 CHO cells was used where four mannosidases were knocked out (*Man1a1/a2/b1/c1*). The only putative mannosidases that are present in these knockout cell lines are EDEM1, 2 and 3. Thus, overexpressing the MLD in these cell lines might enhance any trimming effect on NHK as the presence and effect of other functional mannosidases is minimized.

NHK was co-expressed in the quadruple mannosidase knockout CHO cells with a mock empty plasmid (Figure 3.9, lanes 1-6), the catalytically active Man1b1-FLAG (Figure 3.9, lanes 7-12), EDEM1-FLAG (Figure 3.9, lanes 13-18), EDEM1 (3K)-FLAG (Figure 3.9, lanes 19-24), MLD-FLAG (Figure 3.9, lanes 25-30), MLD (3K)-FLAG (Figure 3.9, lanes 31-36), and MLD Cys-less-FLAG (Figure 3.9, lanes 37-42), in addition

to NHK with the mannosidase inhibitor, kifunensine (Kif) (Figure 3.9, lanes 43-45). Proteins were radiolabeled for 30 min and chased the indicated times.

Consistent with previous data, mannose trimming was abolished upon the addition of kifunensine (Figure 3.9, lanes 43-45) and the mutation the acidic putative active site residues on EDEM1 (Figure 3.9, compare lanes 22-24 to lanes 16-18). Importantly, the MLD also possesses glycan-trimming ability, as observed by the increase in mobility of NHK upon co-expression with MLD (Figure 3.9, lanes 28-30) compared to MLD (3K) (Figure 3.9, lanes 34-36). These results indicate that the MLD is properly folded and possesses glycosidase activity.

Role of IDRs in EDEM1 stability and function

Given that the MLD exhibited similar substrate binding properties as that of the full-length EDEM1, we wanted to determine if it possessed similar inherent properties of EDEM1, specifically its short half-life, and the ability to associate with another known EDEM1 binding partner, ERdj5.

Half-lives: EDEM1 is reported to have a rapid turnover rate with a half-life of ~2 hr (Le Fourn et al., 2009), especially compared to other ER resident proteins such as BiP, a key member of the ER quality control machinery, which is in the range of 28-33 hr (Gülow et al., 2002). Furthermore, proteins that are intrinsically disordered or contain IDRs possess, on average, a shorter half-life than proteins lacking any IDRs (van der Lee et al., 2014). Specifically, proteins containing long stretches of disordered regions (>30 residues) appear to have the shortest half-lives. The EDEM1 N- and C-terminal IDR

regions are predicted to be 71 and 69 amino acids in length, respectively (Figure 3.5A, right panel).

We thus postulated that the MLD construct, which lacks both IDRs, would have the longest half-life. To this end, each construct bearing a C-terminal FLAG epitope was expressed in HEK293T cells and subjected to a pulse-chase experiment after radiolabeling. Following lysis, the proteins were isolated through immunoprecipitation and resolved on SDS-PAGE (Figure 3.10, top panel). The amount of protein remaining at the indicated time points was quantified and normalized to the starting amount (Figure 3.10, bottom panel).

Approximately 50% of EDEM1 FL remained at the 2 hr time point while only ~20% remained at 4 hr. These results are consistent with previous turnover rates of EDEM1 in cell analyses (Le Fourn et al., 2009). However, the half-life of the MLD construct, which lacks both IDRs, was ~4 hr, (~70% remains at 2 hr). Similarly, the constructs lacking each IDR individually (ΔN/ ΔC) have longer half-lives than the full-length construct. These observations further validated the identity and presence of two IDRs on EDEM1 that contribute to the previously observed short half-life of EDEM1.

ERdj5 binding: Since the IDRs were not required for substrate interaction with A1AT misfolded variants (Figure 3.6B, 2.6C and 2.6D), we next determined whether the IDRs of EDEM1were required for binding to the ER oxidoreductase ERdj5. To this end, FLAG-tagged full-length EDEM1, the EDEM1 IDR deletion constructs, and the MLD were co-expressed with MYC-tagged ERdj5 in HEK293T cells. The cells were lysed 24

hr post-transfection and proteins were isolated through co-immunoprecipitation. Binding interactions were monitored through immunoblotting.

An interaction with ERdj5 was recovered with EDEM1 lacking either one of its IDRs (Figure 3.11, compare lanes 5, 6, 8, and 9 to lanes 2 and 3). However, the interaction with ERjd5 was lost with EDEM1 lacking both IDRs as displayed by the MLD (Figure 3.11, compare lanes 11 and 12 to 2 and 3). This indicated that the presence of either IDRs was sufficient to interact with ERdj5 but the interactions was abolished when both IDRs were removed with the EDEM1 MLD.

Taken together, these studies with EDEM1 MLD established its ER localization, determined its substrate binding properties, identified components that support binding to ERdj5, and confirmed it possesses catalytic glycosidase activity in cells.

Conservation of EDEM1 properties in EDEM2 and EDEM3.

To determine if EDEM2 and EDEM3 contain similar properties to EDEM1, EDEM2 and EDEM3 were characterized for substrate binding properties, free thiol content and analyzed for IDRs. Human EDEM2 and EDEM3 were co-expressed in HEK293T cells with WT A1AT, Z, Z Cys256Ser, NHK, NHK Cys256Ser, NHK NOG, and NHK NOG Cys256Ser. The proteins were radiolabeled for 30 min, and chased for 1 hr. Cells were lysed under stringent detergent conditions (TX/SDS), lysates were split into equal portions, and protein complexes were isolated by anti-FLAG or anti-A1AT immunoprecipitation. Neither EDEM2 nor EDEM3 associate with WT A1AT (Figure 3.12A and Figure 3.13A, lane 6).

Like EDEM1 and the MLD, EDEM2 and EDEM3 co-immunoprecipitated with the ERAD clients, Z and NHK (Figure 3.12A and Figure 3.13A, lanes 7 and 9) in a glycan-independent manner (Figure 3.12A and Figure 3.13A, lane 13). However, upon mutating Cys256 to Ser, the interaction was lost (Figure 3.12A and Figure 3.13A, compare lanes 8 to 7, 10 to 9, and 14 to 13), suggesting that the thiol-dependency that is observed with EDEM1 and EDEM1 MLD is a conserved trait among all human EDEM homologues.

Human EDEM2 and EDEM3 possess numerous Cys, 9 and 11, respectively (Figure 3.12B and Figure 3.13B). When subjected to PEG-maleimide modification, both construct displayed reactive thiols at steady state (Figure 3.12B and Figure 3.13B, compare lane 3 to lanes 1, 2 and 4). Additionally, the EDEM2 and EDEM3 protein sequences were queried for IDRs and like EDEM1, both proteins possess IDRs in regions outside the MLD, specifically at the C-terminus (Figure 3.12B and Figure 3.13B).

Together, these results indicate that EDEM1, 2, and 3 possess a conserved redox-sensitivity involved in binding to A1AT ERAD substrates. The proteins are predicted to contain IDRs; however, in the case of EDEM1, these regions do not contribute to Z/NHK binding, as the catalytically active EDEM1 MLD alone is capable of selectively binding to ERAD clients.

Discussion

Protein-to-protein interactions have been observed between EDEM1 and multiple ERAD clients including BACE457, CFTR, Rhodopsin, H2a and A1AT (Cormier et al.,

2009; Gnann et al., 2004; Hosokawa et al., 2001; Kosmaoglou et al., 2009; Molinari et al., 2003; Shenkman et al., 2013). However, the basis for these substrate-binding interactions is uncertain. Here we studied the interaction between EDEM1 and the misfolded A1AT variants Z and NHK. An additional mode of interaction that is redox sensitive was revealed and provided further evidence that the MLD is active and sufficient to selectively bind the A1AT ERAD clients, Z and NHK.

EDEM1 preferentially interacts with Z and NHK, but does not bind to the WT A1AT, suggesting it may recognize elements on these misfolded proteins that are not present on the properly folded substrate (Cormier et al., 2009). In the presence of a reducing agent, the interactions between EDEM1 and Z/NHK were lost under stringent detergent conditions (Figure 3.1). However, under milder detergent condition, the interactions persisted (Figure 3.1) demonstrating the involvement of two types of interactions: a strong covalent-like, oxidation-dependent interaction; as well as a weak, protein-protein interaction as demonstrated by the recovered interaction under milder detergent conditions.

The latter protein-protein interactions are possibly mediated through hydrophobic interactions as such interactions have been demonstrated between EDEM1 and the ERAD client BACE457 (Sokołowska et al., 2015). A model of the EDEM1 MLD structure shows extensive surface exposed hydrophobic patches on EDEM1 (Figure 3.14), all of which may mediate the observed weak protein-protein interactions. Identifying the precise hydrophobic patch(es) involved in this interaction, or determining whether other

ERAD clients or machinery interactions involve hydrophobic interactions with EDEM1 will require further investigation.

The lone cysteine residue located on Z and NHK (Cys256) contributed to the observed oxidation-dependent interaction with EDEM1 (Figure 3.2A, and 2.2B) as the interaction was lost upon mutating the Cys to Ser under strong detergent conditions but persisted under mild detergent conditions. This supports the observed oxidation sensitivity, presumably through a disulfide bond (Figure 3.2B). Interestingly, Cys256 is located in the WT structure in a position that is partially exposed or buried (Figure 3.15).

Mutations as those observed with NHK and Z would be expected to perturb the structure sufficiently to support increased accessibility of Cys256 to quality control factors and ERAD machinery. The presence of aberrant Cys256-mediated dimers that are formed between Z monomers and NHK monomers, that do not occur with WT A1AT, as well as increased secretion of Z upon Cys256 to Ser mutation, implicate a role for the Cys in ER retention of aberrantly folded Z, and perhaps NHK, as well as further provide evidence supporting the increased accessibility of Cys256 on Z compared to WT A1AT.

This suggests that Cys256 is suitably positioned to act as a quality control signal when exposed in aberrant structures. Although, a heterodimer between the two proteins (Z and EDEM1 or NHK and EDEM1) was not readily observable (data not shown), it is likely that since EDEM1 is proposed to exist in the ER as a member of a multi-protein complex, the presence of monomeric or dimeric Z or NHK would not result in an observable mobility shift on non-reducing SDS-PAGE.

A putative model of the EDEM1 MLD showed a conserved barrel structure with the three-putative acidic catalytic residues centered at the core, similar to that of Man1b1 (Figure 3.3E, and 1.5) (Vallée et al., 2000). The model also revealed two potential disulfides as indicated by their predicted proximities, and two unpaired Cys. The predicted map and the presence of reactive thiols, was further tested upon subjection of combinational Cys to Ser mutants of the predicted unpaired Cys residues to peg-maleimide modification (Figure 3.4A).

Given the oxidative nature of the ER and the role of EDEM1 in ERAD, it is surprising that four out of the eight Cys on EDEM1 appear to be accessible to maleimide modification at steady state and suggest that these Cys are likely involved in a functional aspect of EDEM1, either to form direct stable or transient bonds with ERAD clients, ERAD machinery or with other EDEM1 proteins. However, none of the individual Cys were required to interact with Z or NHK (Figure 3.4B) The interaction was only abolished when all Cys were mutated to Ser (Cys-less), in which case the protein was likely unstructured. These results further support the absence of direct involvement of the Cys of EDEM1 in the apparent redox sensitive interaction with Z/NHK.

The redox sensitivity of EDEM1 substrate selection likely involves an oxidoreductase other than ERdj5 since the MLD exhibits redox sensitive binding to Z/NHK (Figure 3.7A and 2.7B) and does not interact with ERdj5 (Figure 3.11). It is likely that the interaction between EDEM1 and ERdj5 does not require the MLD, as EDEM1 appears to interact with ERdj5 through its C-terminal thioredoxin cluster, a region that is not glycosylated (Ushioda et al., 2008).

Several groups have demonstrated an interaction between EDEM1 and multiple oxidoreductases including P5, PDI, ERp57, and ERp72 (Jansen et al., 2012; Jessop et al., 2009). Likewise, ERdj3 was recently implicated in the degradation of the Z variant (Khodayari et al., 2017). Additionally, the EDEM3 MLD was recently discovered to form a disulfide bond with the oxidoreductase ERp46, which promoted the catalytic activity of EDEM3 (Yu et al., 2018). Whether these oxidoreductases or others are involved in the redox-sensitive substrate-binding properties of EDEM1 remains to be determined.

The truncated MLD construct, in which both regions flanking the EDEM1 MLD were removed, was used to assess the requirement of paired Cys residues in the EDEM1-Z/NHK interaction. The fundamental properties of the MLD were characterized. Although the EDEM2 MLD was expressed and characterized both in cells and as a recombinant protein, the properties of the EDEM1 MLD alone are uncharacterized. The EDEM1 MLD construct is targeted to and retained in the ER, in contrast to the EDEM2 MLD (Figure 3.5B and 2.6A) (Mast et al., 2005). Importantly, the MLD alone retained the ability to preferentially interact with ERAD clients in a glycan-independent manner, indicating that the mannosidase-like domain is sufficient to interact and preferentially select A1AT ERAD substrates further reinforcing the MLD requirement in binding to a subset of ERAD clients (Figure 3.6C and 2.6D).

The MLD also exhibited the same oxidation dependent binding and sensitivity to the Z/NHK Cys256 upon stringent detergent condition, indicating that the ability and selectivity for Z and NHK binding is inherent to the MLD and did not require the flanking IDRs (Figure 3.7A and 2.7D). However, the covalent interaction is likely mediated through a co-factor, as neither of the predicted disulfides was involved.

Although the eight-Cys residues on EDEM1 are conserved across species, at least a subset of them appear to function as structural elements of the MLD, as indicated by loss of ERAD client binding in the absence of all Cys residues (Figure 3.8).

In addition, the MLD expressed in a cell line deficient for four mannosidases including Man1a1/a2/b1/c1 exhibited mannose-trimming properties as observed by the mobility shift of NHK on SDS-PAGE (Figure 3.9). The mobility shift was lost upon the mutation of the putative catalytic residues (MLD 3K), suggesting that the catalytically inactive MLD 3K exhibited a dominant negative effect, one in which NHK binds the inactive MLD thus preventing it from interacting with other mannosidases such as EDEM2 or EDEM3 (Figure 3.9) (Ninagawa et al., 2015). EDEM1 does not appear to act solely as a mannosidase as selective interactions with ERAD clients survive prolonged binding required with the co-immunoprecipitation protocol, unlike Man1b1 for which an interaction is not recovered. It is possible that this prolonged interaction indicates a role for EDEM1 in delivering ERAD clients to the retro-translocation machinery. Altogether, these novel findings may facilitate purification of recombinant EDEM1 and its MLD for *in vitro* biochemical characterization, which have previously been unsuccessful and potentially help identify the specific glycan branch on which EDEM1 acts.

In addition to identifying novel redox sensitive properties between EDEM1 or the MLD and two ERAD substrates, we have identified a second IDR located at the C-terminus of EDEM1 (Figure 3.5A). Removing either or both IDRs did not affect the ER targeting or localization of EDEM1 as all constructs received N-linked glycans and exhibited glycoforms that are typically found on ER-resident proteins (Figure 3.6A).

None of the constructs were recovered in the media fractions, confirming their cellular retention (Figure 3.6A). The ER retention of the MLD alone appears to require neither a retention sequence like KDEL nor the N- or C- terminal regions flanking it. Instead, the ER retention of soluble EDEM1 is a property of the MLD unlike that of EDEM2, demonstrating a key difference between the proteins (Figure 3.5B and 2.6A) (Mast et al., 2005). The construct lacking either IDR also retained the glycan-independent preferential interaction with Z and NHK, which is expected as both constructs display intact MLDs (Figure 3.6B and 2.6D).

The present study provides evidence that EDEM1 possesses two IDRs that contribute to its observed short half-life. Unlike other ER resident proteins such BiP, EDEM1 is rapidly turned over and exhibits a half-life of ~2 hr. The stability of EDEM1 upon removal of both IDRs (EDEM1 MLD) appears to double the protein half-life from 2 to 4 hr, which further supports the regions flanking the EDEM1 MLD as intrinsically disordered (Figure 3.10).

The relatively short half-life of EDEM1 is likely linked to its function in ERAD to bind misfolded clients as they accumulate in the ER and target them for degradation. The short half-life is also proposed as a function of ERAD tuning in order to return the ER to basal EDEM1 levels once the stress is alleviated (Merulla et al., 2013). The conservation of the IDRs across EDEM1 in various species further supports their necessity and role in its function (data not shown).

Although neither the N- nor C-terminal IDRs were required for binding to Z or NHK, unlike H2a or soluble tyrosinase, either IDRs appear necessary for binding to

ERdj5 (Figure 3.11) (Marin et al., 2012; Shenkman et al., 2013). Like EDEM1, other proteins such as the E3 ligase San1 and the deubiquitinating enzyme Ubp10 possess IDRs at both their N- and C- termini (Fredrickson et al., 2011; Reed et al., 2015). In both cases, the conformational flexibility of the IDRs allows San1 and Ubp10 to bind multiple partners. EDEM1 may use an analogous mechanism to bind partners such as ERdj5.

EDEM2 and EDEM3 interact with and accelerate the degradation of Z and NHK (Jang et al., 2015; Ninagawa et al., 2015; Hirao et al., 2006). This interaction also appears sensitive to the presence of Cys256 on NHK and Z (Figs. 7*A* and *B*). EDEM2 and EDEM3 also possess reactive thiols at steady state (Figure 3.12A ad 2.13A), and interact with the oxidoreductase TXNDC11 (Timms et al., 2016). Like EDEM1, EDEM2 and EDEM3 are predicted to possess IDRs (Figure 3.12B ad 2.13B). These findings further support conserved properties among the mammalian EDEM protein family.

Together, these findings uncover new modes of interaction that EDEM1 possesses and broaden the binding landscape of EDEM1. Specifically, EDEM1 does not interact with its binding partners or ERAD clients in a "one size fits all" manner. Instead, EDEM1 binding is multifaceted as different components are utilized depending on the properties or requirement of the specific binding partner increasing the versatility of its substrate selectivity.
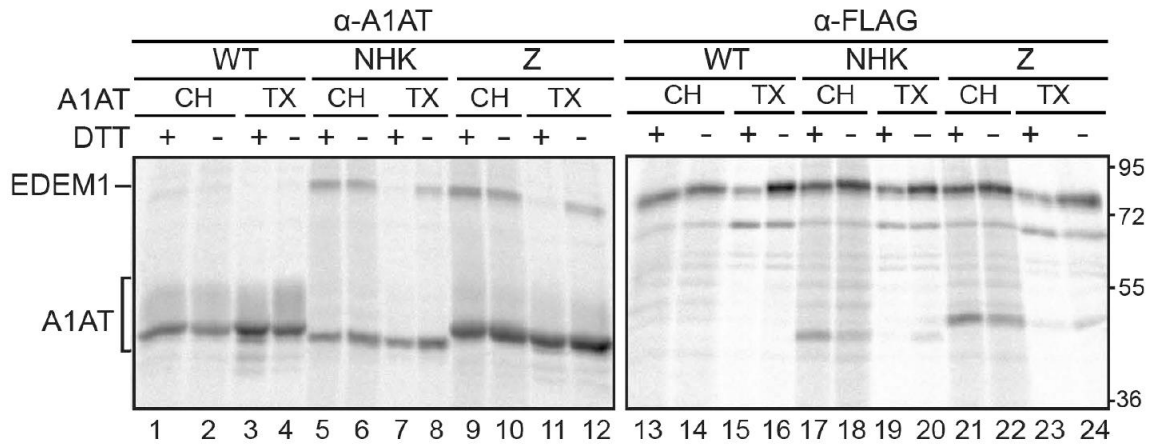
Figure 3.1 EDEM1 binding to ERAD clients A1AT Z and NHK is bipartite

EDEM1-FLAG was transiently transfected with A1AT WT, NHK, or Z in HEK293T cells. Cells were radiolabled with [35S]-Cys/Met for 30 min and chased for 15 min. DTT (5 mM) was added to the cells for 30 min where indicated (+DTT). Cells were lysed in MNT buffer containing Triton X-100 (TX) or CHAPS (CH). Lysates were split in half and EDEM1 and A1AT were isolated using anti-FLAG (α-FLAG) and anti-A1AT (α-A1AT) antisera. The proteins were resolved on 9% reducing SDS-PAGE.
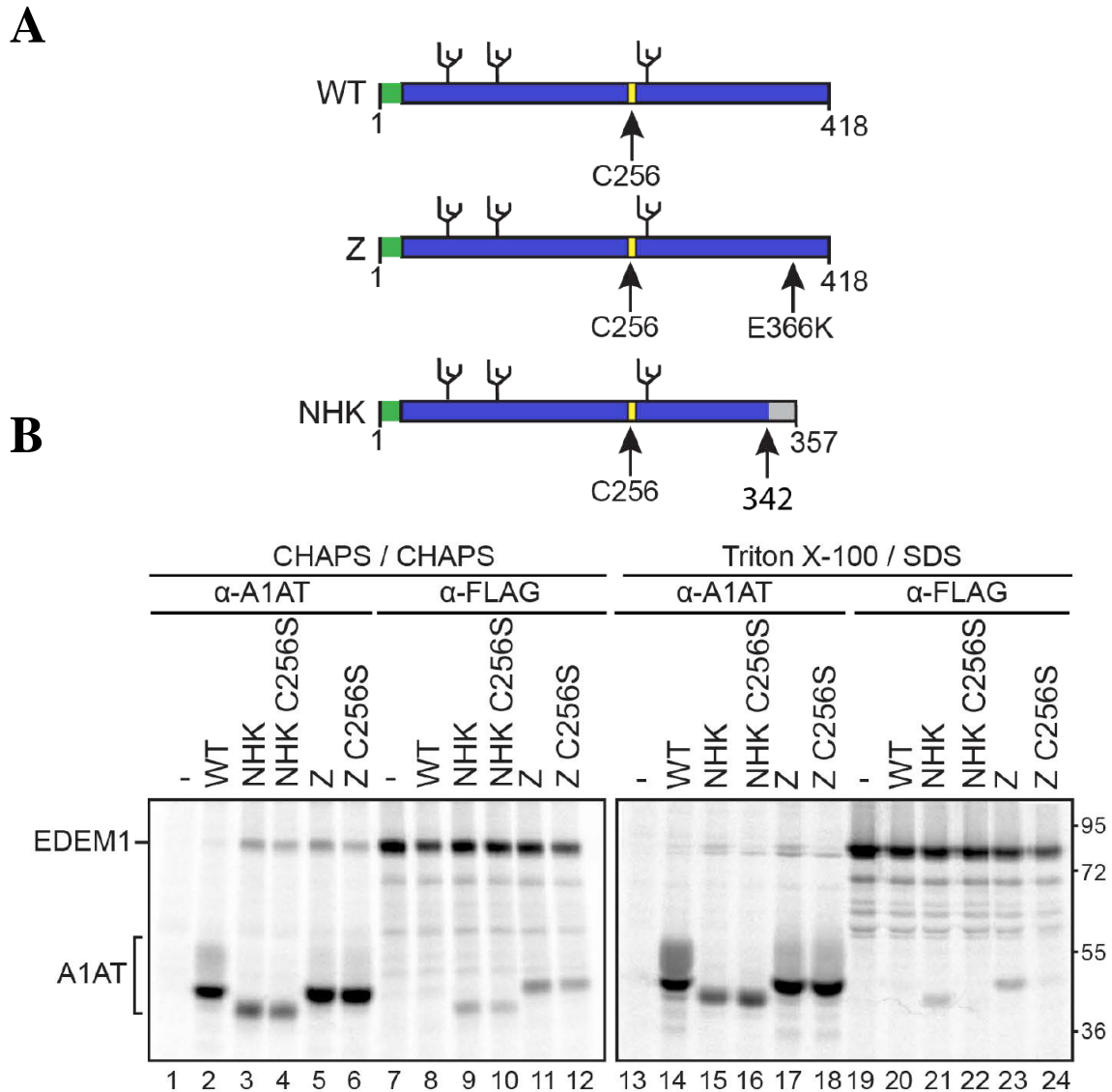
Figure 3.2 EDEM1 binding to ERAD clients A1AT Z and NHK involves C256

(**A**) Cartoon representation of A1AT constructs depicting signal peptide (green), glycosylation sites (black), and Cys256 (yellow). Arrows denote point mutation E366K on Z and frameshift mutation at 342 on NHK. (**B**) EDEM1-FLAG was co-expressed in HEK293T cells with A1AT WT, Z, Z C256S, NHK, or NHK C256S. The proteins were radiolabeled with [35S]-Cys/Met for 30 min and chased for 1 hr. Cells were lysed in 2% CHAPS or MNT buffer containing 0.1% SDS. Half of the cell lysate was subjected to anti-A1AT immunoprecipitation while the other half to anti-FLAG immunoprecipitation, and washed in 0.5% CHAPS or wash buffer containing 0.1% SDS, respectively. Proteins were resolved on 9% reducing SDS-PAGE. Gels are representative of three independent experiments.
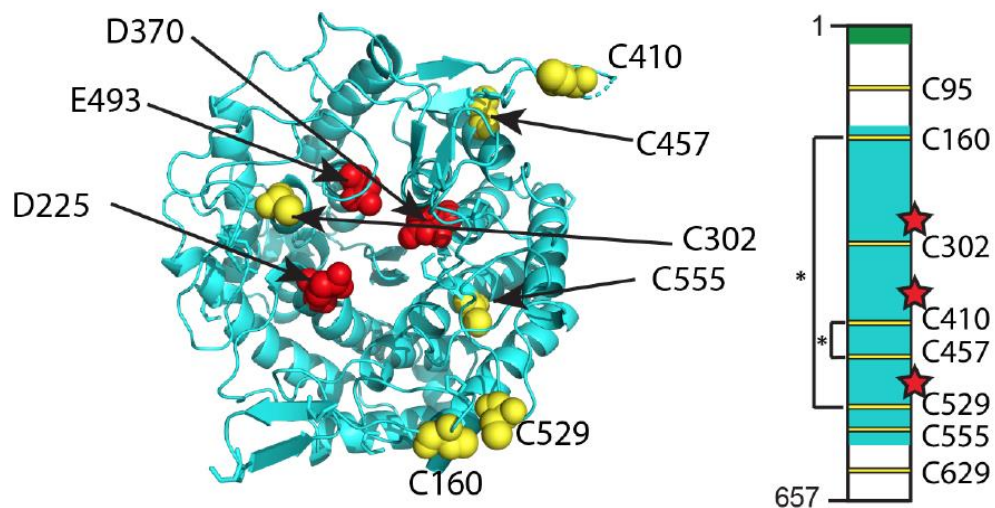
A

B

α-FLAG: IB

| DTT Pretreatment | − | − | + | + |
| PEG-Maleimide | − | + | − | + |

EDEM1-FLAG

175

80

58

1 2 3 4
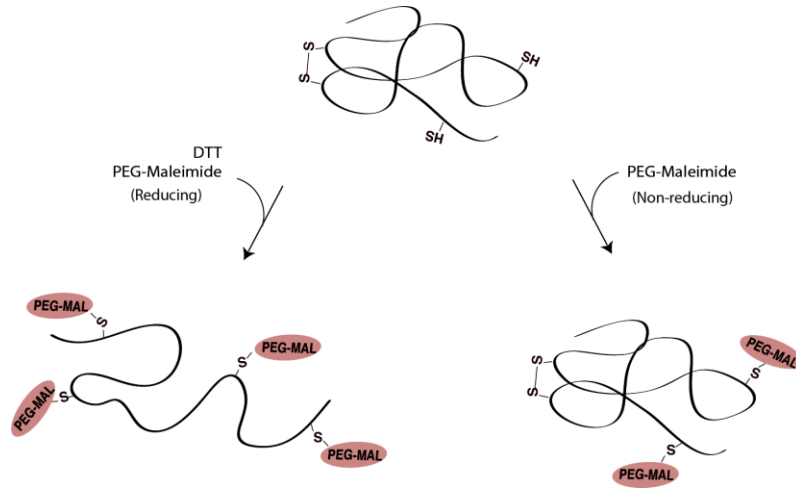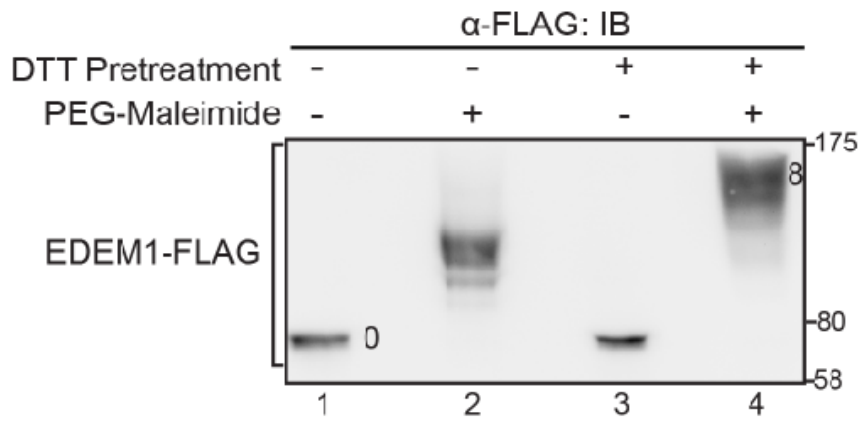
C
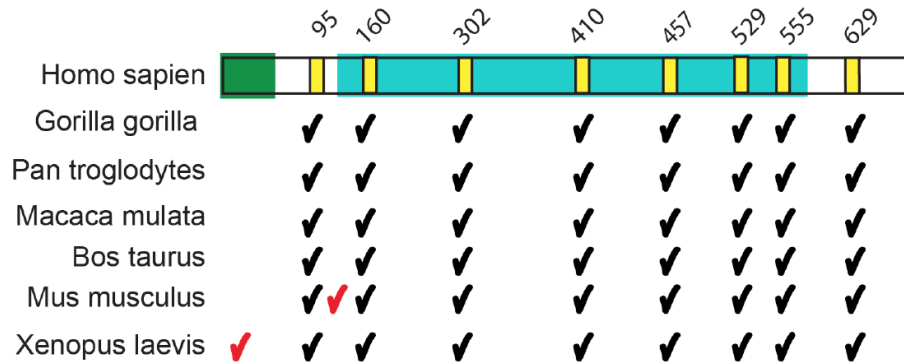
D
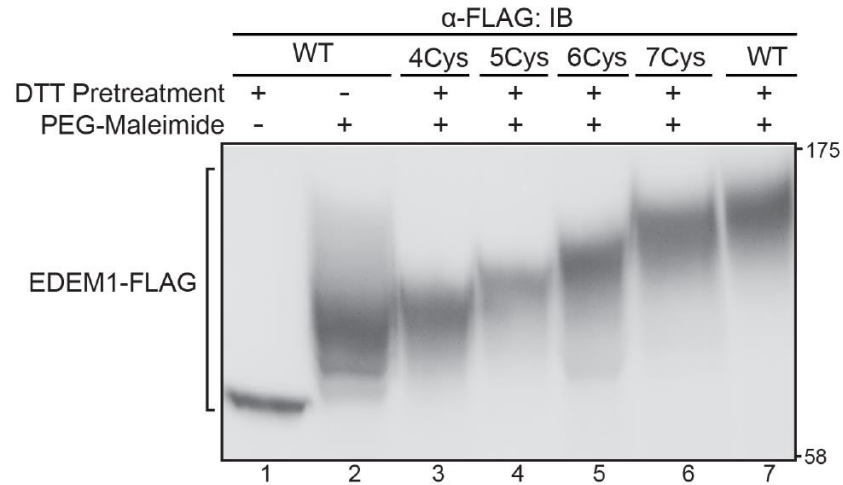
E

Figure 3.3 EDEM1 possesses approximately 4 reactive thiols

(A) Cartoon representation of a protein possessing two cysteines involved in an intramolecular disulfide bond and two unpaired cysteines. The presence of free thiols is analyzed using sulfhydryl-reactive maleimide linked to a polyethylene glycol group (PEG-Mal). Cells expressing the protein of interest are treated with or without DTT to assess reducing and non-reducing states, respectively. Cells are lysed in the presence and absence of PEG-maleimide, and protein samples are resolved by SDS-PAGE. **(B)** EDEM1-FLAG was expressed in HEK293T cells. Cells were pretreated with DTT (5

mM) where indicated (+/-). Cells were lysed in sample buffer containing 5 mM peg-maleimide (+ PEG-Maleimide) or 20 mM NEM (- PEG-Maleimide). Proteins were resolved on 8.5% SDS-PAGE and immunoblotted with FLAG antibody **(C)** Cartoon representation of amino acid sequence alignments (Clustal Omega) of EDEM1 from various species (Accession #:NP_055489.1, XP_004033576.1, JAA36785.1, NP_001252679.1, AAI51306.1, NP_619618.1, and NP_001091440.1) depicting conserved and non-conserved Cys residues, black and red check marks, respectively. **(D)** FLAG-tagged EDEM1 WT, EDEM1 C95/302/555/629S (4Cys), EDEM1 C95/302/629S (5Cys), EDEM1 C95/302S (6Cys), and EDEM1 C95S (7Cys) were transfected in HEK293T cells. 5 mM DTT was added for 1 h where inidcated (+). Cells were lysed in sample buffer containing 5 mM peg-maleimide (+ PEG-Maleimide) or 20 mM NEM (-PEG-Maleimide). Proteins were resolved on 8.5% SDS-PAGE and immunoblotted with FLAG antibody. Gel represents data acquired from three independent experiments. **(E)** Structural model (Phyre2.0) of the MLD (Cyan) showing the three catalytic triad (red) and Cys residues (yellow). Cartoon representation of EDEM1 depicting signal peptide (green), MLD (cyan), putative catalytic residues (red), Cys residues (yellow), and predicted disulfides (*).
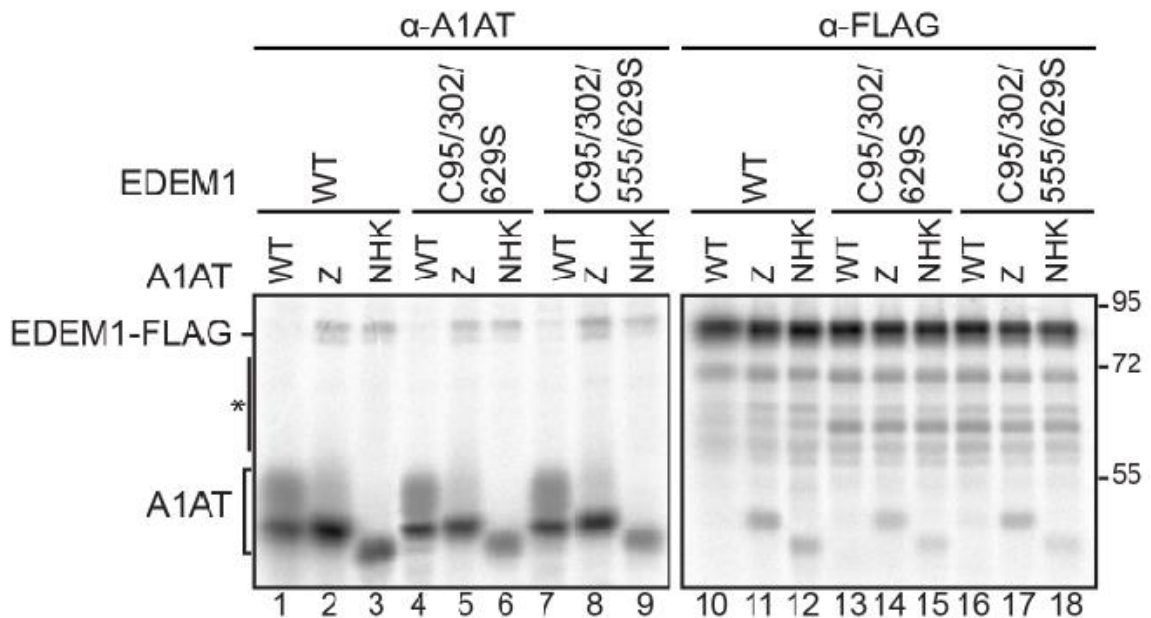
A
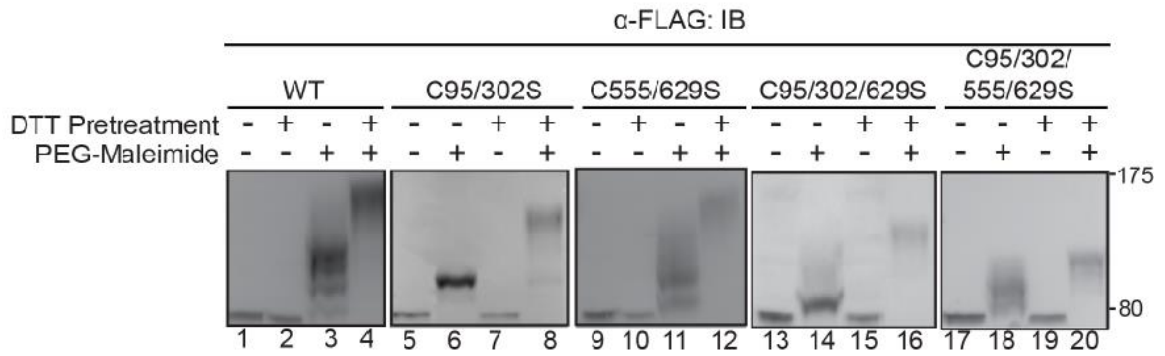
B
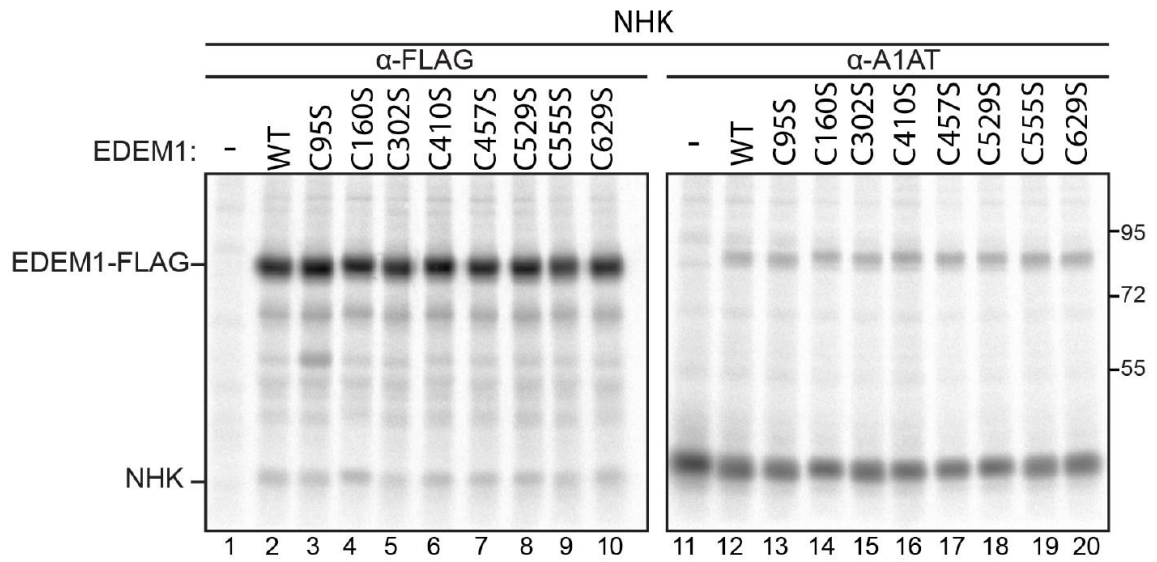
C

Figure 3.4 EDEM1 Cys at position 95/302/555/629 are unpaired but not required
for NHK/Z binding

(A) FLAG-tagged EDEM1 (WT), C95/302S, C555/629S, C95/302/629S, and
C95/302/555/629S were expressed in HEK293T cells. 5 mM DTT was added for 1 h
where inidcated (+). Cells were lysed in sample buffer containing 5 mM peg-maleimide
(+ PEG-Maleimide) or 20 mM NEM (- PEG-Maleimide). Proteins were resolved on
8.5% SDS-PAGE and immunoblotted with FLAG antibody. Gel represents data acquired
from three independent experiments. **(B)** FLAG-tagged EDEM1 WT, C95S, C160S,
C302S, C410S, C457S, C529S, C555S, C629S and empty plasmid (-) were co-expressed
in HEK293T cells with NHK. The proteins were radiolabeled with [35S]-Cys/Met for 30
min and chased for 1 hr. Cells were lysed in MNT buffer containing Triton X-100. Half
of the cell lysate was subjected to anti-A1AT immunoprecipitation while the other half to
anti-FLAG immunoprecipitation, and washed in buffer containing 0.1% SDS. Proteins
were resolved on 9% reducing SDS-PAGE. Gels are representative of three independent
experiments. **(C)** FLAG-tagged EDEM1 (WT), C95/302/629S, and C95/302/555/629S
were co-expressed with A1AT WT, Z, and NHK in cells. Cells were radiolabled with
[35S]-Cys/Met for 30 min and chased for 1 hr. Cells were lysed in MNT buffer
containing 0.1% SDS. Half of the cell lysate was subjected to anti-A1AT and half to anti-
FLAG immunoprecipitation. Proteins were resolved on 8.5% reducing SDS-PAGE.
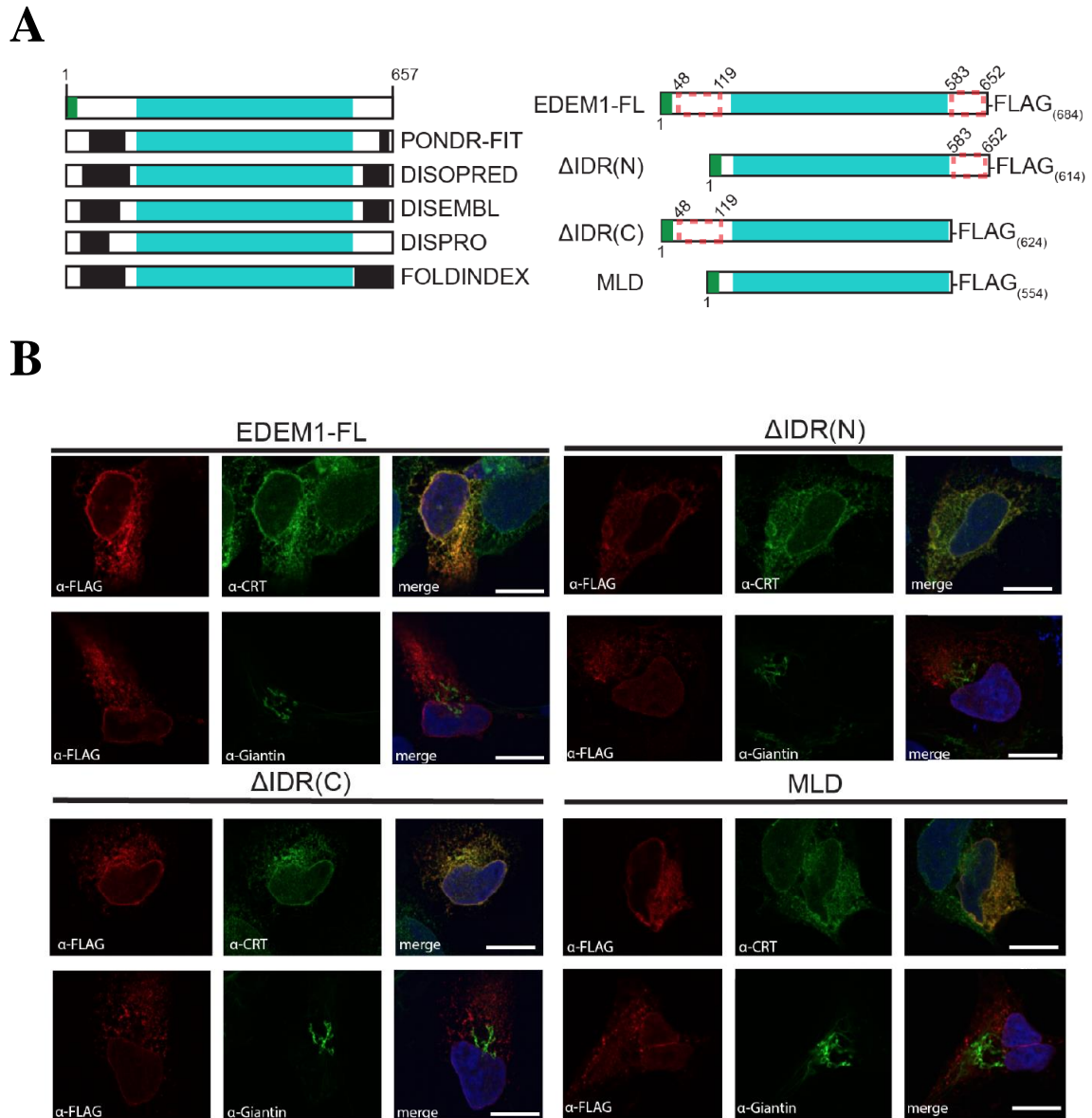Asterisk denotes background bands. Gels are representative of three independent
experiments.

Figure 3.5 EDEM1 constructs lacking either or both IDRs are targeted to the ER

(A) (Left) Cartoon representation of human EDEM1 depicting signal sequence (green), MLD (cyan), and predicted disordered regions (black). (Right) FLAG-tagged EDEM1 constructs lacking either IDRs (ΔIDR N and ΔIDR C) or both (MLD). **(B)** Images of exogenously expressed FLAG-tagged EDEM1, EDEM1 ΔIDR (N), EDEM1 ΔIDR (C), and MLD obtained by confocal microscopy. Fixed cells were stained with FLAG, CRT (ER), or Giantin (Golgi) antisera. Nuclei were visualized by DAPI staining (Blue). Scale bars correspond to 10 μm.
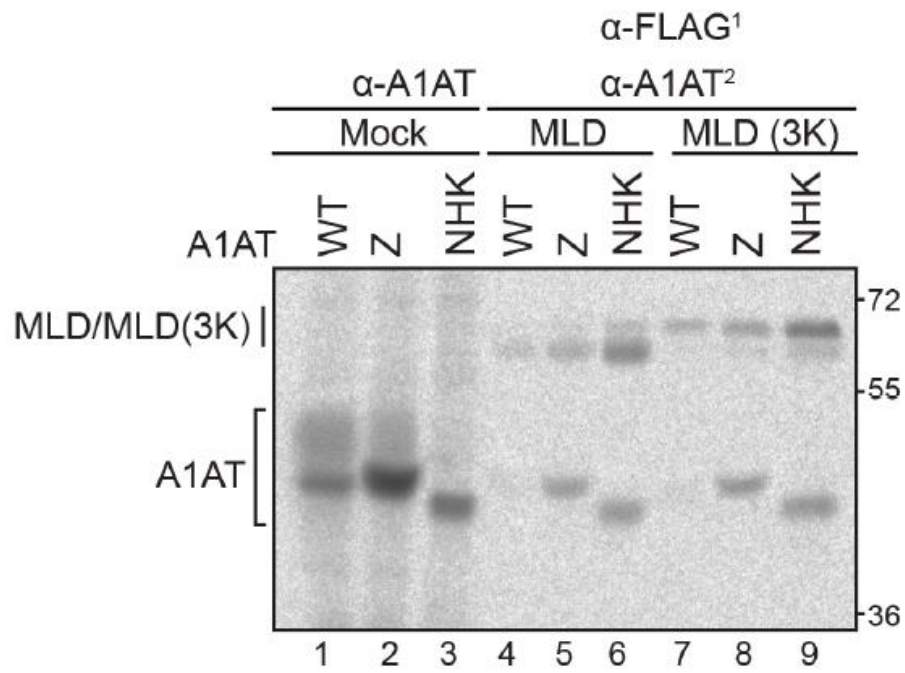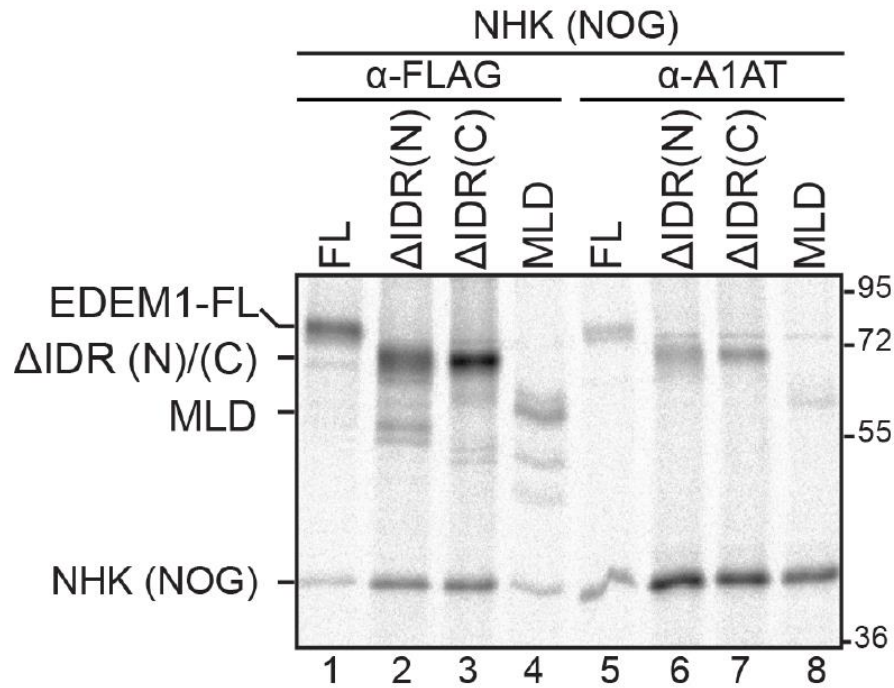
A

B

C

D

73
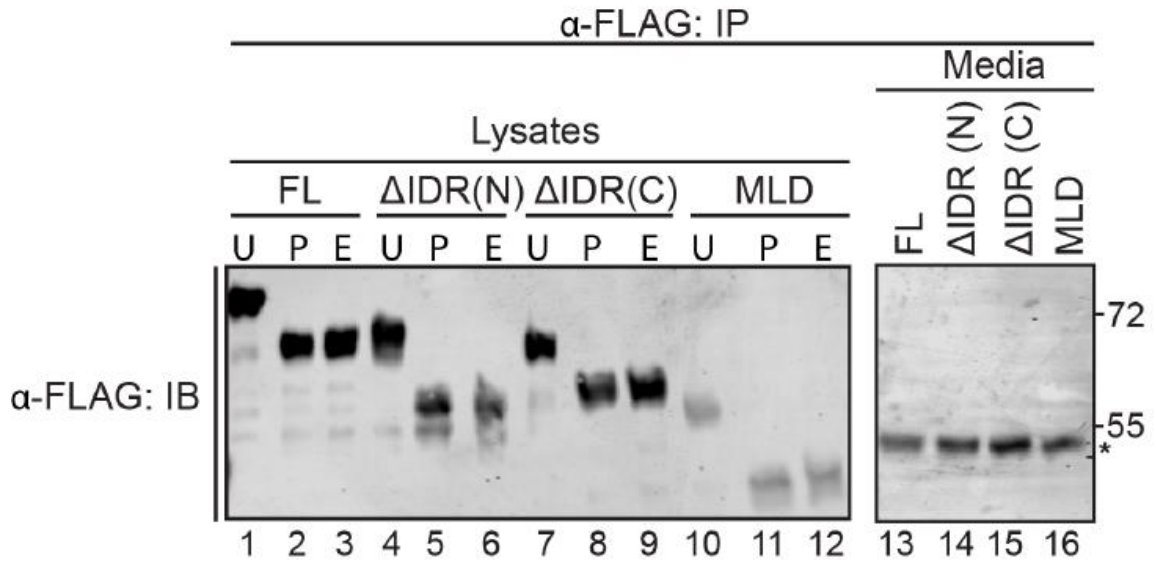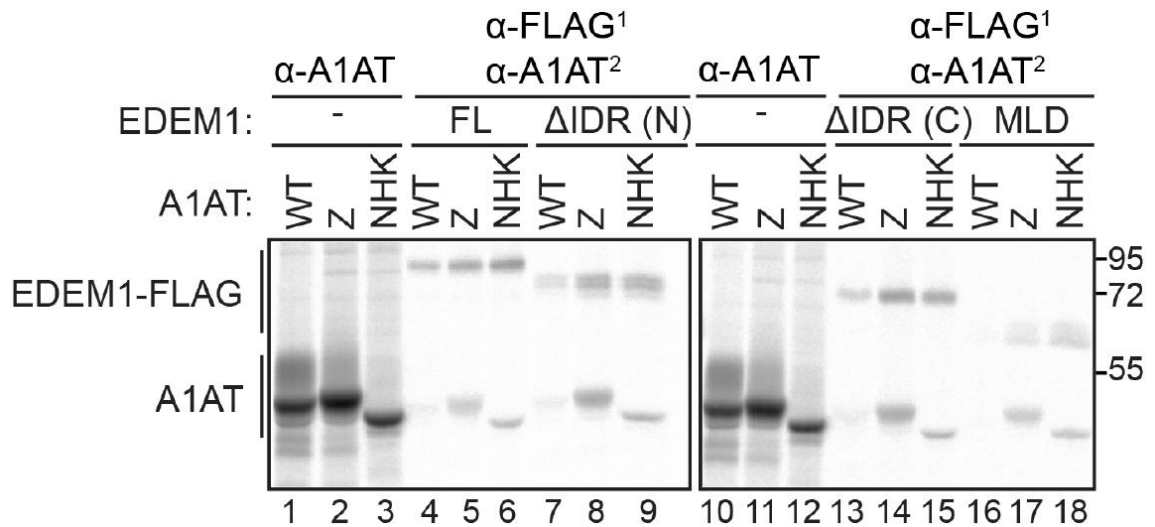
Figure 3.6 EDEM1 lacking IDRs is retained in the ER and preferentially interacts with ERAD substrates in a glycan-independent manner

(A) HEK293T cells were transfected with FLAG-tagged EDEM1-FL, -ΔIDR(N), -ΔIDR(C) and MLD. Cells were lysed in MNT buffer. Lysate and media samples were subjected to anti-FLAG immunoprecipitation and proteins samples were treated with PNGaseF, EndoH, or left untreated (U). Proteins were resolved on a 7.5% reducing SDS-PAGE and immunoblotted against FLAG. Asterisk denotes IgG heavy chain. **(B)** Empty plasmid (-), EDEM1 (FL)-FLAG, ΔIDR(N)-FLAG, ΔIDR(C)-FLAG and MLD-FLAG constructs were co-transfected with the A1AT WT, Z and NHK in HEK293T cells. Proteins were radiolabeled for 30 min with [35S]-Cys/Met and chased for 1 hr. Lysates were subjected to sequential (first anti-FLAG, second anti-A1AT), or single anti-A1AT immunoprecipitation. Proteins were resolved on reducing 8% SDS-PAGE. **(C)** MLD-FLAG, MLD (3K)-FLAG, and empty plasmid (Mock) were co-expressed with WT A1AT, Z, or NHK in HEK293T cells. Cells were radiolabled with [35S]-Cys/Met for 30 min and chased for 1 hr. Cells were lysed in MNT buffer containing Triton X-100. 70% of the lysate was subjected to sequential immunoprecipitation (first anti-FLAG, second anti-A1AT), and 20% to anti-A1AT immunoprecipitation. The proteins were resolved on 8% reducing SDS-PAGE. **(D)** FLAG-tagged EDEM1 WT, ΔIDR (N), ΔIDR (C), and MLD were co-expressed in HEK293T cells with NHK NOG. The proteins were radiolabeled with [35S]-Cys/Met for 30 min and chased for 1 hr. Cells were lysed in MNT buffer. Half of the cell lysate was subjected to anti-FLAG immunoprecipitation while the other half to anti-A1AT immunoprecipitation. Proteins were resolved on 9% reducing SDS-PAGE. Gels are representative of three independent experiments.
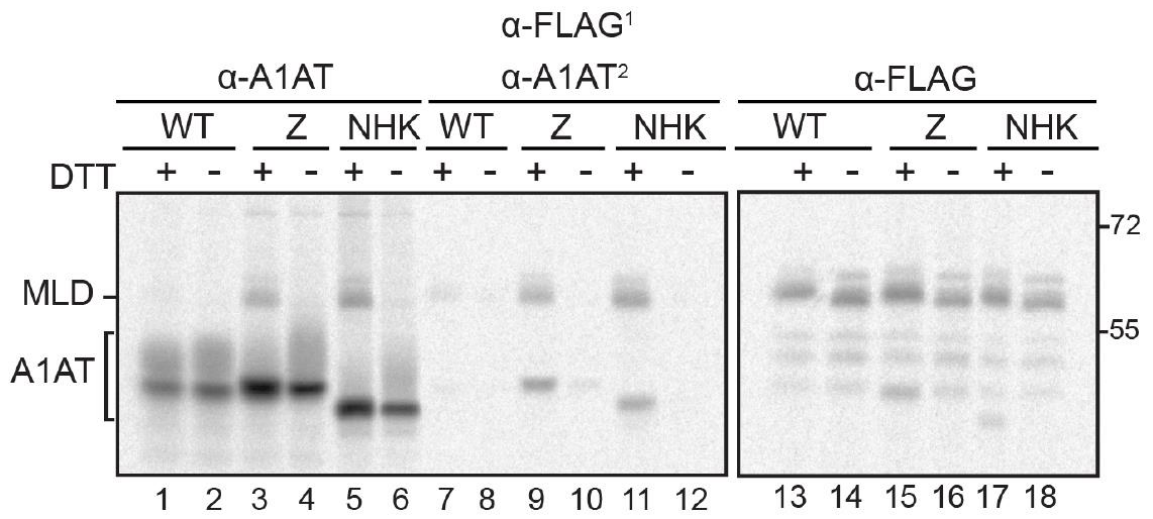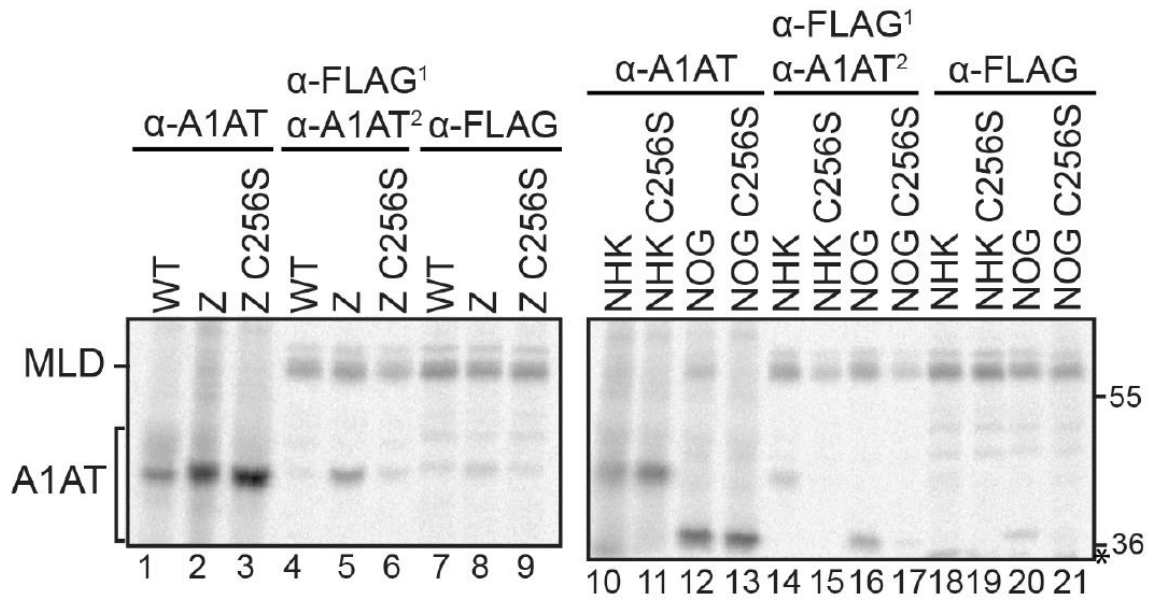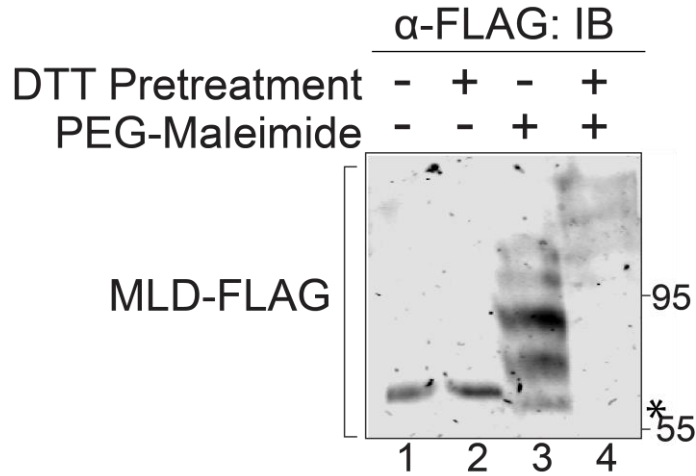
C

Figure 3.7 EDEM1 MLD interacts with Z/NHK through Cys256 and possesses reactive thiols

(A) MLD-FLAG was co-expressed with A1AT WT, Z, or NHK into HEK293T cells. Cells were radiolabled for 30 min and chased for 15 min. DTT (5 mM) was added to the cells for 30 min where indicated (+DTT). Cells were lysed in MNT buffer containing Triton X-100 (TX). A portion of the lysate (65%) was subjected to sequential immunoprecipitation (first anti-FLAG, second anti-A1AT), 20% to anti-A1AT, and 10% to anti-FLAG. The proteins were resolved on 8% reducing SDS-PAGE. **(B)** MLD-FLAG was co-expressed with A1AT WT, Z, Z C256S, NHK, NHK C256S, NHK NOG, and NHK NOG C256S in HEK293T cells. Cells were radiolabled for 30 min and chased for 1 hr and lysed in MNT buffer. Proteins were immunoprecipitated as in A and resolved on 8% reducing SDS-PAGE. Asterisk denotes background band. **(C)** MLD-FLAG was expressed in HEK293T cells. Cells were pretreated for 1 hr with DTT (5 mM) where indicated (+/-). Cells were lysed in sample buffer containing 5 mM peg-maleimide (+ PEG-Maleimide) or 20 mM NEM (- PEG-Maleimide). Proteins were resolved on 8% SDS-PAGE and immunoblotted against FLAG antibody. Gels are representative of three independent experiments.
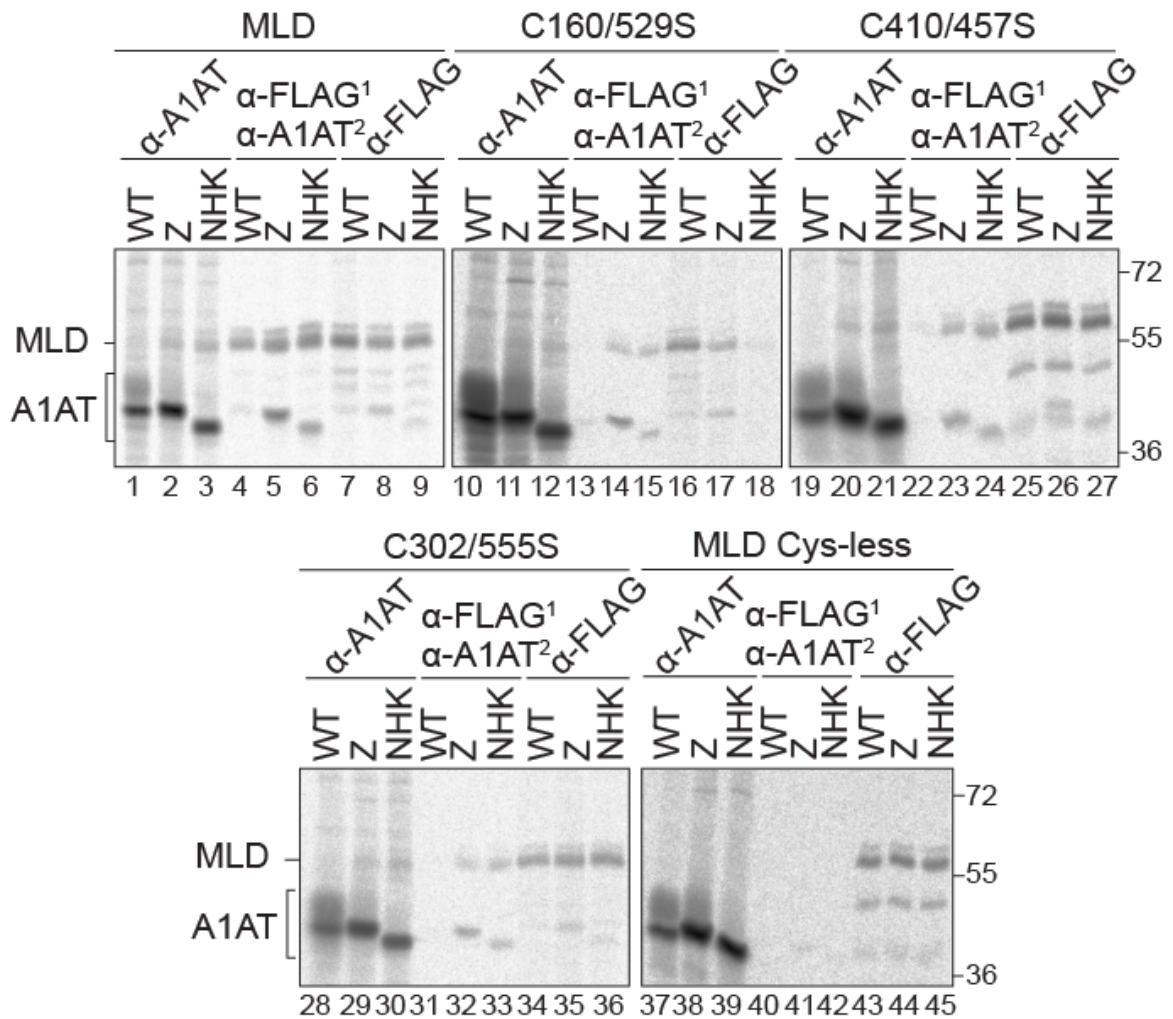
Figure 3.8 EDEM1 MLD Cys-less does not interact with NHK/Z

MLD-FLAG, MLD C160/529S, MLD C410/457S, MLD C302/555S, and MLD Cys-less were co-expressed in HEK293T cells with WT A1AT, Z or NHK. The proteins were radiolabeled for 30 min and chased for 1 hr. Cells were lysed in MNT buffer containing Triton X-100 (TX). A portion of the lysate (65%) was subjected to sequential immunoprecipitation (first anti-FLAG, second anti-A1AT), 20% to anti-A1AT, and 10% to anti-FLAG. The proteins were resolved on 8% reducing SDS-PAGE. Gels are representative of three independent experiments
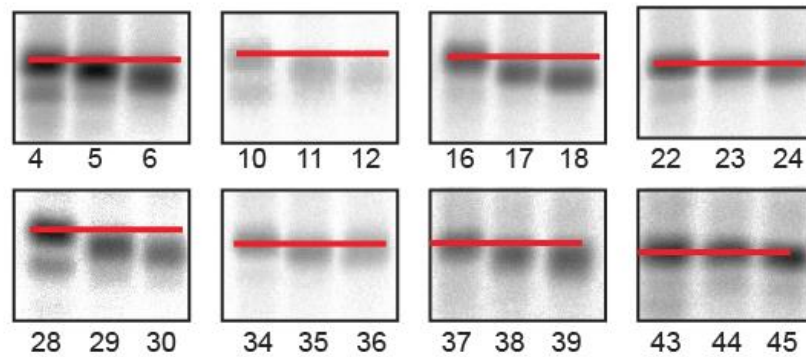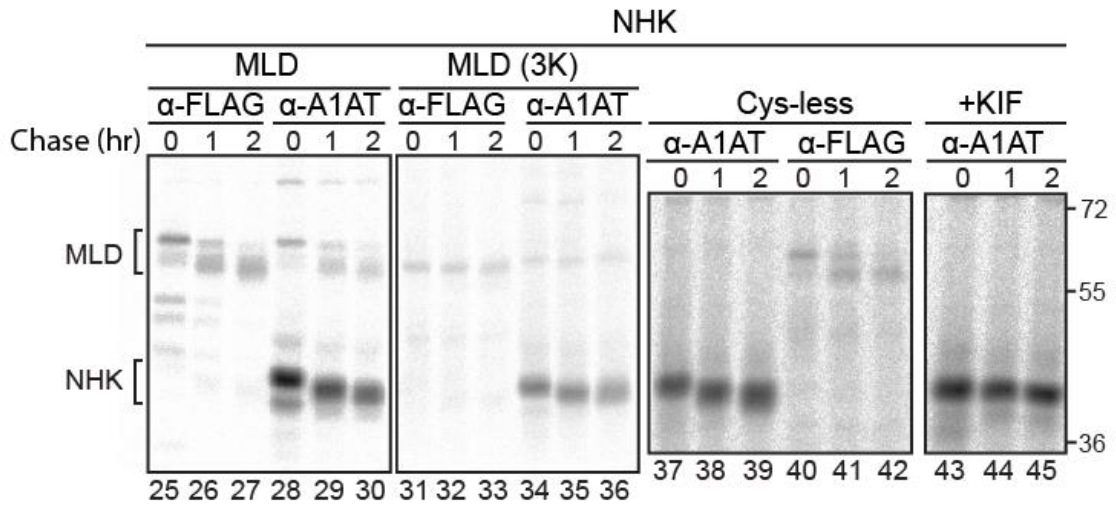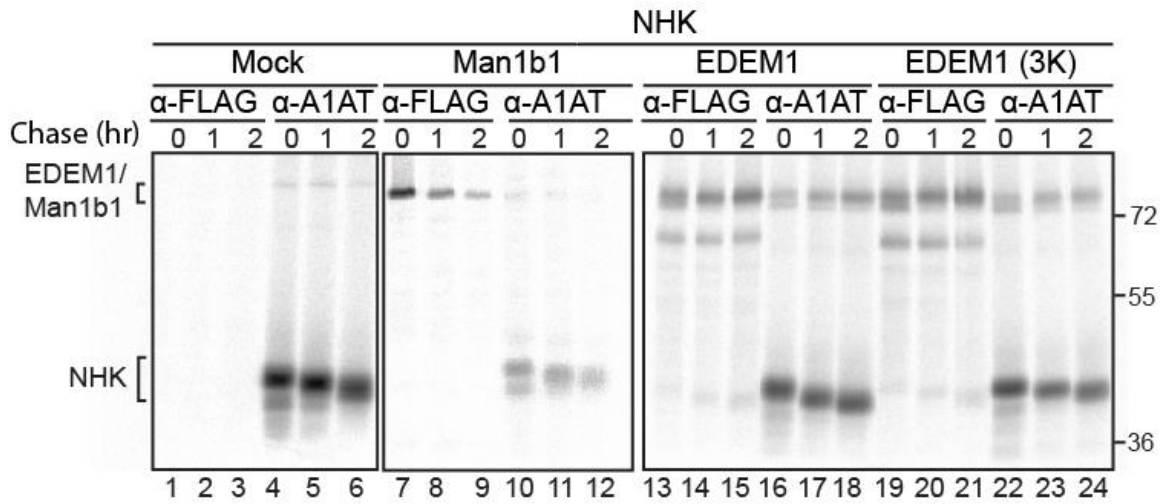
Figure 3.9 EDEM1 MLD promotes glycan trimming

(Top and middle panels) Empty plasmid (Mock), Man1b1-FLAG, EDEM1-FLAG, EDEM1 (3K)-FLAG, MLD-FLAG, MLD (3K)-FLAG, MLD (Cys-less)-FLAG and empty plasmid (mock) were co-expressed with NHK in Man1a1/a2/b1/c1 KO CHO cells. 150 mM Kifunensine (KIF) was added for 5 hr prior to the pulse, where indicated. Proteins were radiolabeled for 30 min with [^{35}S]-Cys/Met and chased for 0, 1, and 2 hr. Cells were lysed in MNT buffer and lysates were divided equally and subjected to anti-FLAG and anti-A1AT immunoprecipitation. Proteins were resolved on reducing 8% SDS-PAGE. (Bottom panels) The NHK bands in the designated lanes was magnified and a red line was drawn through the center of each 0 hr time point and through 2 hr time point to illustrate mobility shifts. Gels are representative of three independent experiments.
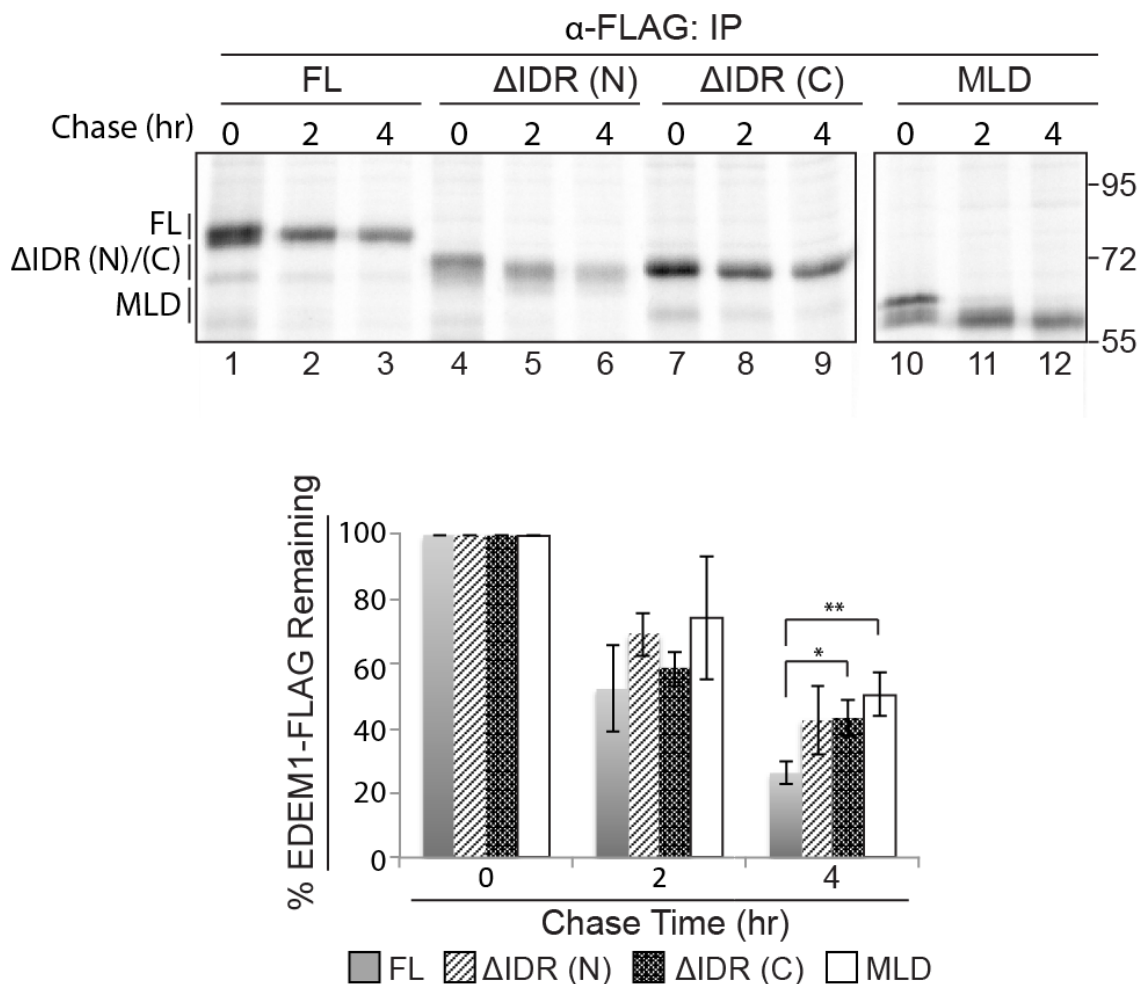
Figure 3.10 EDEM1 IDRs contribute to its rapid turnover

(Top panel) FLAG-tagged EDEM1-ΔIDR(N)/(C) and MLD were transfected into HEK293T. Proteins were radiolabeled for 30 min with [35S]-Cys/Met, and cells were lysed in MNT buffer. Time points were collected at 0, 2, and 4 hr after the pulse. Proteins were resolved on reducing 8% SDS-PAGE. (Bottom panel) The amount of EDEM1 protein remaining at 2 hr and 4 hr was quantified and normalized to the starting material (0 h) and averaged from three independent experiments. Statistical significance between MLD, EDEM1-ΔIDR (N) or (C) and EDEM1 (FL) at 4 hr was determined by an unpaired t-test, the measurement designated (**) has a p value of 0.005, and that of (*) is 0.012. Error bars represent mean ±S.E.
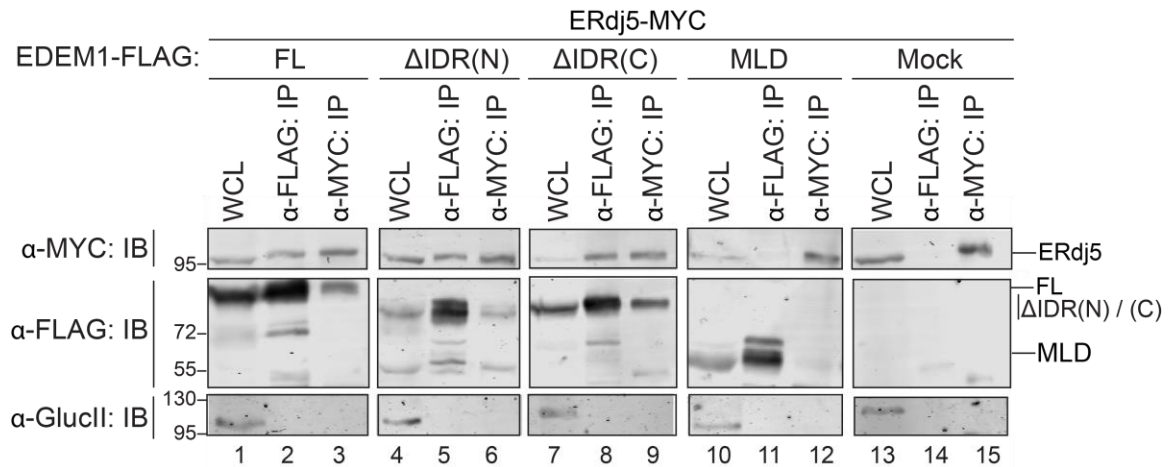
Figure 3.11 EDEM1 IDRs are required for the ERdj5 association

FLAG-tagged EDEM1 (FL), EDEM1-ΔIDR(N), EDEM1-ΔIDR(C), MLD-FLAG, and empty plasmid (mock) were co-expressed with ERdj5-MYC in HEK293T cells. Cells were lysed in HBS buffer containing CHAPS. 10% of the lysate was collected for whole cell lysate (WCL), 40% for anti-FLAG and anti-MYC immunoprecipitation. Proteins were resolved on 8% reducing SDS-PAGE and immunoblotted against MYC, FLAG, and glucosidase II (GlucII). Gels are representative of three independent experiments.

A
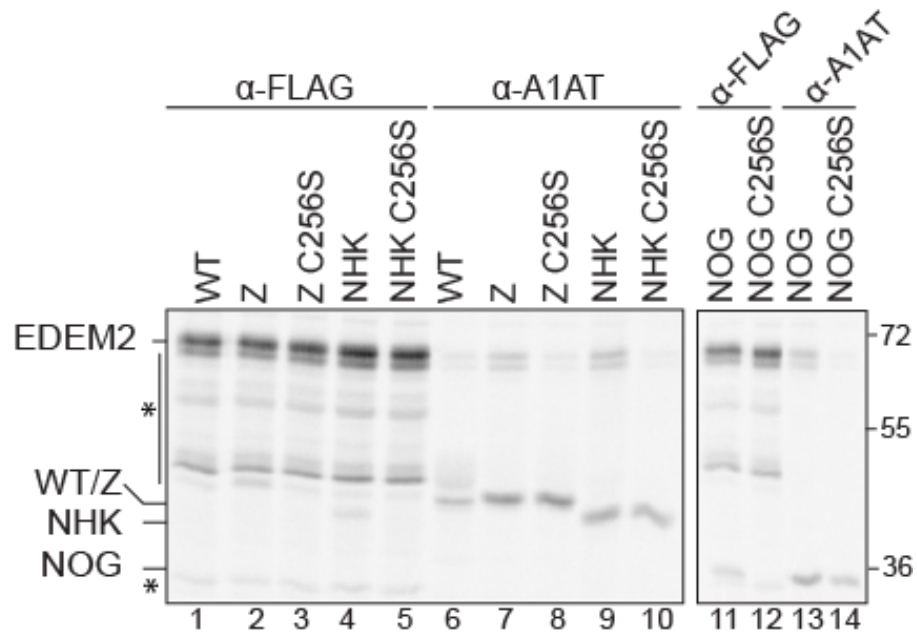
B

Figure 3.12 EDEM2 exhibits thiol-dependent binding to Z/NHK and exposes reactive thiols

(A) EDEM2-FLAG was co-expressed with WT A1AT, Z, Z C256S, NHK, NHK C256S, NHK NOG, and NHK NOG C256S in HEK293T cells. Cells were readiolabeled with [35S]-Cys/Met for 30 min and chased for 1 hr. Cells were lysed in MNT buffer containing Triton X-100. EDEM2 and A1AT variants were isolated using anti-FLAG and anti-A1AT immunoprecipitations, respectively. Proteins were resolved on 9% reducing SDS-PAGE. Asterisks denote background bands. **(B)** (Right panel) EDEM2-FLAG was expressed in HEK293T cells. Cells were pretreated with DTT (5 mM) where indicated (+/-). Cells were lysed in sample buffer containing 5 mM peg-maleimide (+ PEG-Maleimide) or 20 mM NEM (- PEG-Maleimide). Proteins were resolved on 8.5% SDS-PAGE and immunoblotted with FLAG antibody. (Left panel) Cartoon representation of EDEM2 Depicting signal peptide (green), MLD (cyan), Putative catalytic residues (red), Cys residues (yellow), predicted disulfides (*), and predicted IDRs (Red dashed box). Gels are representative of three independent experiments.
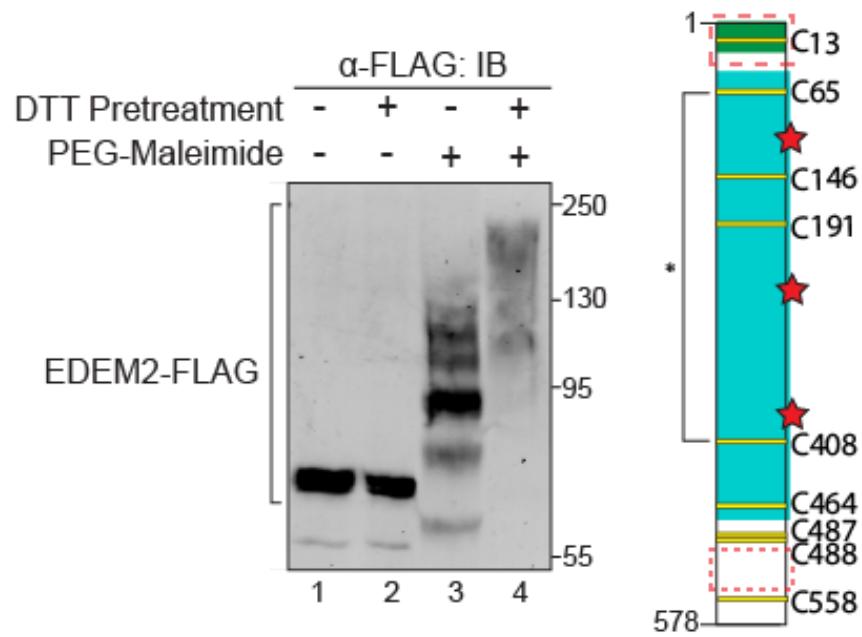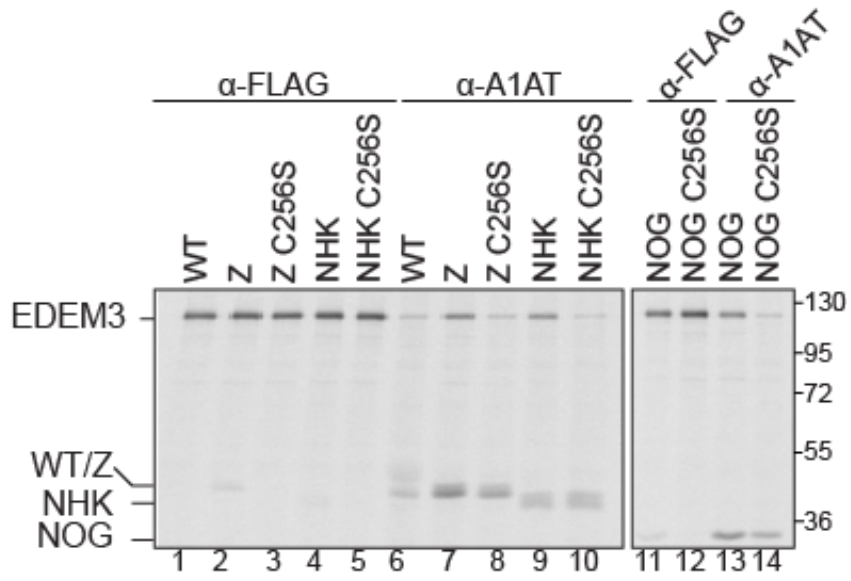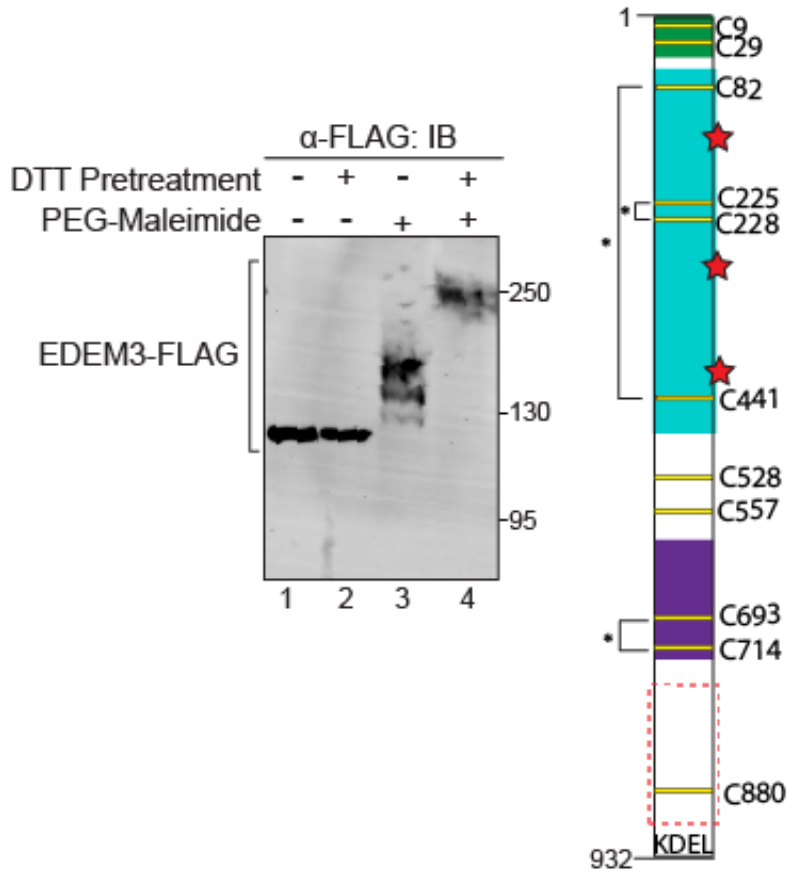
Figure 3.13 EDEM3 exhibits thiol-dependent binding to Z/NHK and exposes reactive thiols

(A) EDEM3-FLAG was co-expressed with WT A1AT, Z, Z C256S, NHK, NHK C256S, NHK NOG, and NHK NOG C256S in HEK293T cells. Cells were readiolabeled with [35S]-Cys/Met for 30 min and chased for 1 hr. Cells were lysed in MNT buffer containing Triton X-100. EDEM2 and A1AT variants were isolated using anti-FLAG and anti-A1AT immunoprecipitations, respectively. Proteins were resolved on 9% reducing SDS-PAGE. Asterisks denote background bands. (B) (Right panel) EDEM3-FLAG was expressed in HEK293T cells. Cells were pretreated with DTT (5 mM) where indicated (+/-). Cells were lysed in sample buffer containing 5 mM peg-maleimide (+ PEG-Maleimide) or 20 mM NEM (- PEG-Maleimide). Proteins were resolved on 8.5% SDS-PAGE and immunoblotted with FLAG antibody. (Left panel) Cartoon representation of EDEM3 depicting signal peptide (green), MLD (cyan), protease-associated domain (purple), putative catalytic residues (red), Cys residues (yellow), predicted disulfides (*), and predicted IDRs (Red dashed box). Gels are representative of three independent experiments.
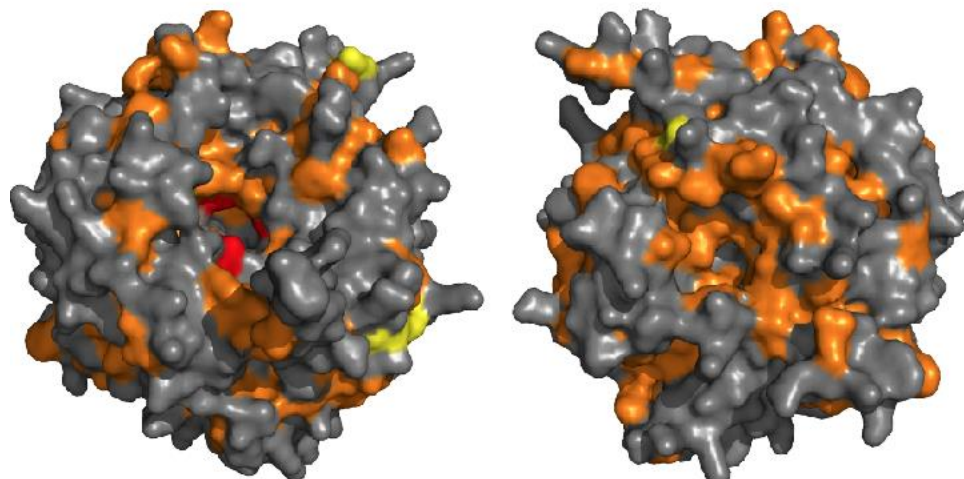
Figure 3.14 Structural model of the human EDEM1 MLD exhibits surface-exposed hydrophobic patches

(Left) Front view of the MLD surface model (Phyre 2.0) (1) depicting three putative catalytic residues (red), Cys residues (yellow), and hydrophobic residues (orange), and Cys residue (yellow). (Right) Back view.
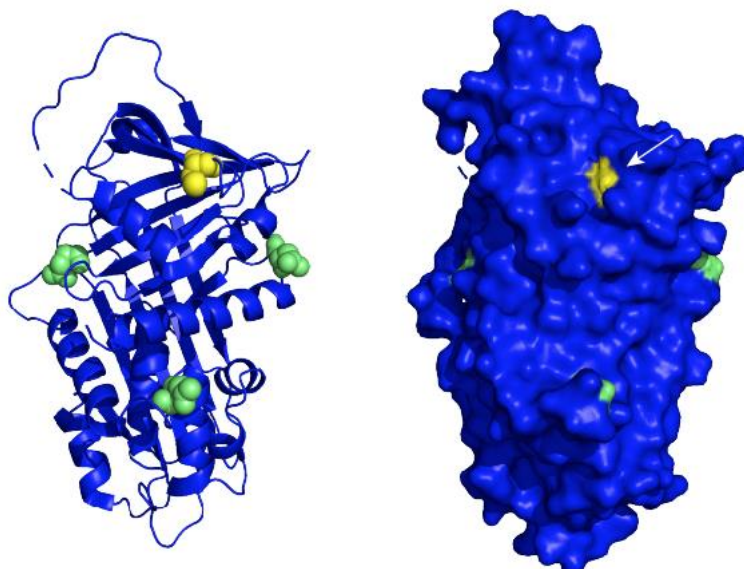
Figure 3.15 A1AT Cys256 is partially buried

(Left) Ribbon representation of A1AT (PDB: 3DRM) depicting three glycosylation sites (green) and Cys256 (yellow). (Right) Surface model of A1AT showing partially buried Cys256 (arrow).

CHAPTER 4

CONCLUSIONS AND FUTURE DIRECTIONS

The ER is a complex organelle that copes with constant stresses due to an influx of nascent polypeptides, which it must process and sort in a crowded environment, all the while avoiding aggregation of misfolded proteins and maintaining proper protein homeostasis. As such, a network of regulated quality control components has evolved to serve as a system of checks and balances to promote protein folding and facilitate degradation. This system is centered around core chaperone proteins, each functioning in distinct ways that act on a variety of substrates ranging from fast folding proteins to slow folding bulky proteins that require multimeric assembly.

A subset of this quality control machinery is specialized in folding, repairing and sorting glycoproteins. Determining the role of EDEM1 in ERAD has been an area of interest and goal for many groups. As more research has been conducted on ERQC ERAD and over the past two decades on EDEM1, we are beginning to uncover EDEM1's unique modes of interaction and its overall function in ERAD. We have demonstrated that EDEM1 exhibits redox-sensitive substrate-binding properties as well as weak protein-protein interactions; further expanding our understanding of the many ways EDEM1 binds its partners. Additionally, we showed that both IDRs, which are responsible for the fast turnover rate of EDEM1, are required for ERdj5 binding but neither was required for NHK binding. Lastly, we demonstrated that the ability to preferentially interact with ERAD substrates and the redox-sensitive binding is an intrinsic property of the MLD.

Determining the oxidative state of EDEM1 and the implications of the redox-sensitive binding

Using detergents of varying strengths and in the presence of the reducing agent DTT, EDEM1 was found to bind NHK and Z through covalent and weak interactions (Figure 3.1). The covalent interactions were mediated through the single Cys residue on NHK and Z (Figure 3.2). Although the Cys residue has previously been implicated in the ER retention and secretion of Z, this is the first time it has been reported to mediate binding to EDEM1 and the first time that a Cys-dependent substrate-binding requirement has been demonstrated for EDEM1.

Many of the known ERAD clients possess Cys residues and some possess unpaired Cys. Like the WT α1-antitrypsin and the ERAD variants, WT transthyretin (TTR) and the ERAD substrate TTR (D18G) possess a single Cys residue that, for the WT, is required for stabilizing the TTR tetramer (Kingsbury et al., 2008). BASE457 is proposed to possesses unpaired Cys residues as suggested by aggregate formation upon treatment with the oxidizing agent diamide (Molinari et al., 2002). While the ERAD-targeted ribophorin 1 (332) possesses no Cys. It would be of interest to see whether the Cys residues on these, particularly BACE457 as its interaction with EDEM1 has been established, and other ERAD clients, are involved in binding to EDEM family proteins. Furthermore, it would be interesting to see whether incorporating a Cys residue on TTR (D18G), which is not a known EDEM1 client, would promote its recognition by EDEM1. Another experiment of interest is to strategically incorporate Cys residues, in such a way that aberrant dimers are not formed, onto properly folded mature proteins like A1AT.

We demonstrated that NHK lacking all three of its glycans (NOG) and possessing the Cys256Ser mutation no longer interacted with EDEM1, while NHK NOG possessing Cys256 did interact (data not shown). Since the glycans are not present on NHK NOG, thus do not mediate an interaction with EDEM1, and the only difference between the two proteins is the presence of Cys256, it would of interest to use this this protein to determine whether EDEM1 recognizes other regions on NHK, such as exposed hydrophobic regions, or whether this interaction is mediated through auxiliary ERAD machinery proteins that do not bind WT A1AT.

A cell-based assay was utilized to identify reactive thiols on EDEM1 using maleimide modification revealed that a subset of the Cys on EDEM1 is unpaired and accessible to maleimide labeling, and a subset is involved in disulfides or inaccessible to modification (Figure 3.3). The purpose of this assay served as a first step in determining whether the Cys on EDEM1 were directly involved in the redox-sensitive interaction with NHK and Z. Although the cell-based maleimide modification technique used in this study is appropriate for revealing reactive thiols, the technique has a few shortcomings especially in terms of determining a disulfide map. For example, the Cys residues that were not accessible to maleimide modification can only be conclusively identified as being involved in disulfides, which encompasses potential disulfides within EDEM1 as well as disulfides between EDEM1 and another protein like an oxidoreductase.

A technique such as mass spectrometry would be better suited for determining the disulfide map of EDEM1. Attempts to identify the EDEM1 disulfide map using mass spectrometry and differential alkylation methods proved challenging. EDEM1 expressed

in mammalian cells in a large-scale setting and isolated through immunoprecipitation was subjected to differential alkylation using N-ethylmaleimide (NEM) and deuterium-labeled N-ethylmaleimide in a recent collaborative effort (data not shown) and uncovered a few issues. First, obtaining adequate amounts of EDEM1 from HEK293T cells through FLAG immunoprecipitation proved challenging, and with each optimization attempts yielding low amounts of EDEM1. Instead, performing affinity column purification or expressing EDEM1 in cells that are more suitable to handle the stresses of EDEM1 overexpression, for instance pancreatic cell lines, would be preferable.

Second, although steps were carried out to label reactive thiols with NEM and any paired Cys with deuterium-labeled NEM, post reduction, it appears that each Cys is involved in forming disulfides to a certain degree, as monitored by NEM: deuterium-labeled NEM ratios. These disulfides are either intermediate disulfides or indicative that the native disulfides on EDEM1 are dynamic, which is difficult to determine using the current method. Furthermore, using this method yielded all Cys except for two as enzymatic cleavage was incomplete. To accurately determine a disulfide map for EDEM1 and identify the Cys that are unpaired, future work should employ techniques to trap peptides linked through disulfide bonds, differentiate intra- from intermolecular disulfides and acquiring purified, natively folded EDEM1 to help resolve issues of trapping non-native intermediate disulfides.

Through a series of Cys to Ser single or combinational point mutations, we determined that not a single Cys is solely responsible for the interaction with NHK through Cys256 nor are the predicted unpaired Cys. Instead, it appears that at least one

set of the predicted disulfides is necessary for this interaction. How this redox-sensitive binding is mediated remains undetermined. Since an EDEM1-NHK dimer is not observable (data not shown), it is likely that the redox-sensitive binding is mediated through an oxidoreductase. Shedding light on this possible mode of interaction could be achieved by employing mass spectrometry in combination with Cys mutations to identify the EDEM1 binding partners under oxidative and reducing conditions. Preliminary data using sucrose sedimentation of the EDEM1 MLD revealed a difference in complex sizes when comparing MLD under oxidative vs. reducing conditions (Figure 4.1). Further experimentation is required to understand the nature of these complexes.

It remains possible that the reason an EDEM1-NHK is not readily observable because EDEM1 exists in a multi-protein complex, as observed from the presence of higher molecular weight species, thus a shift created from a single NHK monomer is not be substantial. Further experiments are required to identify the components of these high molecular weight species. Furthermore, it remains unknown whether EDEM1 or EDEM2 and EDEM3, recognize and accelerate the degradation of monomeric NHK and Z or the aberrant dimers that are not present in WT A1AT. Since these aberrant dimers are formed through Cys256 it is likely that the observed oxidation-sensitivity is a result of the dimer formation, however sorting this out will require careful analysis.

It was recently determined that the oxidoreductase ERp46, through its active Cys-Xxx-Xxx-Cys domain covalently binds to EDEM3 and that Cys83 and Cys441 on EDEM3 confer mannosidase activity of its MLD, as determined by *in vitro* studies (Yu et al., 2018). The EDEM3 Cys83/441 predicted disulfide is homologous to that of EDEM1

Cys160/529. This predicted disulfide is also conserved on EDEM2. Since our data indicate that either of the two predicted disulfides is required for binding to NHK, a follow up experiment would be to determine whether like EDEM3, these predicted disulfides, specifically Cys160/529, are required for MLD function by monitoring the degradation of NHK. A more direct approach is to use purified components and testing the *in vitro* mannosidase activity of EDEM1 MLD Cys-less, MLD possessing only Cys160/529, or only Cys410/457.

In addition to possessing Cys83/441, EDEM3 possess two more Cys that are separated by two amino acids, thus resembling the Cys-Xxx-Xxx-Cys motif of oxidoreductase (Figure 3.13). Although it is not predicted to structurally resemble a thioredoxin domain, as it is located within the EDEM3 MLD, it would be interesting to see whether that apparent Cys-Xxx-Xxx-Cys motif contributes to the observed redox-sensitive interaction with NHK and Z.

Defining the glycan branch selectivity of EDEM proteins

The catalytic activity of the EDEM1 MLD was determined through overexpression of MLD and MLD (3K) with NHK and monitoring the glycan trimming on NHK through gel mobility shifts (Figure 3.9). Although we confirmed the MLD catalytic activity, the branch specificity on which the MLD acts is another source of uncertainty and will require further investigation.

The EDEM1 MLD is homologous to that of α1-2 mannosidases, which act on α1-2-linked mannoses. These mannoses are located on the terminal ends of the B- and C-

branches and the entire A-branch of N-linked glycans of proteins localized in the ER (Figure 1.2). Since there are three EDEM1 homologs and MAN1B1 in the mammalian ER, it is unclear whether these proteins act separately on individual branches or if they are not branch-specific but rather α1-2-linked mannose specific. Determining the branch-specificity of EDEM1 *in vivo* can be addressed using a variety of gene manipulation techniques and knockout cell lines.

Since the A-branch is critical for CNX/CRT binding, whether or not EDEM1 acts on this branch can be determined through a reglucosylation assay that is well established and routinely used in our lab (Pearse and Hebert, 2010; Tannous et al., 2015a). The mutant Chinese hamster ovary cell line, MI8-5, transfers unglucosylated ($Man_9GlcNac_2$) N-linked glycans, which can then acquire a single glucose moiety on the terminal mannose of the A-branch through the activity of UDP-Glc:glycoprotein glucosyltransferase 1 (UGT1) (Hebert et al., 1995). Levels of A-branch reglucosylation can be monitored by inhibiting glucosidase II (Figure 1.3), which removes the glucose moiety added on by UGT1, and subjecting the lysates to affinity pull-down using GST-calreticulin. If EDEM1 acts on the A-branch, then more reglucosylated ERAD substrates will accumulate upon knockout of EDEM1/MLD or EDEM1/MLD (3K). Conversely, lower levels of reglucosylation will be observed in cells overexpressing EDEM1. We have obtained preliminary evidence that a mannosidase may be responsible for extracting substrates from calnexin/calreticulin folding cycles in these cell lines, as mannosidase inhibition through KIF or DMJ resulted in increased reglucosylation (Tannous, 2015).

Since the MI8-5 cell line is derived from mutant hamster cell lines, acquiring the nucleotide sequence of the EDEM1gene-for RNAi purposes may be challenging; therefore it would be ideal to perform these experiments in human cells. We have just acquired CRISPR/Cas9 knocked out *alg6* HEK293 cell that we still need to verify (Figure 4.2). Human cell-line that transfers glycans composed solely of the A-branch through *ALG3/ALG12* can be generated through CRISPR/Cas9 knockout. These mutant cell-lines can then be used to monitor reglucosylation upon EDEM1 overexpression or knockdown, as well as look at mannose trimming through gel mobility shifts to see if EDEM1 acts on the A-branch.

Whether EDEM1 acts on the B-branch can be addressed by creating *ALG12* knockout cells, which will transfer N-linked glycans lacking the C-branch. Determining whether Man_6 glycoforms accumulate in cells overexpressing EDEM1, can be addressed using a pull-down assay using Os9 or Yos9p, or through HPLC mediated glycomics.

Similarly, whether EDEM1 acts on the C-branch can be determined via *ALG3* knockout cells, which will transfer N-linked glycans lacking the B-branch. The effects of EDEM1 on the C-branch can be addressed using a GST-fusion with the OS-9 mannose-6-phosphate receptor homology domain (GST- OS9MRH), since OS-9 possesses high affinity to glycans exposing the C-branch α1,6-linked mannose (Hosokawa et al., 2009).

Lastly, since *ALG12/ALG9* knockout will generate glycoforms lacking the terminal mannose on the C-branch we can then determine whether this mutation bypasses the need for EDEM1 by monitoring if substrates still get targeted for degradation in the absence of EDEM1 (ex. EDEM1 CRISPR/Cas9 knockout). If not, it possible that that

EDEM1 is required to act on the A-branch or that it also functions as a lectin that recognizes the α1-6-linked mannoses to target the ERAD substrate for degradation.

Determining whether the EDEM1 or the MLD preferentially binds untrimmed glycoforms on ERAD machinery such as SEL1L or on ERAD targeted misfolded substrates can also be accomplished using the cell lines MadIA214 which transfer $Glc_1Man_5GlcNAc_2$ *en bloc* and the B3F7 which transfer $Glc_3Man_5GlcNAc_2$ *en bloc* (Ermonval et al., 2001; Stoll et al., 1988; Foulquier et al., 2004). Although these hamster cell-lines have been previously used for ERAD studies, it is not clear that ERAD is functional, as every glycoprotein, including ERAD machinery, would appear to exhibit extensively demannosylated glycans which are thought to be signals for degradation.

Lastly, genomic editing can also be utilized to create human cell lines depleted of EDEM2 and EDEM3, individually or in combination, as has been done in chicken cell lines (Ninagawa et al., 2015). Glycans from these cell lines can be subjected to glycomics to identify the most abundant glycoform from each condition.

Determining the substrate binding properties and characteristics of endogenous EDEM1

Our research has further expanded our knowledge on EDEM1 and its ability to use different binding modalities to interact with substrates or machinery. We also demonstrated mannosidase activity of the EDEM1 MLD. However these conclusions are derived from studies in which EDEM1 is overexpressed, as such they may promote binding and glycan trimming due to the increase in local EDEM1 concentration. This is

especially true when considering that the relative abundance of EDEM1 in mammalian cell is low until it is upregulated by the unfolded protein response. Thus, in order to fine-tune the precise role of EDEM1 in ERAD and ERQC, it is important to study the function and properties of endogenously expressed EDEM1.

Since commercially available antibodies of EDEM1 do not appear specific, as those that we tested either appear to recognize a non-glycosylated protein (~75kD) that does not shift upon treatment with PNGaseF treatment, do not recognize the overexpressed EDEM1, or the protein that is recognized does not appear upregulated by ER-stress. Ideally, monoclonal antibodies with a strong specificity toward EDEM1 should be carefully and strategically generated in order to better study endogenous EDEM1. Since generating antibodies is a time consuming and difficult task that does not guarantee positive results, a more streamlined way to study the binding properties and catalytic activity of EDEM1 is by introducing a C-terminal tag on the endogenous loci using CRISPR/Cas9.

Another unanswered question is how are the soluble MLD and ΔIDR constructs retained in the ER? Full-length EDEM1 exhibits dual topology and exists as a soluble and membrane-bound substrate (Tamura et al., 2011). A preliminary experiment demonstrated that all constructs, which possess the same signal peptide/transmembrane segment as full-length EDEM1, also exhibit dual topology (Figure 4.3). Hence, the ER retention of soluble EDEM1 is inherent to the MLD and possibly mediated through binding to auxiliary proteins; however, which protein and how this is mediated has not yet been determined. This can be addressed through gene silencing, or conditional

silencing, of EDEM1 ER-resident binding partners and monitoring the localization of EDEM1.

Lastly it is not clear if the EDEM1 IDR regions possess machinery-binding properties on their own. Expressing tagged versions of these construct and testing their ability to bind ERdj5 is one way to address this issue. Additionally, these regions could be used as baits to trap and identify EDEM1 binding partners through mass spectrometry. However, these experiments may be problematic as it is likely that the disordered regions could bind proteins non-specifically.

<u>Summary</u>

In this study, we have identified a novel redox-sensitive binding modality on EDEM1, which is employed in the interaction with the ERAD substrates NHK and Z. Specifically, the interaction exhibits characteristics of a covalent interaction and is mediated through the lone Cys residue on NHK. We demonstrated that EDEM1 possess reactive thiols at steady state. However, none of these unpaired Cys are involved in the interaction with NHK/Z. Instead, the Cys that are likely paired appeared involved and possibly through an oxidoreductase other than ERjd5. Future work is required to determine the identity of this oxidoreductase.

In addition to the redox-sensitive binding, we also show that the interaction between EDEM1 and NHK/Z involves weak protein-protein interactions of an undetermined nature. We have confirmed the presence of two intrinsically disordered regions on EDEM1. Both disordered regions are required for maintaining the interaction

with ERdj5. The intrinsic disordered properties of the IDRs contribute to the short half-life of EDEM1.

Lastly, we successfully expressed and characterized the EDEM1 mannosidase-like domain (MLD) in mammalian cells. The MLD not only promotes glycan trimming on NHK, but also exhibits the same redox-sensitive substrate binding properties as that of the full-length protein. Moreover, showing that the MLD alone retains all the substrate binding and catalytic characteristics of EDEM1 sets the stage for future work for examining the biophysical properties of the functional MLD *in vitro*, as attempts to do so in the past with the full length protein have proven unsuccessful.
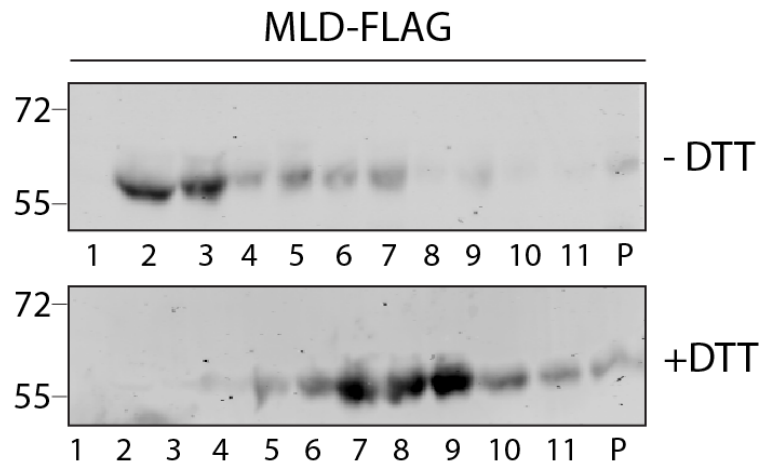
Figure 4.1 EDEM1 MLD sedimentation differs upon addition of DTT

HEK293T cells were transfected with FLAG-tagged EDEM1 MLD and incubated for 48 hr. DTT (5mM) was added for 1 hr prior to lysis. Cells were lysed in MNT buffer, and samples were layered on top of a continuous 10-40 % sucrose gradient in MNT buffer prior to ultracentrifugation. Fractions were collected from the top of the gradient, and proteins were precipitated with trichloroacetic acid. Proteins were resolved on 8.5% SDS-PAGE and immunoblotted against FLAG.
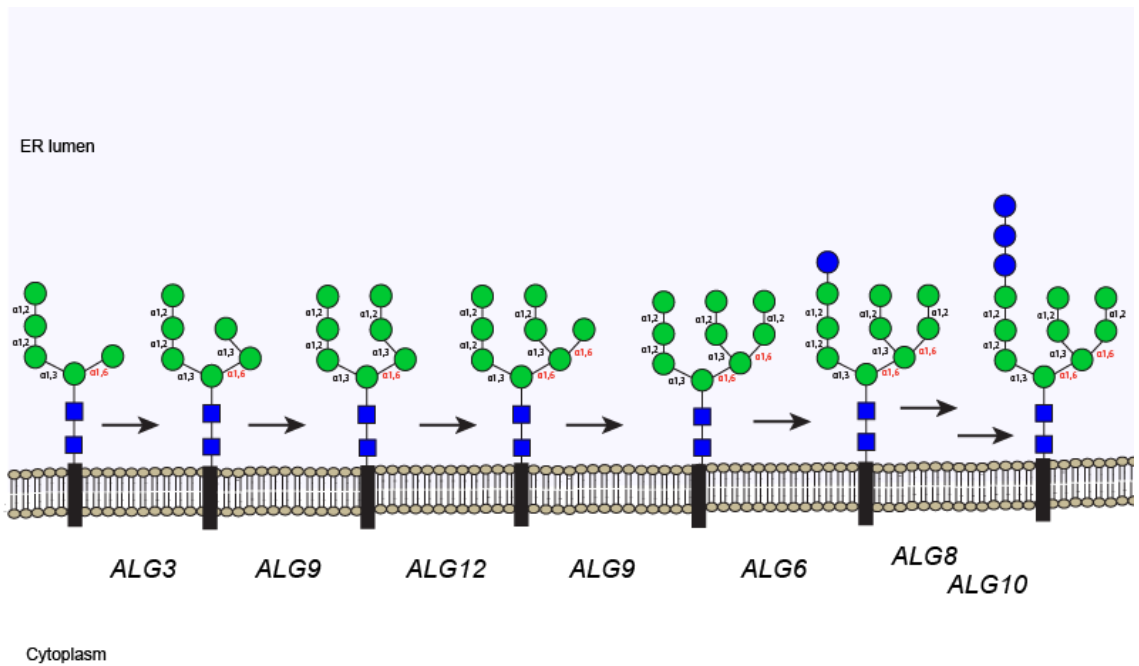
Figure 4.2 Partial schematic of mammalian genes (*ALG*) responsible for the biosynthesis of the B- and C-branches of ER glycans.

The $Man_5GlcNAc_2$ structure is synthesized on a dolichol group (black rectangle). Left to right, *ALG3* and *ALG9* synthesize the B-branch while *ALG12* and *ALG9* create the C-branch. *ALG6*, *ALG8*, and *ALG10* are responsible for adding on the three glucoses (blue circles) to the terminal mannose (green circles) on the A-branch. Red α1,6 linkages denote mannoses recognized by the Os9/Yos9p and XTP3B lectins.

αFLAG: IB
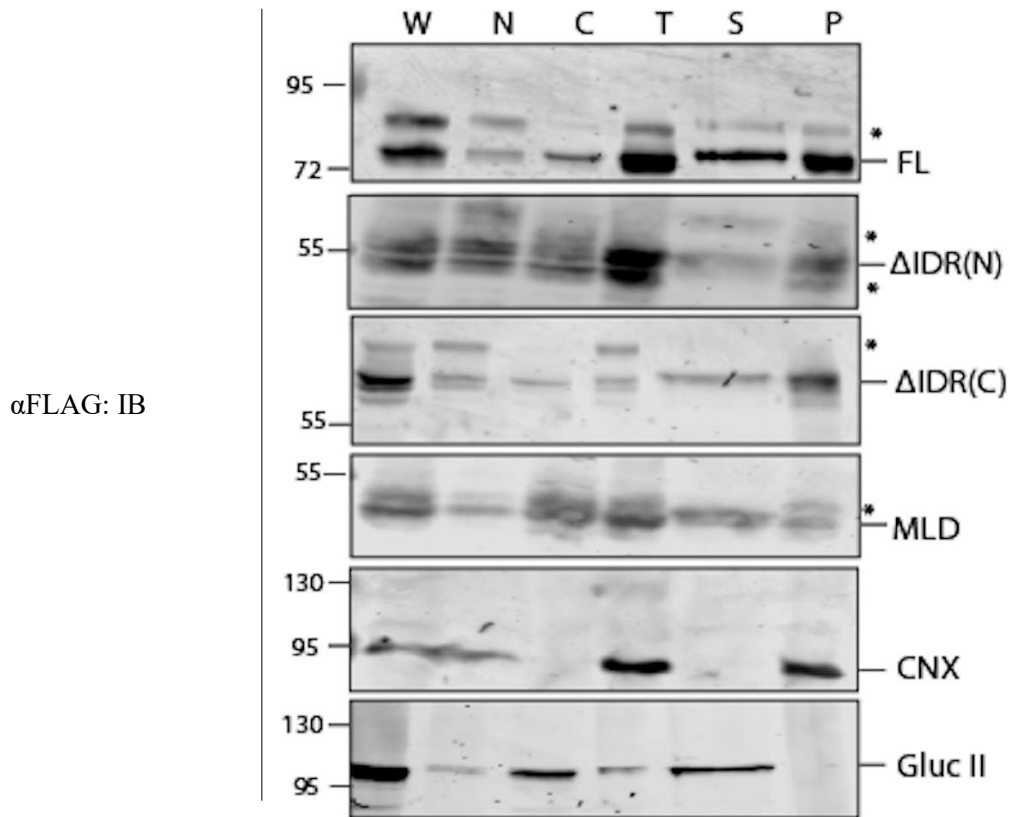
Figure 4.3 EDEM1 FL, ΔIDR (N), ΔIDR (C) and MLD exhibit dual topology and are found in membrane and soluble fractions.

HEK293T cells expressing FLAG-tagged EDEM1 FL, ΔIDR(N), ΔIDR(C) and MLD were homogenized, fractionated and subjected to alkaline extraction. The fractions collected were whole cell lysate (WCL), nucleus (N), cytosol (C), total membrane (TM), as well as supernatant (S) and pellet (P) fractions upon alkaline extraction of the TM. Samples were resolved by reducing 8.5% SDS-PAGE. Asterisks denote non-specific bands.

BIBLIOGRAPHY

Anandasabapathy, N., Ford, G.S., Bloom, D., Holness, C., Paragas, V., Seroogy, C., Skrenta, H., Hollenhorst, M., Fathman, C.G., Soares, L., 2003. GRAIL: an E3 ubiquitin ligase that inhibits cytokine gene transcription is expressed in anergic CD4+ T cells. Immunity 18, 535–547.

Appenzeller-Herzog, C., Ellgaard, L., 2008. The human PDI family: versatility packed into a single fold. Biochim. Biophys. Acta 1783, 535–548. https://doi.org/10.1016/j.bbamcr.2007.11.010

Apweiler, R., Hermjakob, H., Sharon, N., 1999. On the frequency of protein glycosylation, as deduced from analysis of the SWISS-PROT database. Biochim. Biophys. Acta 1473, 4–8.

Arnold, S.M., Fessler, L.I., Fessler, J.H., Kaufman, R.J., 2000. Two homologues encoding human UDP-glucose:glycoprotein glucosyltransferase differ in mRNA expression and enzymatic activity. Biochemistry 39, 2149–2163.

Arnold, S.M., Kaufman, R.J., 2003. The noncatalytic portion of human UDP-glucose: glycoprotein glucosyltransferase I confers UDP-glucose binding and transferase function to the catalytic domain. J. Biol. Chem. 278, 43320–43328. https://doi.org/10.1074/jbc.M305800200

Barlowe, C., Helenius, A., 2016. Cargo Capture and Bulk Flow in the Early Secretory Pathway. Annu. Rev. Cell Dev. Biol. 32, 197–222. https://doi.org/10.1146/annurev-cellbio-111315-125016

Barlowe, C., Orci, L., Yeung, T., Hosobuchi, M., Hamamoto, S., Salama, N., Rexach, M.F., Ravazzola, M., Amherdt, M., Schekman, R., 1994. COPII: a membrane coat formed by Sec proteins that drive vesicle budding from the endoplasmic reticulum. Cell 77, 895–907.

Bause, E., Breuer, W., Schweden, J., Roeser, R., Geyer, R., 1992. Effect of substrate structure on the activity of Man9-mannosidase from pig liver involved in N-linked oligosaccharide processing. Eur. J. Biochem. 208, 451–457.

Belden, W.J., Barlowe, C., 1996. Erv25p, a component of COPII-coated vesicles, forms a complex with Emp24p that is required for efficient endoplasmic reticulum to Golgi transport. J. Biol. Chem. 271, 26939–26946.

Benitez, E.M., Stolz, A., Wolf, D.H., 2011. Yos9, a control protein for misfolded glycosylated and non-glycosylated proteins in ERAD. FEBS Lett. 585, 3015–3019. https://doi.org/10.1016/j.febslet.2011.08.021

Bento, C.F., Renna, M., Ghislat, G., Puri, C., Ashkenazi, A., Vicinanza, M., Menzies, F.M., Rubinsztein, D.C., 2016. Mammalian Autophagy: How Does It Work? Annu. Rev. Biochem. 85, 685–713. https://doi.org/10.1146/annurev-biochem-060815-014556

Bernasconi, R., Pertel, T., Luban, J., Molinari, M., 2008. A dual task for the Xbp1-responsive OS-9 variants in the mammalian endoplasmic reticulum: inhibiting secretion of misfolded protein conformers and enhancing their disposal. J. Biol. Chem. 283, 16446–16454. https://doi.org/10.1074/jbc.M802272200

Bertolotti, A., Zhang, Y., Hendershot, L.M., Harding, H.P., Ron, D., 2000. Dynamic interaction of BiP and ER stress transducers in the unfolded-protein response. Nat. Cell Biol. 2, 326–332. https://doi.org/10.1038/35014014

Bi, X., Mancias, J.D., Goldberg, J., 2007. Insights into COPII coat nucleation from the structure of Sec23.Sar1 complexed with the active fragment of Sec31. Dev. Cell 13, 635–645. https://doi.org/10.1016/j.devcel.2007.10.006

Braakman, I., Lamriben, L., van Zadelhoff, G., Hebert, D.N., 2017. Analysis of Disulfide Bond Formation. Curr Protoc Protein Sci 90, 14.1.1-14.1.21. https://doi.org/10.1002/cpps.43

Breton, C., Snajdrová, L., Jeanneau, C., Koca, J., Imberty, A., 2006. Structures and mechanisms of glycosyltransferases. Glycobiology 16, 29R-37R. https://doi.org/10.1093/glycob/cwj016

Brockmeier, A., Williams, D.B., 2006. Potent lectin-independent chaperone function of calnexin under conditions prevalent within the lumen of the endoplasmic reticulum. Biochemistry 45, 12906–12916. https://doi.org/10.1021/bi0614378

Bukau, B., Horwich, A.L., 1998. The Hsp70 and Hsp60 chaperone machines. Cell 92, 351–366.

Burda, P., Aebi, M., 1999. The dolichol pathway of N-linked glycosylation. Biochim. Biophys. Acta 1426, 239–257.

Burke, J., Lipari, F., Igdoura, S., Herscovics, A., 1996. The Saccharomyces cerevisiae processing alpha 1,2-mannosidase is localized in the endoplasmic reticulum, independently of known retrieval motifs. Eur. J. Cell Biol. 70, 298–305.

Cai, H., Wang, C.C., Tsou, C.L., 1994. Chaperone-like activity of protein disulfide isomerase in the refolding of a protein with no disulfide bonds. J. Biol. Chem. 269, 24550–24552.

Caramelo, J.J., Parodi, A.J., 2008. Getting in and out from calnexin/calreticulin cycles. J. Biol. Chem. 283, 10221–10225. https://doi.org/10.1074/jbc.R700048200

Carvalho, P., Goder, V., Rapoport, T.A., 2006. Distinct ubiquitin-ligase complexes define convergent pathways for the degradation of ER proteins. Cell 126, 361–373. https://doi.org/10.1016/j.cell.2006.05.043

Christianson, J.C., Shaler, T.A., Tyler, R.E., Kopito, R.R., 2008. OS-9 and GRP94 deliver mutant alpha1-antitrypsin to the Hrd1-SEL1L ubiquitin ligase complex for ERAD. Nat. Cell Biol. 10, 272–282. https://doi.org/10.1038/ncb1689

Claessen, J.H.L., Kundrat, L., Ploegh, H.L., 2012. Protein quality control in the ER: balancing the ubiquitin checkbook. Trends Cell Biol. 22, 22–32. https://doi.org/10.1016/j.tcb.2011.09.010

Clerc, S., Hirsch, C., Oggier, D.M., Deprez, P., Jakob, C., Sommer, T., Aebi, M., 2009. Htm1 protein generates the N-glycan signal for glycoprotein degradation in the endoplasmic reticulum. J. Cell Biol. 184, 159–172. https://doi.org/10.1083/jcb.200809198

Cormier, J.H., Pearse, B.R., Hebert, D.N., 2005. Yos9p: a sweet-toothed bouncer of the secretory pathway. Mol. Cell 19, 717–719. https://doi.org/10.1016/j.molcel.2005.08.029

Cormier, J.H., Tamura, T., Sunryd, J.C., Hebert, D.N., 2009. EDEM1 recognition and delivery of misfolded proteins to the SEL1L-containing ERAD complex. Mol. Cell 34, 627–633. https://doi.org/10.1016/j.molcel.2009.05.018

Cruciat, C.-M., Hassler, C., Niehrs, C., 2006. The MRH protein Erlectin is a member of the endoplasmic reticulum synexpression group and functions in N-glycan recognition. J. Biol. Chem. 281, 12986–12993. https://doi.org/10.1074/jbc.M511872200

Dancourt, J., Barlowe, C., 2010. Protein sorting receptors in the early secretory pathway. Annu. Rev. Biochem. 79, 777–802. https://doi.org/10.1146/annurev-biochem-061608-091319

Daniel, P.F., Winchester, B., Warren, C.D., 1994. Mammalian alpha-mannosidases--multiple forms but a common purpose? Glycobiology 4, 551–566.

Danilczyk, U.G., Williams, D.B., 2001. The lectin chaperone calnexin utilizes polypeptide-based interactions to associate with many of its substrates in vivo. J. Biol. Chem. 276, 25532–25540. https://doi.org/10.1074/jbc.M100270200

Dejgaard, K., Theberge, J.-F., Heath-Engel, H., Chevet, E., Tremblay, M.L., Thomas, D.Y., 2010. Organization of the Sec61 translocon, studied by high resolution native electrophoresis. J. Proteome Res. 9, 1763–1771. https://doi.org/10.1021/pr900900x

Denic, V., Quan, E.M., Weissman, J.S., 2006. A luminal surveillance complex that selects misfolded glycoproteins for ER-associated degradation. Cell 126, 349–359. https://doi.org/10.1016/j.cell.2006.05.045

Denisov, A.Y., Määttänen, P., Dabrowski, C., Kozlov, G., Thomas, D.Y., Gehring, K., 2009. Solution structure of the bb' domains of human protein disulfide isomerase. FEBS J. 276, 1440–1449. https://doi.org/10.1111/j.1742-4658.2009.06884.x

Ellgaard, L., Ruddock, L.W., 2005. The human protein disulphide isomerase family: substrate interactions and functional properties. EMBO Rep. 6, 28–32. https://doi.org/10.1038/sj.embor.7400311

Ermonval, M., Kitzmüller, C., Mir, A.M., Cacan, R., Ivessa, N.E., 2001. N-glycan structure of a short-lived variant of ribophorin I expressed in the MadIA214 glycosylation-defective cell line reveals the role of a mannosidase that is not ER mannosidase I in the process of glycoprotein degradation. Glycobiology 11, 565–576.

Foulquier, F., Duvet, S., Klein, A., Mir, A.-M., Chirat, F., Cacan, R., 2004. Endoplasmic reticulum-associated degradation of glycoproteins bearing Man5GlcNAc2 and Man9GlcNAc2 species in the MI8-5 CHO cell line. Eur. J. Biochem. 271, 398–404.

Frand, A.R., Kaiser, C.A., 1999. Ero1p Oxidizes Protein Disulfide Isomerase in a Pathway for Disulfide Bond Formation in the Endoplasmic Reticulum. Molecular Cell 4, 469–477. https://doi.org/10.1016/S1097-2765(00)80198-7

Fredrickson, E.K., Rosenbaum, J.C., Locke, M.N., Milac, T.I., Gardner, R.G., Brodsky, J.L., 2011. Exposed hydrophobicity is a key determinant of nuclear quality control degradation. MBoC 22, 2384–2395. https://doi.org/10.1091/mbc.e11-03-0256

Freeze, H.H., Chong, J.X., Bamshad, M.J., Ng, B.G., 2014. Solving glycosylation disorders: fundamental approaches reveal complicated pathways. Am. J. Hum. Genet. 94, 161–175. https://doi.org/10.1016/j.ajhg.2013.10.024

Frenkel, Z., Gregory, W., Kornfeld, S., Lederkremer, G.Z., 2003. Endoplasmic reticulum-associated degradation of mammalian glycoproteins involves sugar chain trimming to Man6-5GlcNAc2. J. Biol. Chem. 278, 34119–34124. https://doi.org/10.1074/jbc.M305929200

Frickel, E.-M., Frei, P., Bouvier, M., Stafford, W.F., Helenius, A., Glockshuber, R., Ellgaard, L., 2004. ERp57 is a multifunctional thiol-disulfide oxidoreductase. J. Biol. Chem. 279, 18277–18287. https://doi.org/10.1074/jbc.M314089200

Fujimori, T., Kamiya, Y., Nagata, K., Kato, K., Hosokawa, N., 2013. Endoplasmic reticulum lectin XTP3-B inhibits endoplasmic reticulum-associated degradation of a misfolded α1-antitrypsin variant. FEBS J. 280, 1563–1575. https://doi.org/10.1111/febs.12157

Gauss, R., Kanehara, K., Carvalho, P., Ng, D.T.W., Aebi, M., 2011. A Complex of Pdi1p and the Mannosidase Htm1p Initiates Clearance of Unfolded Glycoproteins from the Endoplasmic Reticulum. Molecular Cell 42, 782–793. https://doi.org/10.1016/j.molcel.2011.04.027

Gnann, A., Riordan, J.R., Wolf, D.H., 2004. Cystic fibrosis transmembrane conductance regulator degradation depends on the lectins Htm1p/EDEM and the Cdc48 protein complex in yeast. Mol. Biol. Cell 15, 4125–4135. https://doi.org/10.1091/mbc.E04-01-0024

Gonzalez, D.S., Karaveg, K., Vandersall-Nairn, A.S., Lal, A., Moremen, K.W., 1999. Identification, expression, and characterization of a cDNA encoding human endoplasmic reticulum mannosidase I, the enzyme that catalyzes the first mannose trimming step in mammalian Asn-linked oligosaccharide biosynthesis. J. Biol. Chem. 274, 21375–21386.

Groisman, B., Shenkman, M., Ron, E., Lederkremer, G.Z., 2011. Mannose trimming is required for delivery of a glycoprotein from EDEM1 to XTP3-B and to late endoplasmic reticulum-associated degradation steps. J. Biol. Chem. 286, 1292–1300. https://doi.org/10.1074/jbc.M110.154849

Gülow, K., Bienert, D., Haas, I.G., 2002. BiP is feed-back regulated by control of protein translation efficiency. J. Cell. Sci. 115, 2443–2452.

Hagiwara, M., Maegawa, K.-I., Suzuki, M., Ushioda, R., Araki, K., Matsumoto, Y., Hoseki, J., Nagata, K., Inaba, K., 2011. Structural basis of an ERAD pathway mediated by the ER-resident protein disulfide reductase ERdj5. Mol. Cell 41, 432–444. https://doi.org/10.1016/j.molcel.2011.01.021

Hampton, R.Y., Gardner, R.G., Rine, J., 1996. Role of 26S proteasome and HRD genes in the degradation of 3-hydroxy-3-methylglutaryl-CoA reductase, an integral endoplasmic reticulum membrane protein. Mol. Biol. Cell 7, 2029–2044.

Hara-Kuge, S., Kuge, O., Orci, L., Amherdt, M., Ravazzola, M., Wieland, F.T., Rothman, J.E., 1994. En bloc incorporation of coatomer subunits during the assembly of COP-coated vesicles. J. Cell Biol. 124, 883–892.

Haßdenteufel, S., Johnson, N., Paton, A.W., Paton, J.C., High, S., Zimmermann, R., 2018. Chaperone-Mediated Sec61 Channel Gating during ER Import of Small Precursor Proteins Overcomes Sec61 Inhibitor-Reinforced Energy Barrier. Cell Rep 23, 1373–1386. https://doi.org/10.1016/j.celrep.2018.03.122

Hatahet, F., Ruddock, L.W., 2009. Protein disulfide isomerase: a critical evaluation of its function in disulfide bond formation. Antioxid. Redox Signal. 11, 2807–2850. https://doi.org/10.1089/ars.2009.2466

Hebert, D.N., Foellmer, B., Helenius, A., 1995. Glucose trimming and reglucosylation determine glycoprotein association with calnexin in the endoplasmic reticulum. Cell 81, 425–433.

Hebert, D.N., Molinari, M., 2012. Flagging and docking: dual roles for N-glycans in protein quality control and cellular proteostasis. Trends Biochem. Sci. 37, 404–410. https://doi.org/10.1016/j.tibs.2012.07.005

Hebert, D.N., Molinari, M., 2007. In and out of the ER: protein folding, quality control, degradation, and related human diseases. Physiol. Rev. 87, 1377–1408. https://doi.org/10.1152/physrev.00050.2006

Hegde, R.S., Bernstein, H.D., 2006. The surprising complexity of signal sequences. Trends Biochem. Sci. 31, 563–571. https://doi.org/10.1016/j.tibs.2006.08.004

Hegde, R.S., Kang, S.-W., 2008. The concept of translocational regulation. J. Cell Biol. 182, 225–232. https://doi.org/10.1083/jcb.200804157

Helenius, A., 1994. How N-linked oligosaccharides affect glycoprotein folding in the endoplasmic reticulum. Mol Biol Cell 5, 253–265.

Henrissat, B., 1991. A classification of glycosyl hydrolases based on amino acid sequence similarities. Biochem. J. 280 (Pt 2), 309–316.

Henrissat, B., Bairoch, A., 1996. Updating the sequence-based classification of glycosyl hydrolases. Biochem. J. 316 (Pt 2), 695–696.

Herscovics, A., 2001. Structure and function of Class I alpha 1,2-mannosidases involved in glycoprotein synthesis and endoplasmic reticulum quality control. Biochimie 83, 757–762.

Herscovics, A., Schneikert, J., Athanassiadis, A., Moremen, K.W., 1994. Isolation of a mouse Golgi mannosidase cDNA, a member of a gene family conserved from yeast to mammals. J. Biol. Chem. 269, 9864–9871.

Hirao, K., Natsuka, Y., Tamura, T., Wada, I., Morito, D., Natsuka, S., Romero, P., Sleno, B., Tremblay, L.O., Herscovics, A., Nagata, K., Hosokawa, N., 2006. EDEM3, a Soluble EDEM Homolog, Enhances Glycoprotein Endoplasmic Reticulum-associated Degradation and Mannose Trimming. J. Biol. Chem. 281, 9650–9658. https://doi.org/10.1074/jbc.M512191200

Hoffmann, D., Flörke, H., 1998. A structural role for glycosylation: lessons from the hp model. Fold Des 3, 337–343. https://doi.org/10.1016/S1359-0278(98)00046-7

Hosokawa, N., Kamiya, Y., Kamiya, D., Kato, K., Nagata, K., 2009. Human OS-9, a lectin required for glycoprotein endoplasmic reticulum-associated degradation, recognizes mannose-trimmed N-glycans. J. Biol. Chem. 284, 17061–17068. https://doi.org/10.1074/jbc.M809725200

Hosokawa, N., Tremblay, L.O., Sleno, B., Kamiya, Y., Wada, I., Nagata, K., Kato, K., Herscovics, A., 2010. EDEM1 accelerates the trimming of 1,2-linked mannose on the C branch of N-glycans. Glycobiology 20, 567–575. https://doi.org/10.1093/glycob/cwq001

Hosokawa, N., Wada, I., Hasegawa, K., Yorihuzi, T., Tremblay, L.O., Herscovics, A., Nagata, K., 2001. A novel ER alpha-mannosidase-like protein accelerates ER-associated degradation. EMBO Rep. 2, 415–422. https://doi.org/10.1093/embo-reports/kve084

Hosokawa, N., Wada, I., Nagasawa, K., Moriyama, T., Okawa, K., Nagata, K., 2008. Human XTP3-B forms an endoplasmic reticulum quality control scaffold with the HRD1-SEL1L ubiquitin ligase complex and BiP. J. Biol. Chem. 283, 20914–20924. https://doi.org/10.1074/jbc.M709336200

Iannotti, M.J., Figard, L., Sokac, A.M., Sifers, R.N., 2014. A Golgi-localized Mannosidase (MAN1B1) Plays a Non-enzymatic Gatekeeper Role in Protein Biosynthetic Quality Control. J Biol Chem 289, 11844–11858. https://doi.org/10.1074/jbc.M114.552091

Jaenicke, L.A., Brendebach, H., Selbach, M., Hirsch, C., 2011. Yos9p assists in the degradation of certain nonglycosylated proteins from the endoplasmic reticulum. Mol. Biol. Cell 22, 2937–2945. https://doi.org/10.1091/mbc.E10-10-0832

Jakob, C.A., Bodmer, D., Spirig, U., Battig, P., Marcil, A., Dignard, D., Bergeron, J.J., Thomas, D.Y., Aebi, M., 2001. Htm1p, a mannosidase-like protein, is involved in glycoprotein degradation in yeast. EMBO Rep. 2, 423–430. https://doi.org/10.1093/embo-reports/kve089

Jakob, C.A., Burda, P., Roth, J., Aebi, M., 1998. Degradation of misfolded endoplasmic reticulum glycoproteins in Saccharomyces cerevisiae is determined by a specific oligosaccharide structure. J. Cell Biol. 142, 1223–1233.

Jang, B.-Y., Ryoo, H.D., Son, J., Choi, K.-C., Shin, D.-M., Kang, S.-W., Kang, M.-J., 2015. Role of Drosophila EDEMs in the degradation of the alpha-1-antitrypsin Z variant. Int. J. Mol. Med. 35, 870–876. https://doi.org/10.3892/ijmm.2015.2109

Jansen, G., Määttänen, P., Denisov, A.Y., Scarffe, L., Schade, B., Balghi, H., Dejgaard, K., Chen, L.Y., Muller, W.J., Gehring, K., Thomas, D.Y., 2012. An interaction map of endoplasmic reticulum chaperones and foldases. Mol. Cell Proteomics 11, 710–723. https://doi.org/10.1074/mcp.M111.016550

Jessop, C.E., Watkins, R.H., Simmons, J.J., Tasab, M., Bulleid, N.J., 2009. Protein disulphide isomerase family members show distinct substrate specificity: P5 is targeted to BiP client proteins. J Cell Sci 122, 4287–4295. https://doi.org/10.1242/jcs.059154

Jitsuhara, Y., Toyoda, T., Itai, T., Yamaguchi, H., 2002. Chaperone-like functions of high-mannose type and complex-type N-glycans and their molecular basis. J. Biochem. 132, 803–811.

Karaveg, K., Siriwardena, A., Tempel, W., Liu, Z.-J., Glushka, J., Wang, B.-C., Moremen, K.W., 2005. Mechanism of class 1 (glycosylhydrolase family 47) {alpha}-mannosidases involved in N-glycan processing and endoplasmic reticulum quality control. J. Biol. Chem. 280, 16197–16207. https://doi.org/10.1074/jbc.M500119200

Khodayari, N., Marek, G., Lu, Y., Krotova, K., Wang, R.L., Brantly, M., 2017. Erdj3 Has an Essential Role for Z Variant Alpha-1-Antitrypsin Degradation. J. Cell. Biochem. 118, 3090–3101. https://doi.org/10.1002/jcb.26069

Kingsbury, J.S., Laue, T.M., Klimtchuk, E.S., Théberge, R., Costello, C.E., Connors, L.H., 2008. The Modulation of Transthyretin Tetramer Stability by Cysteine 10 Adducts and the Drug Diflunisal DIRECT ANALYSIS BY FLUORESCENCE-DETECTED ANALYTICAL ULTRACENTRIFUGATION. J. Biol. Chem. 283, 11887–11896. https://doi.org/10.1074/jbc.M709638200

Knittler, M.R., Dirks, S., Haas, I.G., 1995. Molecular chaperones involved in protein degradation in the endoplasmic reticulum: quantitative interaction of the heat shock cognate protein BiP with partially folded immunoglobulin light chains that are degraded in the endoplasmic reticulum. Proc. Natl. Acad. Sci. U.S.A. 92, 1764–1768.

Knop, M., Hauser, N., Wolf, D.H., 1996. N-Glycosylation affects endoplasmic reticulum degradation of a mutated derivative of carboxypeptidase yscY in yeast. Yeast 12, 1229–1238. https://doi.org/10.1002/(SICI)1097-0061(19960930)12:12<1229::AID-YEA15>3.0.CO;2-H

Kornfeld, R., Kornfeld, S., 1985. Assembly of asparagine-linked oligosaccharides. Annu. Rev. Biochem. 54, 631–664. https://doi.org/10.1146/annurev.bi.54.070185.003215

Kosmaoglou, M., Kanuga, N., Aguilà, M., Garriga, P., Cheetham, M.E., 2009. A dual role for EDEM1 in the processing of rod opsin. J. Cell. Sci. 122, 4465–4472. https://doi.org/10.1242/jcs.055228

Kozlov, G., Määttänen, P., Schrag, J.D., Hura, G.L., Gabrielli, L., Cygler, M., Thomas, D.Y., Gehring, K., 2009. Structure of the noncatalytic domains and global fold of the protein disulfide isomerase ERp72. Structure 17, 651–659. https://doi.org/10.1016/j.str.2009.02.016

Kozlov, G., Maattanen, P., Schrag, J.D., Pollock, S., Cygler, M., Nagar, B., Thomas, D.Y., Gehring, K., 2006. Crystal structure of the bb' domains of the protein disulfide isomerase ERp57. Structure 14, 1331–1339. https://doi.org/10.1016/j.str.2006.06.019

Lai, C.W., Otero, J.H., Hendershot, L.M., Snapp, E., 2012. ERdj4 protein is a soluble endoplasmic reticulum (ER) DnaJ family protein that interacts with ER-associated degradation machinery. J. Biol. Chem. 287, 7969–7978. https://doi.org/10.1074/jbc.M111.311290

Lal, A., Pang, P., Kalelkar, S., Romero, P.A., Herscovics, A., Moremen, K.W., 1998. Substrate specificities of recombinant murine Golgi alpha1, 2-mannosidases IA and IB and comparison with endoplasmic reticulum and Golgi processing alpha1,2-mannosidases. Glycobiology 8, 981–995.

Lal, A., Schutzbach, J.S., Forsee, W.T., Neame, P.J., Moremen, K.W., 1994. Isolation and expression of murine and rabbit cDNAs encoding an alpha 1,2-mannosidase involved in the processing of asparagine-linked oligosaccharides. J. Biol. Chem. 269, 9872–9881.

Lamriben, L., Graham, J.B., Adams, B.M., Hebert, D.N., 2016. N-Glycan-based ER Molecular Chaperone and Protein Quality Control System: The Calnexin Binding Cycle. Traffic 17, 308–326. https://doi.org/10.1111/tra.12358

Le Fourn, V., Gaplovska-Kysela, K., Guhl, B., Santimaria, R., Zuber, C., Roth, J., 2009. Basal autophagy is involved in the degradation of the ERAD component EDEM1. Cellular and Molecular Life Sciences 66, 1434–1445. https://doi.org/10.1007/s00018-009-9038-1

Li, Z., Stafford, W.F., Bouvier, M., 2001. The metal ion binding properties of calreticulin modulate its conformational flexibility and thermal stability. Biochemistry 40, 11193–11201.

Liu, Y.-C., Fujimori, D.G., Weissman, J.S., 2016. Htm1p-Pdi1p is a folding-sensitive mannosidase that marks N-glycoproteins for ER-associated protein degradation. Proc. Natl. Acad. Sci. U.S.A. 113, E4015-4024. https://doi.org/10.1073/pnas.1608795113

Marin, M.B., Ghenea, S., Spiridon, L.N., Chiritoiu, G.N., Petrescu, A.-J., Petrescu, S.-M., 2012. Tyrosinase degradation is prevented when EDEM1 lacks the intrinsically disordered region. PLoS ONE 7, e42998. https://doi.org/10.1371/journal.pone.0042998

Mast, S.W., Diekman, K., Karaveg, K., Davis, A., Sifers, R.N., Moremen, K.W., 2005. Human EDEM2, a novel homolog of family 47 glycosidases, is involved in ER-associated degradation of glycoproteins. Glycobiology 15, 421–436. https://doi.org/10.1093/glycob/cwi014

Mast, S.W., Moremen, K.W., 2006. Family 47 alpha-mannosidases in N-glycan processing. Meth. Enzymol. 415, 31–46. https://doi.org/10.1016/S0076-6879(06)15003-X

Matagne, A., Dobson, C.M., 1998. The folding process of hen lysozyme: a perspective from the "new view." Cell. Mol. Life Sci. 54, 363–371. https://doi.org/10.1007/s000180050165

Mazzarella, R.A., Srinivasan, M., Haugejorden, S.M., Green, M., 1990. ERp72, an abundant luminal endoplasmic reticulum protein, contains three copies of the active site sequences of protein disulfide isomerase. J. Biol. Chem. 265, 1094–1101.

Menon, S., Lee, J., Abplanalp, W.A., Yoo, S.-E., Agui, T., Furudate, S.-I., Kim, P.S., Arvan, P., 2007. Oxidoreductase interactions include a role for ERp72 engagement with mutant thyroglobulin from the rdw/rdw rat dwarf. J. Biol. Chem. 282, 6183–6191. https://doi.org/10.1074/jbc.M608863200

Merulla, J., Fasana, E., Soldà, T., Molinari, M., 2013. Specificity and Regulation of the Endoplasmic Reticulum-Associated Degradation Machinery. Traffic 14, 767–777. https://doi.org/10.1111/tra.12068

Molinari, M., Calanca, V., Galli, C., Lucca, P., Paganetti, P., 2003. Role of EDEM in the release of misfolded glycoproteins from the calnexin cycle. Science 299, 1397–1400. https://doi.org/10.1126/science.1079474

Molinari, M., Galli, C., Piccaluga, V., Pieren, M., Paganetti, P., 2002. Sequential assistance of molecular chaperones and transient formation of covalent complexes during protein degradation from the ER. J. Cell Biol. 158, 247–257. https://doi.org/10.1083/jcb.200204122

Moremen, K.W., Trimble, R.B., Herscovics, A., 1994. Glycosidases of the asparagine-linked oligosaccharide processing pathway. Glycobiology 4, 113–125.

Mueller, B., Lilley, B.N., Ploegh, H.L., 2006. SEL1L, the homologue of yeast Hrd3p, is involved in protein dislocation from the mammalian ER. J. Cell Biol. 175, 261–270. https://doi.org/10.1083/jcb.200605196

Munro, S., 2001. The MRH domain suggests a shared ancestry for the mannose 6-phosphate receptors and other N-glycan-recognising proteins. Curr. Biol. 11, R499-501.

Nakatsukasa, K., Brodsky, J.L., 2008. The recognition and retrotranslocation of misfolded proteins from the endoplasmic reticulum. Traffic 9, 861–870. https://doi.org/10.1111/j.1600-0854.2008.00729.x

Nakatsukasa, K., Nishikawa, S., Hosokawa, N., Nagata, K., Endo, T., 2001. Mnl1p, an alpha -mannosidase-like protein in yeast Saccharomyces cerevisiae, is required for endoplasmic reticulum-associated degradation of glycoproteins. J. Biol. Chem. 276, 8635–8638. https://doi.org/10.1074/jbc.C100023200

Neutzner, A., Neutzner, M., Benischke, A.-S., Ryu, S.-W., Frank, S., Youle, R.J., Karbowski, M., 2011. A systematic search for endoplasmic reticulum (ER) membrane-associated RING finger proteins identifies Nixin/ZNRF4 as a regulator of calnexin stability and ER homeostasis. J. Biol. Chem. 286, 8633–8643. https://doi.org/10.1074/jbc.M110.197459

Ninagawa, S., Okada, T., Sumitomo, Y., Horimoto, S., Sugimoto, T., Ishikawa, T., Takeda, S., Yamamoto, T., Suzuki, T., Kamiya, Y., Kato, K., Mori, K., 2015. Forcible destruction of severely misfolded mammalian glycoproteins by the non-glycoprotein ERAD pathway. J Cell Biol 211, 775–784. https://doi.org/10.1083/jcb.201504109

Ninagawa, S., Okada, T., Sumitomo, Y., Kamiya, Y., Kato, K., Horimoto, S., Ishikawa, T., Takeda, S., Sakuma, T., Yamamoto, T., Mori, K., 2014. EDEM2 initiates mammalian glycoprotein ERAD by catalyzing the first mannose trimming step. J. Cell Biol. 206, 347–356. https://doi.org/10.1083/jcb.201404075

O'Connor, S.E., Imperiali, B., 1998. A molecular basis for glycosylation-induced conformational switching. Chemistry & Biology 5, 427–437. https://doi.org/10.1016/S1074-5521(98)90159-4

Oda, Y., Hosokawa, N., Wada, I., Nagata, K., 2003. EDEM as an acceptor of terminally misfolded glycoproteins released from calnexin. Science 299, 1394–1397. https://doi.org/10.1126/science.1079181

Oka, O.B.V., Bulleid, N.J., 2013. Forming disulfides in the endoplasmic reticulum. Biochim. Biophys. Acta 1833, 2425–2429. https://doi.org/10.1016/j.bbamcr.2013.02.007

Olivari, S., Cali, T., Salo, K.E.H., Paganetti, P., Ruddock, L.W., Molinari, M., 2006. EDEM1 regulates ER-associated degradation by accelerating de-mannosylation of folding-defective polypeptides and by inhibiting their covalent aggregation. Biochem. Biophys. Res. Commun. 349, 1278–1284. https://doi.org/10.1016/j.bbrc.2006.08.186

Olivari, S., Galli, C., Alanen, H., Ruddock, L., Molinari, M., 2005. A novel stress-induced EDEM variant regulating endoplasmic reticulum-associated glycoprotein degradation. J. Biol. Chem. 280, 2424–2428. https://doi.org/10.1074/jbc.C400534200

Ou, W.J., Bergeron, J.J., Li, Y., Kang, C.Y., Thomas, D.Y., 1995. Conformational changes induced in the endoplasmic reticulum luminal domain of calnexin by Mg-ATP and Ca2+. J. Biol. Chem. 270, 18051–18059.

Pan, S., Cheng, X., Sifers, R.N., 2013. Golgi-situated endoplasmic reticulum α-1, 2-mannosidase contributes to the retrieval of ERAD substrates through a direct interaction with γ-COP. Mol Biol Cell 24, 1111–1121. https://doi.org/10.1091/mbc.E12-12-0886

Pan, S., Wang, S., Utama, B., Huang, L., Blok, N., Estes, M.K., Moremen, K.W., Sifers, R.N., 2011. Golgi localization of ERManI defines spatial separation of the mammalian glycoprotein quality control system. Mol Biol Cell 22, 2810–2822. https://doi.org/10.1091/mbc.E11-02-0118

Parodi, A., Cummings, R.D., Aebi, M., 2015. Glycans in Glycoprotein Quality Control, in: Varki, A., Cummings, R.D., Esko, J.D., Stanley, P., Hart, G.W., Aebi, M., Darvill, A.G., Kinoshita, T., Packer, N.H., Prestegard, J.H., Schnaar, R.L., Seeberger, P.H. (Eds.), Essentials of Glycobiology. Cold Spring Harbor Laboratory Press, Cold Spring Harbor (NY).

Pearse, B.R., Hebert, D.N., 2010. Lectin chaperones help direct the maturation of glycoproteins in the endoplasmic reticulum. Biochim. Biophys. Acta 1803, 684–693. https://doi.org/10.1016/j.bbamcr.2009.10.008

Pelletier, M.F., Marcil, A., Sevigny, G., Jakob, C.A., Tessier, D.C., Chevet, E., Menard, R., Bergeron, J.J., Thomas, D.Y., 2000. The heterodimeric structure of glucosidase II is required for its activity, solubility, and localization in vivo. Glycobiology 10, 815–827.

Prilusky, J., Felder, C.E., Zeev-Ben-Mordehai, T., Rydberg, E.H., Man, O., Beckmann, J.S., Silman, I., Sussman, J.L., 2005. FoldIndex: a simple tool to predict whether a given protein sequence is intrinsically unfolded. Bioinformatics 21, 3435–3438. https://doi.org/10.1093/bioinformatics/bti537

Quan, E.M., Kamiya, Y., Kamiya, D., Denic, V., Weibezahn, J., Kato, K., Weissman, J.S., 2008. Defining the glycan destruction signal for endoplasmic reticulum-associated degradation. Mol. Cell 32, 870–877. https://doi.org/10.1016/j.molcel.2008.11.017

Reed, B.J., Locke, M.N., Gardner, R.G., 2015. A Conserved Deubiquitinating Enzyme Uses Intrinsically Disordered Regions to Scaffold Multiple Protein Interaction Sites. J. Biol. Chem. 290, 20601–20612. https://doi.org/10.1074/jbc.M115.650952

Riemer, J., Appenzeller-Herzog, C., Johansson, L., Bodenmiller, B., Hartmann-Petersen, R., Ellgaard, L., 2009. A luminal flavoprotein in endoplasmic reticulum-associated degradation. Proc. Natl. Acad. Sci. U.S.A. 106, 14831–14836. https://doi.org/10.1073/pnas.0900742106

Rutkevich, L.A., Cohen-Doyle, M.F., Brockmeier, U., Williams, D.B., 2010. Functional Relationship between Protein Disulfide Isomerase Family Members during the Oxidative Folding of Human Secretory Proteins. Mol Biol Cell 21, 3093–3105. https://doi.org/10.1091/mbc.E10-04-0356

Saeed, M., Suzuki, R., Watanabe, N., Masaki, T., Tomonaga, M., Muhammad, A., Kato, T., Matsuura, Y., Watanabe, H., Wakita, T., Suzuki, T., 2011. Role of the endoplasmic reticulum-associated degradation (ERAD) pathway in degradation of hepatitis C virus envelope proteins and production of virus particles. J. Biol. Chem. 286, 37264–37273. https://doi.org/10.1074/jbc.M111.259085

Saeki, Y., Kudo, T., Sone, T., Kikuchi, Y., Yokosawa, H., Toh-e, A., Tanaka, K., 2009. Lysine 63-linked polyubiquitin chain may serve as a targeting signal for the 26S proteasome. EMBO J. 28, 359–371. https://doi.org/10.1038/emboj.2008.305

Saito, Y., Ihara, Y., Leach, M.R., Cohen-Doyle, M.F., Williams, D.B., 1999. Calreticulin functions in vitro as a molecular chaperone for both glycosylated and non-glycosylated proteins. EMBO J. 18, 6718–6729. https://doi.org/10.1093/emboj/18.23.6718

Sakoh-Nakatogawa, M., Nishikawa, S.-I., Endo, T., 2009. Roles of protein-disulfide isomerase-mediated disulfide bond formation of yeast Mnl1p in endoplasmic reticulum-associated degradation. J. Biol. Chem. 284, 11815–11825. https://doi.org/10.1074/jbc.M900813200

Schrag, J.D., Bergeron, J.J., Li, Y., Borisova, S., Hahn, M., Thomas, D.Y., Cygler, M., 2001. The Structure of calnexin, an ER chaperone involved in quality control of protein folding. Mol. Cell 8, 633–644.

Schulz, M.A., Tian, W., Mao, Y., Van Coillie, J., Sun, L., Larsen, J.S., Chen, Y.-H., Kristensen, C., Vakhrushev, S.Y., Clausen, H., Yang, Z., 2018. Glycoengineering design options for IgG1 in CHO cells using precise gene editing. Glycobiology. https://doi.org/10.1093/glycob/cwy022

Shailubhai, K., Pukazhenthi, B.S., Saxena, E.S., Varma, G.M., Vijay, I.K., 1991. Glucosidase I, a transmembrane endoplasmic reticular glycoprotein with a luminal catalytic domain. J. Biol. Chem. 266, 16587–16593.

Shenkman, M., Groisman, B., Ron, E., Avezov, E., Hendershot, L.M., Lederkremer, G.Z., 2013. A shared endoplasmic reticulum-associated degradation pathway involving the EDEM1 protein for glycosylated and nonglycosylated proteins. J. Biol. Chem. 288, 2167–2178. https://doi.org/10.1074/jbc.M112.438275

Shental-Bechor, D., Levy, Y., 2008. Effect of glycosylation on protein folding: a close look at thermodynamic stabilization. Proc. Natl. Acad. Sci. U.S.A. 105, 8256–8261. https://doi.org/10.1073/pnas.0801340105

Sickmeier, M., Hamilton, J.A., LeGall, T., Vacic, V., Cortese, M.S., Tantos, A., Szabo, B., Tompa, P., Chen, J., Uversky, V.N., Obradovic, Z., Dunker, A.K., 2007. DisProt: the Database of Disordered Proteins. Nucleic Acids Res. 35, D786-793. https://doi.org/10.1093/nar/gkl893

Sokołowska, I., Piłka, E.S., Sandvig, K., Węgrzyn, G., Słomińska-Wojewódzka, M., 2015. Hydrophobicity of protein determinants influences the recognition of substrates by EDEM1 and EDEM2 in human cells. BMC Cell Biol 16. https://doi.org/10.1186/s12860-015-0047-7

Sousa, M., Parodi, A.J., 1995. The molecular basis for the recognition of misfolded glycoproteins by the UDP-Glc:glycoprotein glucosyltransferase. EMBO J. 14, 4196–4203.

Sousa, M.C., Ferrero-Garcia, M.A., Parodi, A.J., 1992. Recognition of the oligosaccharide and protein moieties of glycoproteins by the UDP-Glc:glycoprotein glucosyltransferase. Biochemistry 31, 97–105.

Stigliano, I.D., Alculumbre, S.G., Labriola, C.A., Parodi, A.J., D'Alessio, C., 2011. Glucosidase II and N-glycan mannose content regulate the half-lives of monoglucosylated species in vivo. Mol. Biol. Cell 22, 1810–1823. https://doi.org/10.1091/mbc.E11-01-0019

Stoll, M.S., Mizuochi, T., Childs, R.A., Feizi, T., 1988. Improved procedure for the construction of neoglycolipids having antigenic and lectin-binding activities, from reducing oligosaccharides. Biochem. J. 256, 661–664.

Stolz, A., Wolf, D.H., 2010. Endoplasmic reticulum associated protein degradation: a chaperone assisted journey to hell. Biochim. Biophys. Acta 1803, 694–705. https://doi.org/10.1016/j.bbamcr.2010.02.005

Su, K., Stoller, T., Rocco, J., Zemsky, J., Green, R., 1993. Pre-Golgi degradation of yeast prepro-alpha-factor expressed in a mammalian cell. Influence of cell type-specific oligosaccharide processing on intracellular fate. J. Biol. Chem. 268, 14301–14309.

Takeda, Y., Seko, A., Hachisu, M., Daikoku, S., Izumi, M., Koizumi, A., Fujikawa, K., Kajihara, Y., Ito, Y., 2014. Both isoforms of human UDP-glucose:glycoprotein glucosyltransferase are enzymatically active. Glycobiology 24, 344–350. https://doi.org/10.1093/glycob/cwt163

Tamura, T., Cormier, J.H., Hebert, D.N., 2011. Characterization of early EDEM1 protein maturation events and their functional implications. J. Biol. Chem. 286, 24906–24915. https://doi.org/10.1074/jbc.M111.243998

Tang, H.-Y., Huang, C.-H., Zhuang, Y.-H., Christianson, J.C., Chen, X., 2014. EDEM2 and OS-9 Are Required for ER-Associated Degradation of Non-Glycosylated Sonic Hedgehog. PLoS One 9. https://doi.org/10.1371/journal.pone.0092164

Tannous, A., 2015. NEW INSIGHTS INTO THE ROLE OF THE UDP-GLUCOSE: GLYCOPROTEIN GLUCOSYLTRANSFERASE 1 IN THE ENDOPLASMIC RETICULUM QUALITY CONTROL. Doctoral Dissertations.

Tannous, A., Patel, N., Tamura, T., Hebert, D.N., 2015a. Reglucosylation by UDP-glucose:glycoprotein glucosyltransferase 1 delays glycoprotein secretion but not degradation. Mol. Biol. Cell 26, 390–405. https://doi.org/10.1091/mbc.E14-08-1254

Tannous, A., Pisoni, G.B., Hebert, D.N., Molinari, M., 2015b. N-linked sugar-regulated protein folding and quality control in the ER. Semin. Cell Dev. Biol. 41, 79–89. https://doi.org/10.1016/j.semcdb.2014.12.001

Tessier, D.C., Dignard, D., Zapun, A., Radominska-Pandya, A., Parodi, A.J., Bergeron, J.J., Thomas, D.Y., 2000. Cloning and characterization of mammalian UDP-glucose glycoprotein: glucosyltransferase and the development of a specific substrate for this enzyme. Glycobiology 10, 403–412.

Tian, G., Xiang, S., Noiva, R., Lennarz, W.J., Schindelin, H., 2006. The crystal structure of yeast protein disulfide isomerase suggests cooperativity between its active sites. Cell 124, 61–73. https://doi.org/10.1016/j.cell.2005.10.044

Timms, R.T., Menzies, S.A., Tchasovnikarova, I.A., Christensen, L.C., Williamson, J.C., Antrobus, R., Dougan, G., Ellgaard, L., Lehner, P.J., 2016. Genetic dissection of mammalian ERAD through comparative haploid and CRISPR forward genetic screens. Nat Commun 7, 11786. https://doi.org/10.1038/ncomms11786

Tremblay, L.O., Herscovics, A., 1999. Cloning and expression of a specific human alpha 1,2-mannosidase that trims Man9GlcNAc2 to Man8GlcNAc2 isomer B during N-glycan biosynthesis. Glycobiology 9, 1073–1078.

Trombetta, E.S., Simons, J.F., Helenius, A., 1996. Endoplasmic reticulum glucosidase II is composed of a catalytic subunit, conserved from yeast to mammals, and a tightly bound noncatalytic HDEL-containing subunit. J. Biol. Chem. 271, 27509–27516.

Trombetta, S.E., Parodi, A.J., 1992. Purification to apparent homogeneity and partial characterization of rat liver UDP-glucose:glycoprotein glucosyltransferase. J. Biol. Chem. 267, 9236–9240.

Tu, B.P., Ho-Schleyer, S.C., Travers, K.J., Weissman, J.S., 2000. Biochemical Basis of Oxidative Protein Folding in the Endoplasmic Reticulum. Science 290, 1571–1574. https://doi.org/10.1126/science.290.5496.1571

Tulsiani, D.R., Touster, O., 1988. The purification and characterization of mannosidase IA from rat liver Golgi membranes. J. Biol. Chem. 263, 5408–5417.

Ushioda, R., Hoseki, J., Araki, K., Jansen, G., Thomas, D.Y., Nagata, K., 2008. ERdj5 is required as a disulfide reductase for degradation of misfolded proteins in the ER. Science 321, 569–572. https://doi.org/10.1126/science.1159293

Vallée, F., Lipari, F., Yip, P., Sleno, B., Herscovics, A., Howell, P.L., 2000. Crystal structure of a class I α1,2-mannosidase involved in N-glycan processing and endoplasmic reticulum quality control. EMBO J 19, 581–588. https://doi.org/10.1093/emboj/19.4.581

van den Berg, B., Chung, E.W., Robinson, C.V., Mateo, P.L., Dobson, C.M., 1999. The oxidative refolding of hen lysozyme and its catalysis by protein disulfide isomerase. EMBO J 18, 4794–4803. https://doi.org/10.1093/emboj/18.17.4794

van der Goot, A.T., Pearce, M.M.P., Leto, D.E., Shaler, T.A., Kopito, R.R., 2018. Redundant and Antagonistic Roles of XTP3B and OS9 in Decoding Glycan and Non-glycan Degrons in ER-Associated Degradation. Mol. Cell 70, 516-530.e6. https://doi.org/10.1016/j.molcel.2018.03.026

van der Lee, R., Buljan, M., Lang, B., Weatheritt, R.J., Daughdrill, G.W., Dunker, A.K., Fuxreiter, M., Gough, J., Gsponer, J., Jones, D.T., Kim, P.M., Kriwacki, R.W., Oldfield, C.J., Pappu, R.V., Tompa, P., Uversky, V.N., Wright, P.E., Babu, M.M., 2014. Classification of Intrinsically Disordered Regions and Proteins. Chemical Reviews 114, 6589–6631. https://doi.org/10.1021/cr400525m

Wang, C., Li, W., Ren, J., Fang, J., Ke, H., Gong, W., Feng, W., Wang, C.-C., 2013. Structural insights into the redox-regulated dynamic conformations of human protein disulfide isomerase. Antioxid. Redox Signal. 19, 36–45. https://doi.org/10.1089/ars.2012.4630

Ward, J.J., McGuffin, L.J., Bryson, K., Buxton, B.F., Jones, D.T., 2004. The DISOPRED server for the prediction of protein disorder. Bioinformatics 20, 2138–2139. https://doi.org/10.1093/bioinformatics/bth195

Wijeyesakere, S.J., Gagnon, J.K., Arora, K., Brooks, C.L., Raghavan, M., 2015. Regulation of calreticulin-major histocompatibility complex (MHC) class I interactions by ATP. Proc. Natl. Acad. Sci. U.S.A. 112, E5608-5617. https://doi.org/10.1073/pnas.1510132112

Wijeyesakere, S.J., Rizvi, S.M., Raghavan, M., 2013. Glycan-dependent and -independent interactions contribute to cellular substrate recruitment by calreticulin. J. Biol. Chem. 288, 35104–35116. https://doi.org/10.1074/jbc.M113.507921

Wolf, D.H., Stolz, A., 2012. The Cdc48 machine in endoplasmic reticulum associated protein degradation. Biochim. Biophys. Acta 1823, 117–124. https://doi.org/10.1016/j.bbamcr.2011.09.002

Xue, B., Dunbrack, R.L., Williams, R.W., Dunker, A.K., Uversky, V.N., 2010. PONDR-FIT: a meta-predictor of intrinsically disordered amino acids. Biochim. Biophys. Acta 1804, 996–1010. https://doi.org/10.1016/j.bbapap.2010.01.011

Yamaguchi, D., Hu, D., Matsumoto, N., Yamamoto, K., 2010. Human XTP3-B binds to alpha1-antitrypsin variant null(Hong Kong) via the C-terminal MRH domain in a glycan-dependent manner. Glycobiology 20, 348–355. https://doi.org/10.1093/glycob/cwp182

Yang, Z., Steentoft, C., Hauge, C., Hansen, L., Thomsen, A.L., Niola, F., Vester-Christensen, M.B., Frödin, M., Clausen, H., Wandall, H.H., Bennett, E.P., 2015. Fast and sensitive detection of indels induced by precise gene targeting. Nucleic Acids Res. 43, e59. https://doi.org/10.1093/nar/gkv126

Yu, S., Ito, S., Wada, I., Hosokawa, N., 2018. ER-resident protein 46 (ERp46) triggers the mannose-trimming activity of ER degradation-enhancing α-mannosidase-like protein 3 (EDEM3). J. Biol. Chem. https://doi.org/10.1074/jbc.RA118.003129